Master's thesis

NTNU
Norwegian University of Science and Technology
Faculty of Information Technology and Electrical Engineering
Department of Electric Power Engineering

Oda Andrea Hjelme

Optimal PV Inverter Active and Reactive Power Control in Distribution Grids With High Amounts of Solar PV

Master's thesis in Master of Energy and Environmental Engineering
Supervisor: Magnus Korpås
March 2019

NTNU
Norwegian University of Science and Technology

Oda Andrea Hjelme

Optimal PV Inverter Active and Reactive Power Control in Distribution Grids With High Amounts of Solar PV

Master's thesis in Master of Energy and Environmental Engineering
Supervisor: Magnus Korpås
March 2019

Norwegian University of Science and Technology
Faculty of Information Technology and Electrical Engineering
Department of Electric Power Engineering

NTNU
Norwegian University of
Science and Technology

Problem description

The increasing integration of photovoltaic solar panels (PV) is bringing new challenges to power system operators. As this technology is mostly connected at a low voltage (LV) level, the major impacts in the power system are seen in the distribution grids. In particular, large amounts of distributed generation may give rise to technical issues such as overloading and overvoltages, and thus lower power quality.

The purpose of this project is to analyze how utilization of smart photovoltaic inverters can mitigate the negative impacts from high amounts of solar photovoltaic active power generation in distribution networks. The objectives of the thesis are:

- Give a brief introduction to relevant system theory and previous research in the area.
- Formulate an optimization model for a 3 bus power network in The General Algebraic Modeling System (GAMS) to understand the basics of optimization and the new control variables regarding controllable inverters.
- Analyze the impact of high amounts of solar photovoltaics in a low voltage grid using real grid, load demand and photovoltaic active power generation data.
- Investigate how controllable inverters can mitigate the negative impacts caused by high amounts of solar photovoltaic active power generation in the distribution network using an expanded version of the optimization model, including multi-objective formulations.
- Investigate different inverter control options and identify which control option is more advantageous for overvoltage, power quality, and active power savings.
- Preform sensitivity analysis on voltage limits.

An existing grid model developed in GAMS will be used as basis for the simulations carried out in the project. This model will be further extended to assess the problems formulated above. The analyses will be conducted on realistic case studies based on power system data from NTE.

Preface

This Master's thesis is the conclusion of my Masters of Science degree (MSc) in Energy and Environmental Engineering with the Department of Electric Power Engineering at Norwegian University of Science and Technology (NTNU). The thesis addresses optimal control of photovoltaic inverters for overvoltage mitigation in distribution power networks.

I would like to thank my supervisor Magnus Korpås for great guidance throughout the semester. Your inputs and guidance have been highly appreciated. I would like to express gratitude to my co-supervisor Salman Zaferanlouei for helping me out with the simulation model. I am thankful for your fast responses and helpful guidance. I would also like to thank Marianne Blikø at NTE for your help in the initial phase of the project.

Finally, I would like to express gratitude towards to my friends and family for all your love and support.

Trondheim, March 2019

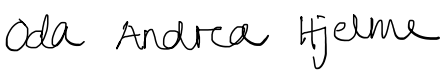

Oda Andrea Hjelme

Abstract

Photovoltaic solar panels are being installed in low voltage distribution networks at an increasing rate. This brings new challenges to the power system operators. In particular, large amounts of distributed generation give rise to technical issues such as overloading of the power network cables, overvoltages and thus lower power quality. In hours of high generation, overvoltage problems can be avoided by curtailment of active power generation or by reactive power absorption in the photovoltaic inverters. In turn, smart utilization of photovoltaic inverters can increase the distribution network's hosting capacity for distributed active power generation.

In this thesis, control of photovoltaic inverters for overvoltage mitigation in a low voltage distribution grid in Steinkjer, with high amounts of photovoltaic power generation is studied. An optimal power flow optimization model is built and simulated using GAMS (The General Algebraic Modeling System). Optimal set-points for photovoltaic inverter active and reactive power outputs are found by minimization of four different objectives: (i) network active power losses, (ii) voltage deviations, (iii) photovoltaic active power curtailment, and (iv) overall active power losses (network and curtailment).

The main results reveal that control of photovoltaic inverters is effective for overvoltage mitigation and for increasing the distribution grid's hosting capacity for distributed generation. Active power curtailment for overvoltage mitigation results in the lowest network active power losses. Reactive power control eliminate the need for active power curtailment. The network losses are increased compared to active power curtailment due to the reactive power absorption and higher active power generation. The distribution grid can tolerate higher amounts of active power generation with regards to overvoltages compared to overloading of the power cables. The overloading is increased by adding reactive power control to the inverters. This is due to increased reactive power line flows.

Sensitivity analysis on upper voltage limits show that reductions in overall active power losses (network and curtailment) can be obtained by accepting higher voltage variations. This is because by allowing higher voltages, the reactive power line flows and the required amount of curtailed active power generation can be reduced. Thus, one should carefully consider the consequences when setting absolute voltage boundaries.

Sammendrag

Solceller installeres i det lavspente distribusjonsnettet i stadig økende grad. Dette fører til nye utfordringer for kraftnettoperatørene. Spesielt gir store mengder distribuert energiproduksjon opphav til overbelastning av kraftledningene, overspenninger, og dermed lavere leveringskvalitet. I timer med høy energiproduksjon kan overspenningsproblemer unngås ved kutting av aktiv effekt eller ved absorbsjon av reaktiv effekt i vekselretterene mellom solcellene og nettet. Smart utnyttelse av vekselrettere kan derfor øke distribusjonsnettets evne til å tolerere aktiv effektproduksjon.

I denne oppgaven vurderes kontroll av vekselrettere for å begrense overspenningsproblemer i et lavspent distribusjonsnett i Steinkjer, med store mengder energiproduksjon fra solceller. En optimeringsmodell for optimal kraftflyt er utviklet og simulert i GAMS (The General Algebraic Modeling System). Optimale settpunkter for aktiv og reaktiv effektproduksjon for solcellesystemene er funnet ved å minimere fire ulike nyttefunksjoner: (i) nettverkstap, (ii) spenningsavvik, (iii) aktiv effektkutting, og (iii) totale effekttap (nettverkstap og aktiv effektkutting).

Hovedresultatene viser at kontroll av vekselrettere tilkoblet solkraftsystemer er effektivt for å unngå overspenningsproblemer og til å øke distribusjonsnettets kapasitet for distribuert energiproduksjon. Kutting av effekttopper for å unngå overspenning gir lavest nettverkstap. Reaktiv effektkontroll fører til at kutting av effekttopper ikke er nødvendig. Nettverkstapene er høyere sammenlignet med aktiv effektkontroll på grunn av den reaktive effekten som absorberes i vekselretterene og høyere aktiv effektproduksjon. Distribusjonsnettet kan tolerere større mengder aktiv effektproduksjon med hensyn til overspenninger i forhold til overbelastning av kraftledningene. Overbelastningen økes ved reaktiv effektkontroll i vekselretterne. Dette skyldes økt reaktiv effektflyt i kraftledningene.

Sensitivitetsanalyse på øvre spenningsgrenser viser at reduksjon i totale aktive effekttap (nettverkstap og aktiv effektkutting) kan oppnås ved å akseptere høyere spenningsvariasjoner. Dette skyldes at ved å tillatte høyere spenninger kan mengden absorbert reaktiv effekt og kuttet aktiv effektproduksjon reduseres. Derfor bør man vurdere konsekvensene nøye før man setter absolutte spenningsgrenser.

Acronyms

AC Alternating current

AMS Advanced measurement and control systems

APC Active power curtailment

DC Direct current

DG Distributed generation

DSO Distribution system operator

FACTS Flexible AC transmission system

GAMS The general algebraic modelling system

HV High voltage

LV Low voltage

NLP Nonlinear programming

NTE Nord-Trøndelag Elektrisitetsverk

OLTC On-load tap changer

OPF Optimal power flow

PF Power factor

pu Per unit

PV Photovoltaic

RPC Reactive power control

STATCOM Static synchronous compensator

Contents

List of Figures

List of Tables

1 Introduction

1.1 Background and objective

1.1.1 Solar power in Norway

The installed capacity of photovoltaic (PV) systems in Norway is increasing and at the end of 2017 the installed capacity reached 45 MWp [1]. Also the request for residential roof-top solar PV is increasing. Some of the reasons for the observed and assumed future growth are decreasing prices of solar PV systems, EL-certificates and increased interest in environmental questions. The hydropower in Norway makes it easier to integrate large amounts of unpredictable energy resources (PV, wind etc.) into the power system compared to in other countries, due to the regulation opportunities hydropower provide [1].

New forms for communication, new business models and new management systems become available as a consequence of the ongoing digitization of the power industry. In Norway, advanced measurement and control systems (AMS) are being installed in all households, and hour-by-hour measurements of power consumption and generation will become available. Elhub [1] shall form a common data hub for the electricity grid in Norway and will include all power data throughout Norway, and may be utilized for local marketplaces for energy exchange. The Norwegian energy company Otovos "Nabostrøm" is planning to use Elhub to visualize trade between customers with solar PV systems and customers who want locally produced green electricity. Otovo buys excess power from the PV owners and sells the power to the consumers that want to buy locally produced power [1]. In turn this might motivate end-users to install higher PV capacities.

The report "Solcellesystemer og sol i systemet" from Multiconsult and Asplan Viak Mars 2018 [1] present some possible challenges that may arise. High penetration of PV systems in the distribution network is

assumed to cause significant overvoltage issues, significant overloading issues and changes in the reactive power balance. Generally, the main issues will occur when PV systems are connected at the end of a radial in weak distribution networks. The power networks in more urban areas such as in the south-east of Norway are relatively strong and are assumed to tolerate the integration in a better manner. Smart utilization of PV inverters may be an alternative to increase the power system capacity. This may reduce the estimated needs for investments in the Norwegian power network [1].

1.1.2 Challenges and mitigation methods

The increasing integration of photovoltaic solar panels is bringing new challenges to the power system operators. PV systems are mostly connected at a low voltage (LV) level, thus the major impacts on the power system are in the distribution grids. A number of research papers have identified the potential challenges and impacts from integration of distributed generation units in LV distribution networks [2, 3]. The negative impacts include overvoltages, voltage unbalance, poor power quality, reverse power flows, voltage fluctuations and increased power losses. The voltage unbalance depends on how the solar PVs and loads are distributed in different phases of the LV distribution feeder. Voltage rise has been found to be one of the significant factors that limits the integration of high levels of solar power generation into radial distribution systems. These voltage variations are observed to increase with the level of PV penetration.

Possible mitigation methods to voltage variations and unbalance problems are many. Network upgrading is a traditional solution. Other solutions include OLTC (on-load tap changer), fixed or switched capacitors, and active power curtailment (APC). New techniques including inverter-based reactive power control, use of energy storage and flexible AC transmission system (FACTS) controllers have been proposed [2]. In a review of the mentioned techniques [2], FACTS controllers was found to be most effective. However, their current application at the distribution level is very limited and very little literature exists on FACTS controllers for voltage regulation in radial distribution systems with high PV penetrations. Reactive power support from PV inverters is gaining more attention and is thought to become an important tool for overvoltage prevention, voltage regulation and power factor correction [2].

1.1.3 PV inverter control for voltage-regulation

Several papers have investigated the effect of local voltage control by PV inverters [4–8]. Reactive power generation from the inverter can increase the voltage locally in undervoltage situations. In overvoltage situations, reactive power can be absorbed to decrease the voltage magnitude. Such reactive power control strategies may lead to high network currents and in turn higher active power losses. An additional solution to overvoltage problems are active power curtailment strategies that curtail PV active power during peak hours [8]. However, curtailment is unprofitable for the PV owner.

Reactive power support has significantly less effect in low voltage power networks compared to higher voltage networks. Due to higher R/X ratios, low voltage networks are more sensitive to active power compared to reactive power, and thus the supply of active power causes a noticeable increase in voltage magnitudes. For that reason a combination of reactive power support and active power curtailment is desired for overvoltage mitigation in low voltage networks [5]. Additional reasons for a combination of the control methods are that active power curtailment is unprofitable for the PV owner and that reactive power compensation leads to increased network active power losses. Reference [9] proposes that provision of reactive power from a generation unit with capacity exceeding 3.68 kVA should become mandatory in low voltage grids, because the supply of active power causes a significant voltage increase in low voltage grids.

In theory, the inverter can generate reactive power to support the network also when the sun does not shine. For example, Varma et.al. [10] investigate utilization of the PV inverter as a static synchronous compensator (STATCOM), also called a PV-STATCOM, in distribution systems. A PV-STATCOM can provide voltage control during critical system needs on a 24/7 basis. The entire inverter capacity can be utilized for STATCOM operation in the night, when the generation is zero. However, PV inverters on the market are limited by their manufacturers to two quadrant operation and can only supply reactive power compensation in hours of active power generation [11]. In addition to being a tool for voltage-regulation, the inverter may work as a communication unit for energy management. Smart control systems can make it possible for the distribution system operator (DSO) to buy services that the PV inverters can provide. Thus, each PV inverter provides a new tool for the distribution utilities to optimize its performance [12].

1.1.4 Optimal operation of smart PV inverters for improved operation of power networks

Several papers have studied optimal operation of PV inverters to improve the operation of a power network. A multi-objective optimization approach is derived in several papers [4–7]. The objectives usually include to minimize voltage magnitude deviation over the network, network active power losses and curtailment of PV active power generation. The equality constraints are typically the real and reactive power flow equations. The inequality constraints are the operational constraints of the network. The inverter constraints include a restriction for active power output limited by the available active power generation and restrictions for the reactive power output limited by the power factor (PF) capability and rated apparent power of the PV inverter.

Different inverter controls have been formulated in different papers [4–7]. In [6] and [5], PV inverter active power-voltage (P-V) and reactive power-voltage (Q-V) droop controls are utilized. An other approach is to find optimal PV inverter real and reactive power set-points based on feasible operating ranges [4, 7]. Research shows that optimal PV inverter real and reactive power set-points are successful for overvoltage mitigation in residential power networks with high PV penetrations [4, 7]. In addition, optimal set-points of the inverters results in lower voltage deviations and lower overall active power losses (network losses and curtailed PV active power) compared to fixed inverter settings [6] or PV active power curtailment alone [4, 5].

1.1.5 Objective

This thesis aims to asses how the presence of controllable PV inverters can mitigate the negative impacts from high amounts of solar PV in a distribution network. This shall be done by building an optimization model that aims to minimize network power losses, curtailed PV active power generation and voltage deviations. The objectives of the thesis include:

- Give a brief introduction to relevant system theory and previous research in the area.
- Formulate an optimization model for a 3 bus power network in GAMS to understand the basics of optimization and the new control variables regarding controllable inverters.
- Analyze the impact of high amounts of solar photovoltaics in a low voltage grid using real grid, load demand and photovoltaic active power generation data.

- Investigate how controllable inverters can mitigate the negative impacts caused by high amounts of solar photovoltaic active power generation in the distribution network using an expanded version of the optimization model, including multi-objective formulations.
- Investigate different inverter control options and identify which control option is more advantageous for overvoltage, power quality, and active power savings.
- Preform sensitivity analysis on voltage limits.

1.2 Approach

The system theory is used to formulate mathematical equations and constraints, together forming the optimization model. The resulting nonlinear optimization problem is written into GAMS and solved using nonlinear programming (NLP). Grid and load data fitted to the standard MATPOWER format for conventional load flow analysis in MATPOWER are provided by Lillebø [13]. Data for solar PV active power generation was generated using *Renewables.ninja* in my project thesis [14]. The simulation results obtained from running the optimization problem in GAMS are imported to Matlab in order to make presentable plots and graphs.

1.3 Limitations

The load demand and solar PV system outputs are assumed to be equally distributed between the phases. Thus, the power system is assumed to be balanced and voltage unbalance is not included in the analysis. Other assumptions and limitations are given in Section 4.1.

1.4 Structure of the thesis

Chapter 1 reviews the potential challenges associated with high penetration of PV power generation in low voltage power networks. In addition possible mitigation methods to voltage regulation are discussed and PV inverter control is introduced. A brief introduction to research on optimal operation of PV inverters for improved power network performance is also given.

Chapter 2, *Distribution grids with high amounts of solar PV*, explains how distributed generation affect the voltage magnitudes and network power losses. The operational range for different PV inverter controls are also explained.

Chapter 3, *Optimal power flow*, gives an introduction to power flow studies and optimal power flow. A short introduction to the multi-objective optimization technique is also given.

The mathematical formulation of the optimization problem is presented in Chapter 4, *Mathematical formulation of the problem*. The optimization objectives are presented as well as the constraints of the problem.

Chapter 5, *Computer implementation*, presents the implementation of the optimization model.

Chapter 6, *Case study description*, presents the distribution network of study, as well as load demand and PV active power generation data.

The simulation results are presented and analyzed in Chapter 7, *Results*.

The main findings from the results are discussed in Chapter 8, *Discussion*.

Chapter 8, *Conclusion*, concludes and summarize the main findings of the study.

Chapter 9, *Further work*, gives some suggestions for further work.

In Appendix A, simulation results for a high PV scenario (doubled installed PV capacity) are presented. The main results from single-objective optimization are summarized in Appendix B. In Appendix C, the PV inverter power factor at the most critical node is presented for a low PV scenario.

2 | Distribution grids with high amounts of solar PV

High amounts of solar PV power generation may cause overvoltages and increased active power losses in distribution networks. In this chapter the necessary theoretical framework to understand this will be presented. The chapter will also present smart PV inverters and explain how they may be utilized to solve overvoltage problems by reactive power control and active power curtailment.

First, some basic theory about distribution networks is given including nominal voltage level and acceptable voltage deviations from nominal. The total power loss is high in the distribution network lines compared to in high voltage (HV) networks due to low voltage and high current [15]. The term R/X ratio will also be explained in this chapter. Due to high R/X ratios in low voltage grids, the distribution grids are more susceptible to voltage change from active power compared to reactive power [16].

2.1 Distribution networks

The Norwegian electrical power grid is divided into two networks; the transmission network and the distribution network. The transmission grid comprise power lines connecting producers and consumers from different parts of the country, as well as power lines to other countries. The transmission grid mainly consists of 300 or 420 kV transmission lines. The distribution network comprise the grid connecting the transmission grid to the lower voltage distribution networks, and the grid supplying the end-users such as households and industry. The voltage level in the distribution grid range from 220 kV to 230/400 V in the LV network [17]. This project focuses on distributed power generation connected to the low voltage part of the distribution network, i.e. at a voltage level of 230/400 V.

2.1.1 Voltage limitations in the low voltage distribution network

The voltage drops when loads are connected to a power system, and increases if generation units are connected, as explained in Section 2.2.1. Voltages that deviate from nominal value may lead to technical issues and poor power quality, among other things [2]. Therefore, limits for allowable voltage deviations from nominal voltage are defined.

In the Norwegian regulations for quality of supply [18], it is stated that the DSO shall ensure that the voltage stays within ± 10% of the nominal value for slow variations in voltage. The maximum permissible voltage change caused by distributed generation is limited to 3%, compared to the system voltage without distributed generation, according to VDEs standard for power generation systems [19]. The power company Nord-Trøndelag Elektrisitetsverk (NTE) practices somewhat different limits for voltage deviation. They use the following voltage bounds for analyzes of the power network; at a voltage level of 230/400 V, the permissible range is from -7% to +8% of nominal voltage. However, in NTEs guide for prosumers [20] the voltage limits are more strict and the change in voltage from nominal value is limited to 5%. In this project a conservative range of ± 5% of nominal voltage will be used.

2.1.2 Apparent power and displacement power factor

In an alternating current (AC) electrical power system the power flow consist of both real power, P, and reactive power, Q. The active and reactive powers are important factors for the voltage along a line, as well as for the system power losses. The active and reactive powers are combined to the complex apparent power, $S = P + jQ$. The ratio between the real power and apparent power is defined as the displacement power factor of the power flowing, and the terms leading or lagging power factor refer to whether the phase of the current is leading or lagging the phase of the voltage. A lower absolute value for the power factor means that a larger amount of the apparent power is reactive power.

$$PF = cos(\phi) = \frac{P}{S} \tag{2.1}$$

where S is the magnitude of the apparent power given by:

$$S = \sqrt{P^2 + Q^2} \tag{2.2}$$

2.1.3 R/X ratio of a power network

The effect of active and reactive power on voltage in a power transmission network depends on the ratio between the line resistance and reactance [2]. This ratio is referred to as the R/X ratio. In distribution networks, the line resistance is usually much higher than the line reactance, resulting in high R/X ratios. The R/X ratio in higher voltage networks are typically lower, due to lower line resistances and higher reactances. For low voltage networks the R/X ratio can be up to 10, while medium voltage networks typically have a R/X ratio around 1. In addition, the R/X ratio is larger for underground cables compared to for overhead lines. The R/X ratio of a power network is an important parameter as the voltage sensitivity to active and reactive power is heavily influenced by this ratio. This will be explained in Section 2.4.2.

2.2 Distribution networks with distributed power generation

Distributed power generation impact the voltage profile and the power losses in a power network. This will be explained in this section considering the two bus system given in Figure 2.1. The system consists of a branch connected between a sending end node, *S*, and a receiving end node, *N*. The receiving end is attached to a load, $P_L + jQ_L$, and a distributed generation (DG) unit, $P_{DG} + jQ_{DG}$. $P_S + jQ_S$ is the sending end active and reactive powers. V_S and V_N are the sending and receiving end voltage magnitudes and I is the current flowing through the branch with resistance R and reactance X.

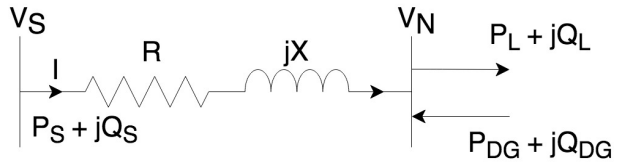

Figure 2.1: A two bus system with load and generation at the end of the line.

2.2.1 Impact of distributed generation on the voltage profile

The effect of active power on voltage is primarily proportional to the line resistance, while the change in voltage due to reactive power is primarily proportional to the line reactance in distribution networks [21]. The voltage change across a line $\Delta V = V_N - V_S$ can be approximated as [22]

$$\Delta V \approx \frac{R(P_L + P_{DG}) + X(Q_L + Q_{DG})}{V_N} \tag{2.3}$$

where the active and reactive powers are defined as power injections to the receiving end bus. A load is a negative injection and will cause the voltage to drop. Opposite, distributed generation represent a positive injection and will lead to a voltage increase. The total voltage change is divided into voltage change caused by the load, ΔV_L, and voltage change caused by the distributed generation unit, ΔV_{DG}.

$$\Delta V = \Delta V_L + \Delta V_{DG} \tag{2.4}$$

where

$$\Delta V_L = \frac{RP_L + XQ_L}{V_N} \tag{2.5}$$

$$\Delta V_{DG} = \frac{RP_{DG} + XQ_{DG}}{V_N} \tag{2.6}$$

Note that the active power consumption of the load, P_L, is negative while the active power injection of the DG unit, P_{DG}, is positive.

The loads in the distribution grid are usually mostly resistive with a power factor close to 1. Consequently, the voltage drop caused by a load mainly depends on the resistance of the line and the size of the load. If the active power generation of the DG unit exceeds the load demand, excess energy is fed into the grid and the power flow reverses. Hence, a voltage increase will occur if reactive power is neglected and the resulting bidirectional power flow into the grid creates potential overvoltage problems.

2.2.2 Impact of distributed generation on network power losses

Distributed power generation will lead to increased network power losses if the presence of the DG unit contributes to an increase in the power flowing in the power transmission network. Possible causes for increase in power flows are high reverse power flows or increased reactive currents due to reactive power generation/ absorption from the generation unit. Opposite, if the unit contributes to reduce the power flow, the network power loss may be reduced.

As a result of low voltage and high current, the total power losses in low voltage networks are higher compared to for high voltage networks. As a consequence of high losses, the cost of power increases and the voltage profile worsens [15]. The total power loss in a power transmission system can be decomposed into two parts; real power loss, P_{Loss}, and reactive power loss, Q_{Loss}. The power loss for the line connect-

ing the sending end and receiving end buses in Figure 2.1 can be expressed by the following equations [15].

$$P_{Loss} = RI^2 \tag{2.7}$$

$$Q_{Loss} = XI^2 \tag{2.8}$$

$$I = \sqrt{\frac{P_S^2 + Q_S^2}{V_S^2}} \tag{2.9}$$

The power balance on the line is given by

$$P_S = P_L - P_{DG} + P_{Loss} \tag{2.10}$$

$$Q_S = Q_L - Q_{DG} + Q_{Loss} \tag{2.11}$$

P_S	Sending end active power
Q_S	Sending end reactive power
I	Value of the current flowing through the branch connected between nodes S and N.

2.3 Solar PV inverters

Solar PV inverters can be utilized to mitigate overvoltage problems in the distribution power grid. Solar PV panels generate direct current (DC) and are usually connected to an inverter that converts the direct current into alternating current. Most PV inverters interconnected to the distribution network operate at unity power factor, $PF = 1$, meaning they only produce active power [11]. However, PV inverters are capable of absorbing or generating reactive power and thereby reduce or increase the voltage magnitude in the grid connection point as explained in Section 2.2.1.

The inverters have two possibilities of operation; two quadrant and full quadrant operations. However, most PV inverters on the market today are limited to two quadrant operation with a limited power factor capability range. The resulting operating range is discussed in Section 2.3.1. A consequence of the limited power factor is limited reactive power capability as discussed in Section 2.3.2. Introduction of solar PV in the low voltage distribution network needs to obey standards. These standards are presented in Section

2.3.3. Possible inverter control strategies and the operational space for active and reactive power PV inverter outputs for different control strategies are discussed in Section 2.3.4-2.3.6.

2.3.1 Operating range

PV inverters are rated in terms of an apparent power rating, S. The apparent power rating represent the inverter capacity and limits the PV inverter active and reactive power outputs. The inverters have two possibilities of operation; two quadrant and full quadrant operation. However, only two quadrant operation is possible for PV inverters without storage [2]. The resulting operating range is represented by the right semicircle in Figure 2.2 with radius S in the PQ space.

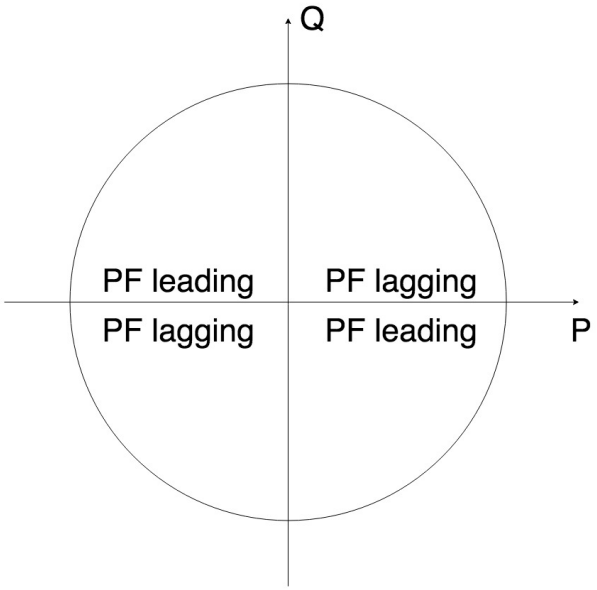

Figure 2.2: PV inverter operating range in the PQ space.

The full capacity of a PV inverter can in theory be utilized for generating or consuming reactive power. In a two quadrant operation, the PV inverter consumes reactive power at a leading power factor (also referred to as capacitive operation) and generate reactive power at a lagging power factor (also referred to as inductive operation). The reactive power management does dot require energy from the PV array, and hence the inverters are capable of providing reactive power when the generation is zero. However, the inverters on the market today have limited power factor capability and are not designed to provide reactive power while generating no real power [11]. The PV inverter power factor range is limited by the manufacturers to limit the amount of wear on the device as well as to limit the operating losses. Typical

power factor ranges for PV inverters can be 0.8/0.9/0.95 lagging to 0.8/0.9/0.95 leading [11].

The apparent power output from the PV inverter is given by $S_{PV} = P_{PV} + jQ_{PV}$, where the active and reactive power outputs can be written as:

$$P_{PV} = S_{PV} \times cos(\phi) \tag{2.12}$$

$$Q_{PV} = S_{PV} \times sin(\phi) \tag{2.13}$$

where

$$S_{PV} = \sqrt{P_{PV}^2 + Q_{PV}^2} \tag{2.14}$$

$$\phi = cos^{-1}(PF) \tag{2.15}$$

2.3.2 Reactive power capability

PV inverters are usually specified by its apparent power rating and its power factor capability, and the reactive power capability of the inverter depends on these specifications. The PV inverter will loose its reactive power capability if the real power produced by the PV array is equal to the inverter apparent power rating, S. Nevertheless, some reactive power capability can be retained by over-sizing the inverter [2]. If the inverter is overrated such that $S_{PV,max} > P_{PV,max}$, the inverter will be able to consume or generate reactive power at maximum PV array generation, $P_{PV,max}$. The amount of reactive power, Q_{PV}, that can be consumed/ generated follows from the inequality

$$\sqrt{P_{PV}^2 + Q_{PV}^2} \leq S_{PV,max} \tag{2.16}$$

Thus, the reactive power capability at maximum PV power generation follows as

$$Q_{PV}(P_{PV,max})) \leq \sqrt{S_{PV,max}^2 - P_{PV,max}^2} \tag{2.17}$$

The power factor limitations of an inverter also limits the inverter's reactive power capability. More reactive power can be provided by reducing the operating power factor for a given amount of power generation, P_{PV}. This follows if the reactive power output is written in terms of the power factor and active

power generation,

$$\begin{aligned} Q_{PV} &= S_{PV} \times sin(\phi) \\ &= P_{PV} \times tan(\phi) \\ &= P_{PV} \times tan(cos^{-1}(PF)) \end{aligned} \tag{2.18}$$

Thus, for a given power generation, P_{PV}, the available reactive power is limited by the power factor limit, PF_{min}. For an inverter with minimal power factor limit of 0.8, the reactive power output is limited to 75% of the active power generation:

$$\begin{aligned} Q_{PV} &\leq P_{PV} \times tan(cos^{-1}(PF_{min})) \\ &\leq P_{PV} \times 0.75 \end{aligned} \tag{2.19}$$

2.3.3 Standards for PV systems connected to low voltage distribution networks

The distributed generation interconnection standards that target PV systems in the low voltage distribution grid are the German norm VDE 4105-2011 [19] and the European norm EN 50438:2013 [23]. The standards include requirements for reactive power capability, allowable voltage rise caused by distributed generation units and apparent power limits for single-phase installations, among other things.

According to standard VDE 4105:2011 [19], the power generation systems shall contribute to the static voltage stability in the low voltage network if required due to network related circumstances and by the network operator. Table 2.1 shows the requirements on reactive power capabilities. Generators with apparent power ratings up to 13.8 kVA are required to be able to provide power factors up to 0.95 lagging/leading. Displacement power factors up to 0.9 must be supported if the apparent power rating exceeds 13.8 kVA.

Table 2.1: Requirements on reactive capability for power generation systems in the distribution network. From the German norm VDE 4105-2011 [19].

Rated power of the solar PV system	Power factor range
$S_{max} \leq 13.8$ kVA	0.95 lagging to 0.95 leading
$S_{max} > 13.8$ kVA	0.90 lagging to 0.90 leading

The allowable voltage rise for distributed generation units in the low voltage distribution networks are limited to 3% according to VDE 4105-2011 [19]. In NTEs guide for prosumers [20], the permissible voltage

change is limited to 5%. The allowable voltage rise constrain the permissible installed power rating of the unit. However, in order to be characterized as a prosumer, the power fed into the grid must never exceed 100 kW [24].

Power generation systems may be single-phase or three-phase connected to the network. To avoid voltage unbalance, maximum apparent power ratings for single-phase connected systems are set. In VDE 4105-2011 [19], the limit for single-phase installations in the low voltage networks is set to 4.6 kVA. In NTEs guide for prosumers [20], the limit is set to 3.6 kVA. For apparent power ratings exceeding the limit for single-phase installations several single-phase connections or three-phase inverters are required.

2.3.4 Voltage control functions of PV inverters

Several local voltage control functions are available for PV inverters, including static control (constant Q or constant PF), voltage dependent reactive power consumption/generation Q(V), power factor dependent on active power PF(P) and voltage dependent curtailment of active power P(V) control. The PV inverter operates by adjusting its active and reactive power outputs as a function of a quantity measured at the connection point [21].

Static control: Constant Q or constant PF

In the constant Q method, the reactive power consumption is constant independent of voltage and active power generation. In the constant PF control method, the PV inverter provides reactive power proportional to the active power generation. Typical values for constant power factor are 0.9 or 0.95 leading. It is not advised to use these static control functions because of high reactive currents in the grid which in turn leads to higher network power losses [21].

Voltage dependent reactive power consumption/generation: Q(V)

In the Q(V) method, the consumption or generation of reactive power is a function of the voltage measured. Reactive power is consumed when the voltage exceeds a certain threshold. Contrary, when the voltage falls below a certain threshold, reactive power is injected to increase the voltage. The relation

between Q and V is linear and a deadband can be applied around the nominal voltage to avoid reactive power provision during acceptable voltage deviations [21].

Power factor dependent on active power: PF(P)

In the PF(P) method, the power factor is dependent on the active power generation. During high feed-in power, the reactive power consumption is increased by linearly reducing the value of the operating power factor. The power factor is set to unity when the active power generation is low. This method controls the voltage indirectly as high power generation is often correlated to high voltage [21].

Voltage dependent curtailment of active power: P(V)

Voltage dependent curtailment of active power implies that active power is gradually decreased if the voltage exceeds a certain threshold. This control method can contribute to increase the annual amount of active power generation as a higher capacity of PV can be installed without causing overvoltages in the power system. However, the PV system will be less profitable due to reduced revenue from power generation [21].

2.3.5 Control of PV inverters

PV inverters can either be controlled locally or by a remote control interface. In local control the inverter adjust the active and reactive power set-points as a function of a quantity measured (voltage, active power etc.) at the connection point. In a remote control interface the desired set-points can be calculated centrally and the set-points are further transmitted to the PV inverters. Remote control can improve the utilization of PV inverter control, but relies on a strong communication infrastructure [21].

2.3.6 Operational space for different control strategies

The different control strategies result in different available operating ranges for active and reactive power PV inverter outputs. For two quadrant inverter operation, the available operating space is limited by the apparent power rating of the inverter, S_{max}, and the power generated by the PV array, $P_{PV,max}$. This is common for all control strategies.

If an active power curtailment (APC) strategy is implemented at an inverter, active power is curtailed to obtain the desired amount of power. The feasible operating points for this strategy is illustrated by the orange line in Figure 2.3a. PV inverters that only allow reactive power control (RPC) and no curtailment are capable of operating at operating points at the orange line in Figure 2.3b, provided that the power factor capability is not limiting. The inverter can absorb or generate reactive power depending on its rating and the generated active power. The inverter will only be able to provide reactive power compensation at $P_{PV,max}$ if the inverter is overrated, that is S_{max}>$P_{PV,max}$ (see Section 2.3.2).

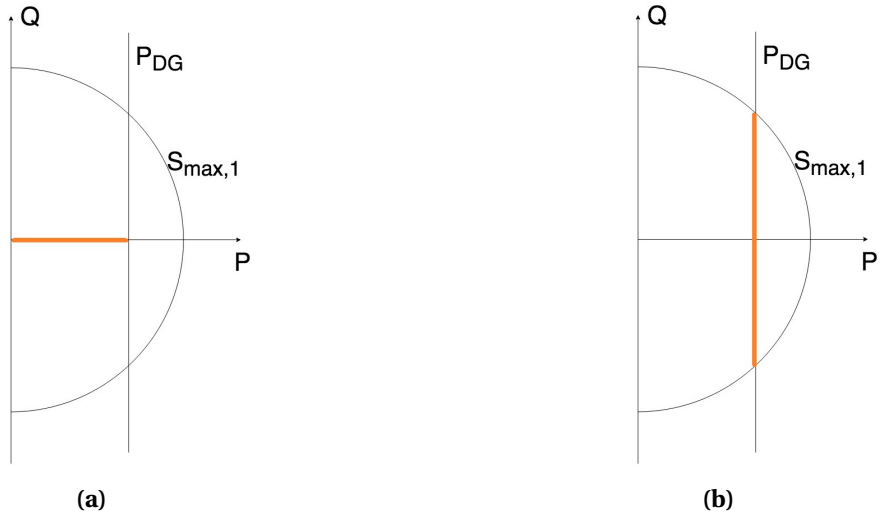

Figure 2.3: Operating range for: (a) Active power curtailment (APC) at unity power factor, (b) Reactive power control (RPC) only. Figures inspired by [4].

Active power curtailment and reactive power control can be combined to provide increased flexibility. By combining the two strategies the resulting operating space will be significantly larger compared to active power curtailment or reactive power control alone. The resulting operating space is illustrated by the orange area in Figure 2.4a. As stated in Section 2.3.1, the power factor range of the PV inverters are typically limited to 0.8-0.95 leading/lagging. Thus, the operating range will be reduced. The resulting operating space is given by the orange area in Figure 2.4b.

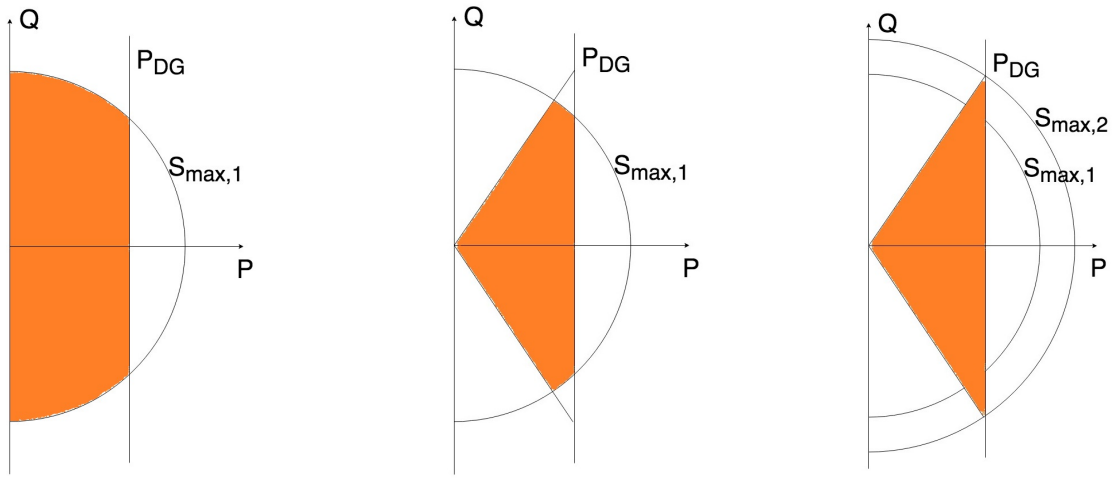

Figure 2.4: Operating range for a combination of the control strategies active power curtailment and reactive power control. (a) No limit on power factor capability, (b) Limited power factor capability, (c) Limited power factor capability and increased apparent power rating. Figures inspired by [4].

As stated above, the inverter can be overrated to enable reactive power compensation at maximum active power generation. In Figure 2.4b, the reactive power capability is limited by the apparent power rating $S_{max,1}$ at active power generation P_{DG}. To increase the reactive power absorption (or generation) some active power generation needs to be curtailed. In this project it is assumed that the inverter is oversized such that the inverter can provide reactive power compensation at $P_{PV,max}$ and minimum power factor. The operating space for this strategy is given by the orange area in Figure 2.4c with increased apparent power rating, $S_{max,2} > S_{max,1}$. For instance, a minimum power factor of 0.8 means an overrating of the inverter of 25%. This can be seen from Equation 2.20, with $Q_{pv,max}$ from Equation 2.19.

$$\begin{aligned} S_{pv} &= \sqrt{P_{pv,max}^2 + Q_{pv,max}^2} \\ &= \sqrt{P_{pv,max}^2 + (0.75 \times P_{pv,max})^2} \\ &= P_{pv,max}\sqrt{1 + 0.75^2} \\ &= P_{pv,max} \times 1.25 \end{aligned} \tag{2.20}$$

2.4 Effectiveness of PV inverter control

2.4.1 Impact of the power factor

In Section 2.2.1 an often used approximation for voltage change along a line was explained. High feed-in power from a generation unit will cause the voltage to rise. The voltage rise can be limited if the generation unit consumes reactive power at a leading power factor. Undervoltage situations can occur in high load situations. In these situations, the distributed generation unit can increase the voltage by generating reactive power at a lagging power factor. Figure 2.5 shows the impact of distributed generation on the voltage profile for different inverter settings. Operating at a lower power factor means that a higher fraction of the apparent power is reactive power. Thus, the voltage rise can be reduced even more by operating at a lower value for the leading power factor.

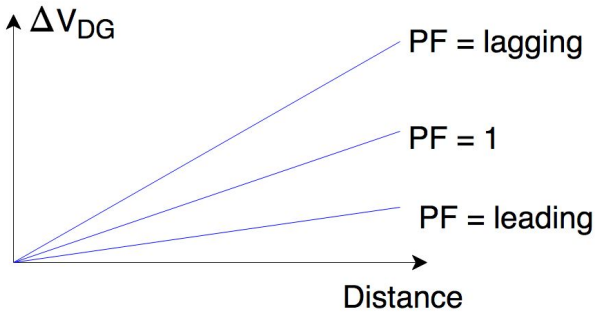

Figure 2.5: Impact of operating power factor on voltage change along a power line. The x-axis represent the length of the power line.

2.4.2 Impact of the R/X ratio of the power network

The voltage sensitivity to active and reactive power is heavily influenced by the R/X ratio of the power network. The coupling between active power, P, and voltage magnitude, $|V|$, and the coupling between reactive power, Q and voltage angle, δ, is strong in systems with high R/X ratios. On the other hand, the coupling between P and δ, and Q and $|V|$, is weak. The opposite is true for low R/X ratios [16]. The R/X ratios in distribution systems are high, and hence the distributions systems are more susceptible to voltage change from active power than reactive power. The impact of the power networks R/X ratio will be illustrated below by calculating the voltage change caused by a generation unit in networks with

different R/X ratios.

In a medium voltage network with a R/X ratio of 1, active and reactive power will impact the change in voltage in equal manner. Lets say that the inverter is overrated and that the inverter is operating at power factor of 0.8 leading, and thus $Q_{DG} = -0.75 \times P_{DG}$ (from Equation 2.18). For this medium voltage network, the reactive power consumption can compensate for 75% of the voltage rise caused by generation (from Equation 2.6):

$$\begin{aligned} \Delta V_{DG,HV}^{Qcontrol} &= \frac{RP_{DG} + XQ_{DG}}{V_N} \\ &= \frac{RP_{DG} - R(0.75P_{DG})}{V_N} \\ &= \frac{0.25RP_{DG}}{V_N} \\ &= 25\%\Delta V_{DG}^{noQcontrol} \end{aligned} \tag{2.21}$$

Similarly, for a low voltage grid with a R/X ratio of 10, 7.5% of the voltage rise caused by distributed generation can be compensated for by reactive consumption considering the same power factor:

$$\begin{aligned} \Delta V_{DG,HV}^{Qcontrol} &= \frac{RP_{DG} + XQ_{DG}}{V_N} \\ &= \frac{RP_{DG} - 0.1R(0.75P_{DG})}{V_N} \\ &= \frac{0.925RP_{DG}}{V_N} \\ &= 92.5\%\Delta V_{DG}^{noQcontrol} \end{aligned} \tag{2.22}$$

Thus, the effect of reactive power consumption is significantly lower in the low voltage network due to a higher R/X ratio. The voltage drop caused by distributed generation for different R/X ratios is illustrated in Figure 2.6.

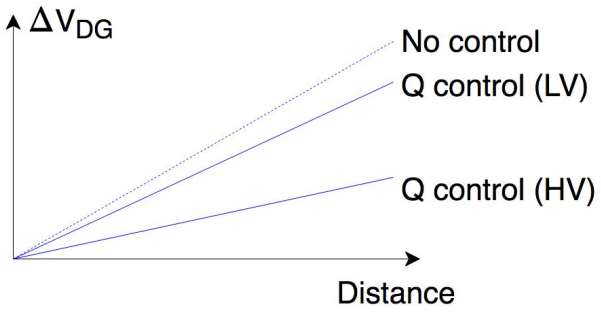

Figure 2.6: Voltage-lowering effect of reactive power absorption in low and high voltage networks. The x-axis represent the length of the power line.

3 | Optimal power flow

This chapter will give an introduction to power flow studies, optimal power flow and multi-objective optimization. Optimal power flow is used to optimize the operation of the distribution power network and to optimize the PV inverter active and reactive power outputs. The theory regarding power flow studies and optimal power flow is taken from the book *Power System Analysis* written by Hadi Saadat [16], and the theory regarding multi-objective optimization is taken from chapter Multi-objective Optimization written by Kalyanmoy Deb in the book *Search Methodologies* [25].

3.1 Power flow studies and optimal power flow

A power flow study is a steady-state analysis of the flow of electrical power in a power system. Power flow studies are important for planning, economic scheduling and control of an existing system, as well as planning of the future expansion of it. The analysis is usually simplified by the following assumptions [16]:

- The system operates under balanced conditions. In a balanced system all loads and generators are equally distributed across all three phases.
- The system can be represented by a single-phase model. Hence, the system is simplified to one phase instead of three.
- All impedances/admittances are in per unit [pu] on a common MVA base.

In a power flow analysis, the four quantities, voltage magnitude, $|V|$, phase angle, δ, real power injection, P_i, and reactive power injection, Q_i, are associated to each bus. Two of the quantities are known for each bus. The buses are usually classified into three types; reference bus (slack bus), generator bus (P-V

bus) and load bus (P-Q bus). The active power and voltage magnitude are specified at a generator bus, while the active and reactive powers are specified at a load bus. The voltage magnitude at the slack bus is assumed to be 1 per unit (pu), and the angle is set to 0 rad and works as an angular reference for all other buses.

The power flow equations used for power flow analysis are derived from the nodal analysis equations for the power system. In order to derive the power flow equations, the system is most often expressed in matrix notation, where $Y_{BUS} = G + jB$ is the admittance matrix of the network. I_{BUS} is the vector of injected bus currents, V_{BUS} is the vector of bus voltages and n is the number of buses in the system.

$$\Big[I_{BUS}\Big] = \Big[Y_{BUS}\Big]\Big[V_{BUS}\Big] \tag{3.1}$$

$$\begin{bmatrix} I_1 \\ \vdots \\ I_i \\ \vdots \\ I_n \end{bmatrix} = \begin{bmatrix} Y_{11} & \cdots & Y_{1i} & \cdots & Y_{1n} \\ \vdots & \cdots & \vdots & \cdots & \vdots \\ Y_{i1} & \cdots & Y_{ii} & \cdots & Y_{in} \\ \vdots & \cdots & \vdots & \cdots & \vdots \\ Y_{n1} & \cdots & Y_{ni} & \cdots & Y_{nn} \end{bmatrix} \begin{bmatrix} V_1 \\ \vdots \\ V_i \\ \vdots \\ V_n \end{bmatrix} \tag{3.2}$$

The apparent power at bus i, S_i, can be decomposed into active and reactive power injections:

$$S_i = P_i + jQ_i = V_i\Big(\sum_{i=1}^{n} Y_{ij}^* V_{ij}^*\Big) \tag{3.3}$$

$$P_i = \sum_{j=1}^{n} |V_i||V_j||Y_{ij}|cos\big(\theta_{ij} - \delta_i + \delta_j\big) \tag{3.4}$$

$$Q_i = -\sum_{j=1}^{n} |V_i||V_j||Y_{ij}|sin\big(\theta_{ij} - \delta_i + \delta_j\big) \tag{3.5}$$

where V_i and δ_i are the voltage magnitude and angle at bus i, and Y_{ij} and θ_{ij} are the magnitude and angle of admittance matrix element (i, j). Equations 3.4 and 3.5 are known as the real and reactive power flow equations. By solving for the unknown variables at each bus, the load flow solution is obtained. The power flow equations are nonlinear, and thus a numerical iterative algorithm is required to solve the equations.

3.1.1 Optimal power flow

The optimal power flow (OPF) technique is used to optimize the operation of an electric power system subject to the physical constraints imposed by electrical laws and engineering limits. Typical objectives are to minimize economic costs or power transmission losses. In the problem formulation, the power flow equations (Equations 3.4 and 3.5) are usually used as equality constraints. The inequality constraints usually represent physical limitations of the system such as upper and lower bus voltage limits and active and reactive power limits on generation buses.

3.2 Multi-objective optimization

Multi-objective optimization (MOO) considers optimization problems having more than one objective function to be optimized simultaneously. The objectives are usually conflicting, and a single solution that simultaneously optimizes each objective may not exist. Conflicting objectives in an optimal power flow problem can be minimization of voltage deviations and curtailment of power generation. As explained in Section 2.2.1, high reverse power flows from distributed generation may cause overvoltages and thus increased voltage deviations.

A multi-objective optimization problem can be denoted as:

$$\begin{aligned} \text{Minimize} \quad & F(x) = \big(f_1(x), f_2(x), ..., f_m(x)\big) \\ \text{subject to} \quad & h(x) = 0 \\ & g(x) \leq 0 \end{aligned} \tag{3.6}$$

where m is the number of objective functions, and h(x) and g(x) denotes the equality and inequality constraints, respectively.

Multi-objective optimization problems with conflicting objectives usually have no single solution, but a set of non-dominated, alternative solutions. These solutions are known as the Pareto optimal set of the problem and are considered equally good. The set of solutions often provide a clear front, the Pareto optimal front, on an objective space plotted with the objective values. A decision process is necessary in order to select a suitable comprise solution from the alternative solutions.

3.2.1 Weighted-sum approach

A widely used method to solve multi-objective optimization problems is the weighted-sum approach. In this method the multi-objective optimization problem is converted into a single-objective optimization problem by pre-multiplying each objective with a weight. The weighting coefficients are real values representing the relative importance of the objectives, and are typically chosen such that their sum is one, $\sum_{i=1}^{m} w_i = 1$. Appropriate scaling of the objectives is of great importance in this method, and normalizing of the objectives usually yield good results [26]. Using the weighted-sum approach, the above problem can be formulated as:

$$\begin{aligned} \text{Minimize} \quad & F(x) = \sum_{i=1}^{m} w_i f_i(x) \\ \text{subject to} \quad & h(x) = 0 \\ & g(x) \leq 0 \end{aligned} \tag{3.7}$$

The solution to the simplified problem can under some conditions be a Pareto optimal point. Thus, by changing the weight vector, different Pareto optimal solutions can be obtained and a Pareto optimal front can be approximated. An advantage with a method optimizing a linear combination of the objectives is that no interactions with a decision maker is needed, as only one single solution is found.

4 | Mathematical formulation of the problem

The purpose of this thesis it to investigate how controllable PV inverters can mitigate to limit some expected disadvantages associated with high amounts of solar power generation in the distribution power networks. This is approached by developing and testing four different control objectives, each representing a challenge or disadvantage. The objectives include to minimize network active power losses, voltage deviations, PV active power curtailment, and overall active power losses (network active power losses and PV active power curtailment). The objectives are proved efficient for improving the power network performance in the papers [4] and [7].

This chapter will give the mathematical formulation of the optimization problem. First, the single-objective optimization with the objectives to minimize network active power losses (O1), voltage deviations (O2), and PV active power curtailment (O3) are formulated. Second, a multi-objective optimization based on objectives O1 and O3 is formulated. This multi-objective optimization problem is transformed into a single-objective optimization problem using the weighted-sum approach with the objectives equally weighted. The resulting single-objective optimization problem is referred to as objective 4 (O4), overall active power losses. Finally, a multi-objective optimization problem based on objectives O1, O2, and O3 is formulated, where objectives O1 and O3 are transformed into the single-objective O4, before the multi-objective optimization of objectives O2 and O4 is transformed into a single-objective optimization problem using the weighted-sum approach. The objectives are scaled and different values of weights are assigned to the objectives.

4.1 Assumptions

The following assumptions have been made in the simulations:

- The power system operates under balanced conditions. In a balanced system all loads and generators are equally distributed across all three phases. This is assumed to solve the load flow problems in MATPOWER and GAMS.
- The system can be represented by a single-phase model. Hence, the system is simplified to one phase instead of three. Also to solve the load flow problems in MATPOWER and GAMS.
- The apparent power rating of the inverter is assumed to be overrated compared to the active power rating, such that reactive power compensations at $PF = PF_{min}$ and $P_{PV,max}$ is possible. Hence, the inverters are overrated by 25% for $PF_{min} = 0.8$. This is calculated in Equation 2.20 and illustrated in Figure 2.4c.
- The transformer connected to the main grid is assumed to have sufficient capacity to export all excess energy from PV power generation since the focus is on voltage problems in this project.
- The cable's rated power threshold is not taken into account in the simulations since the focus is on voltage problems.

4.2 Notations

Sets

i	-	Set of buses, $i \in$ [1,N]
t	-	Set of hours, $t \in$ [1,T]
$slackbus$	-	Bus acting as the slack bus, $\in$ [76]
$generator$	-	Set of buses acting as a generator bus, $\in$ [76]
$pvbus$	-	Set of buses with PV active power generation, $\in$ [1,54]
$notgeneratorandpvbus$	-	Set of bus bars connecting the transformer feeder lines to the end-user branches , $\in$ [55,75]

Parameters

$\|Y_{ij}\|$	-	Magnitude of admittance matrix element (i,j) [pu]
θ_{ij}	-	Angle of admittance matrix element (i,j) [radians]
P_{Li}^{t}	-	Active load demand at time t [pu]
Q_{Li}^{t}	-	Reactive load demand at time t [pu]
$P_{PVi,max}^{t}$	-	Maximum available active power solar generation at time t [pu]
PF^{min}	-	Minimal power factor of PV inverter [-]
V^{min}	-	Minimum voltage magnitude [pu]
V^{max}	-	Maximum voltage magnitude [pu]
δ^{min}	-	Minimum voltage angle [radians]
δ^{max}	-	Maximum voltage angle [radians]
P_{slack}^{min}	-	Lower bound for active power import at the slack bus [pu]
P_{slack}^{max}	-	Upper bound for active power import at the slack bus [pu]
Q_{slack}^{min}	-	Lower bound for reactive power import at the slack bus [pu]
Q_{slack}^{max}	-	Upper bound for reactive power import at the slack bus [pu]

Variables

V_{i}^{t}	-	Voltage magnitude at bus i and time t [pu]
δ_{i}^{t}	-	Voltage angle at bus i and time t [radians]
P_{i}^{t}	-	Active power injection to bus i at time t [pu]
Q_{i}^{t}	-	Reactive power injection to bus i at time t [pu]
P_{Gi}^{t}	-	Active power generation at bus i and time t [pu]
Q_{Gi}^{t}	-	Reactive power generation at bus i and time t [pu]
P_{PVi}^{t}	-	Active power PV inverter output at bus i and time t [pu]
Q_{PVi}^{t}	-	Reactive power PV inverter output at bus i and time t [pu]
$P_{curtail,i}^{t}$	-	Curtailed active solar power at bus i and time t [pu]

4.3 Single-objective optimization

4.3.1 Objective 1: Minimization of network active power losses

Active power losses in a power system are related to the flow of current in the power lines. If the PV power generation exceeds the load demand at a bus, PV active power can either be curtailed or be exported from the bus into the grid. Export of excess energy results in increased power flows and hence increased power loss. In addition, reactive power flows from reactive power compensation in the PV inverters results in increased active power losses.

To ensure stability in the power system, the total generation must equal to the total load in the system plus the total active power losses. Hence, the total active power losses at time t can be given by:

$$P^t_{loss} = \sum_{i=1}^{N} P^t_{Gi} - \sum_{i=1}^{N} P^t_{Li} \tag{4.1}$$

Objective 1 is to minimize the network active power losses, and is given by:

$$\text{Minimize} \quad F = \sum_{t=1}^{T} \left(\sum_{i=1}^{N} P^t_{Gi} - \sum_{i=1}^{N} P^t_{Li} \right) \tag{4.2}$$

4.3.2 Objective 2: Minimization of voltage deviations

Equation 2.3 relates the net load on a node to voltage change on a power line. The equation shows that if the PV power generation exceeds the load demand at a bus, the voltage magnitude at the current bus will increase. In this objective the aim is to minimize the change in voltage magnitude from 1 pu at all buses, and thus ensure a flat voltage profile. Because the change can be both negative and positive, the voltage change is squared. The sum of voltage change from 1 pu in the system at time t can be written as:

$$V^t_{dev} = \sum_{i=1}^{N} (1 - V^t_i)^2 \tag{4.3}$$

Objective 2 is to minimize voltage deviations from 1 pu at all buses, and is given by:

$$\text{Minimize} \quad F = \sum_{t=1}^{T}\left(\sum_{i=1}^{N}(1-V_i^t)^2\right) \tag{4.4}$$

4.3.3 Objective 3: Minimization of PV active power curtailment

PV active power is curtailed when the objective is to minimize active power losses or voltage deviation. In this objective the aim is to minimize the PV active power curtailment while keeping the voltage magnitude within the upper and lower bounds. The difference between the maximum available solar power generation, $P^t_{PVi,max}$ and the active power PV inverter output, P^t_{PVi}, is defined as the curtailed PV active power, $P^t_{curtail,i}$, at bus i and time t:

$$P^t_{curtail,i} = P^t_{PVi,max} - P^t_{PVi} \tag{4.5}$$

Minimizing the PV active power curtailment is the same as maximizing the PV active power in the system:

$$\text{Maximize} \quad F = \sum_{t=1}^{T}\left(\sum_{i=1}^{N}(P^t_{PVi})\right) \tag{4.6}$$

Further, maximizing the PV active power in the system is the same as minimizing its negative. We denote $P^t_{curtail}$ as:

$$P^t_{curtail} = \sum_{i=1}^{N}(-P^t_{PVi}) \tag{4.7}$$

Objective 3 is to minimize PV active power curtailment, and is given by:

$$\text{Minimize} \quad F = \sum_{t=1}^{T}\left(\sum_{i=1}^{N}(-P^t_{PVi})\right) \tag{4.8}$$

4.3.4 Objective 4: Minimization of overall active power losses

Both the network active power losses and the PV active power curtailment represent loss of energy in the power system. It is of interest to analyze how minimizing the sum of these losses will effect the active and reactive power inverter outputs. Objective 4 is to minimize the total active power losses and can be formulated as a sum of objective 1 and 3, with the objectives equally weighted. The total active power losses at time t can be written as:

$$P^t_{loss,overall} = \sum_{i=1}^{N} P^t_{Gi} - \sum_{i=1}^{N} P^t_{Li} + \sum_{i=1}^{N} (P^t_{PVi,max} - P^t_{PVi}) \tag{4.9}$$

As for objective 3, $P^t_{PVi,max}$ is extracted. $P^t_{loss,tot}$ is denoted as:

$$P^t_{loss,tot} = \sum_{i=1}^{N} P^t_{Gi} - \sum_{i=1}^{N} P^t_{Li} + \sum_{i=1}^{N} (-P^t_{PVi}) \tag{4.10}$$

Objective 4 is to minimize the total active power loss in the power system including network active power losses and PV active power curtailment:

$$\text{Minimize} \quad F = \sum_{t=1}^{T} \left(\sum_{i=1}^{N} P^t_{Gi} - \sum_{i=1}^{N} P^t_{Li} + \sum_{i=1}^{N} (-P^t_{PVi}) \right) \tag{4.11}$$

4.4 Multi-objective optimal power flow problem

4.4.1 Multi-objective optimization using the weighted sum method

A multi-objective optimization problem with the four objectives in Section 4.3 can be converted into a single-objective optimization problem by using the weighted-sum approach (Section 3.2.1). The four objectives can be summed if they are scaled such that they are of similar magnitude. One way to scale the objectives is to divide each objective by an adequate scaling factor s, and common practice is to use the maximum of each objective as the scale factor. The multi-objective optimization problem can be written

as the following using the weighted-sum approach, where w_i are weights:

$$\text{Minimize} \quad F = \sum_{t=1}^{T} w_1 J_1^t + w_2 J_2^t + w_3 J_3^t + w_4 J_4^t \tag{4.12}$$

$$J_1^t = \frac{P_{loss}^t}{s_1} \tag{4.13}$$

$$J_2^t = \frac{V_{dev}^t}{s_2} \tag{4.14}$$

$$J_3^t = \frac{P_{curtail}^t}{s_3} \tag{4.15}$$

$$J_4^t = \frac{P_{loss,tot}^t}{s_4} \tag{4.16}$$

In [7], the weighted-sum approach is used to find a solution to the formulated multi-objective optimization problem in the paper, and the scaling factors are chosen to be the maxima of each objective.

4.5 Restrictions

The objective functions are optimized with respect to some constrained variables. This optimal power flow optimization problems include equality constraints and inequality constrains related to power flow studies and power network limitations, as well as for the PV inverter outputs.

4.5.1 Restrictions related to power flow studies and power network limitations

Equality constraints

The real and reactive power flow equations (Equation 3.4 and 3.5) represent equality constraints in the optimization problem. The injected power to a certain bus is given by the difference in power generation and load demand at that bus. Thus, the restrictions for active- and reactive power injections can be written as:

$$P_{Gi}^t - P_{Li}^t = \sum_{j=1}^{N} |V_i^t||V_j^t||Y_{ij}|cos\left(\theta_{ij} - \delta_i^t + \delta_j^t\right) \tag{4.17}$$

$$Q_{Gi}^t - Q_{Li}^t = -\sum_{j=1}^{N} |V_i^t||V_j^t||Y_{ij}|sin\left(\theta_{ij} - \delta_i^t + \delta_j^t\right) \tag{4.18}$$

It is common practice to model the slack bus with a constant voltage magnitude of 1.0 pu and a phase angle of 0 radians. Thus,

$$V_{slackbus}^t = 1 \tag{4.19}$$

$$\delta_{slackbus}^t = 0 \tag{4.20}$$

The PV inverter outputs are added to all buses with PV power generation by setting the generation at the bus equal to the PV inverter outputs:

$$P_{G,pvbus}^t = P_{PV,pvbus}^t \tag{4.21}$$

$$Q_{G,pvbus}^t = Q_{PV,pvbus}^t \tag{4.22}$$

The generation at the bus bars connecting the transformer feeder lines to the end-user branches are set to zero:

$$P_{G,notgeneratorandpvbus}^t = 0 \tag{4.23}$$

$$Q_{G,notgeneratorandpvbus}^t = 0 \tag{4.24}$$

Inequality constraints

The voltage magnitude and phase angle at each bus are limited by upper and lower bounds.

$$V^{min} \leq V_i^t \leq V^{max} \tag{4.25}$$

$$\delta^{min} \leq \delta_i^t \leq \delta^{max} \tag{4.26}$$

The limit on power that can be drawn from the upstream power network (or exported to the upstream power network) is given in the following. Note that it is assumed that the upper and lower limits on import/ export are not limiting the flow of excess power caused by PV power generation in the simulations.

$$P_{slackbus}^{min} \leq P_{G,slackbus}^t \leq P_{slackbus}^{max} \tag{4.27}$$

$$Q^{min}_{slackbus} \leq Q^{t}_{G,slackbus} \leq Q^{max}_{slackbus} \tag{4.28}$$

4.5.2 Restrictions related to controllable PV inverters

The PV inverters are modelled by inequality constraints representing the capability limits of the PV inverters. The active power PV inverter output at bus i and time t is limited by the inequality constraint:

$$0 \leq P^{t}_{PVi} \leq P^{t}_{PVi,max} \tag{4.29}$$

The reactive power PV inverter output at bus i and time t is limited by the active power PV inverter output and the minimal power factor PF_{min} of the inverter (Equation 2.19). It is assumed that the inverter is overrated and that the operating range is given by Figure 2.4c.

$$Q^{t}_{PVi,max} = P^{t}_{PVi} \times tan(cos^{-1}(PF_{min})) \tag{4.30}$$

$$-Q^{t}_{PVi,max} \leq Q^{t}_{PVi} \leq Q^{t}_{PVi,max} \tag{4.31}$$

In the simulations without reactive power control (in the only APC control), the reactive power inverter outputs are set to zero:

$$Q^{t}_{PVi} = 0 \tag{4.32}$$

4.6 Model formulation

The full model formulation, including the objective and constraints introduced in the previous sections, is given below.

$$\text{Min} \quad \sum_{t=1}^{T}\left[\frac{w_1}{s_1}\Big(\sum_{i=1}^{N}P_{Gi}^t-\sum_{i=1}^{N}P_{Li}^t\Big)+\frac{w_2}{s_2}\Big(\sum_{i=1}^{N}(1-V_i^t)^2\Big)+\frac{w_3}{s_3}\Big(\sum_{i=1}^{N}(-P_{PVi}^t)\Big)+\frac{w_4}{s_4}\Big(\sum_{i=1}^{N}P_{Gi}^t-\sum_{i=1}^{N}P_{Li}^t+\sum_{i=1}^{N}(-P_{PVi}^t)\Big)\right]$$

$$\begin{aligned}
\text{subject to} \quad P_{Gi}^t-P_{Li}^t &= \sum_{j=1}^{N}|V_i^t||V_j^t||Y_{ij}|cos\big(\theta_{ij}-\delta_i^t+\delta_j^t\big)\\
Q_{Gi}^t-Q_{Li}^t &= -\sum_{j=1}^{N}|V_i^t||V_j^t||Y_{ij}|sin\big(\theta_{ij}-\delta_i^t+\delta_j^t\big)\\
V_{slackbus}^t &= 1\\
\delta_{slackbus}^t &= 0\\
V_i^t &\geq V^{min}\\
V_i^t &\leq V^{max}\\
\delta_i^t &\geq \delta^{min}\\
\delta_i^t &\leq \delta^{max}\\
P_{G,slackbus}^t &\geq P_{slackbus}^{min}\\
P_{G,slackbus}^t &\leq P_{slackbus}^{max}\\
Q_{G,slackbus}^t &\geq Q_{slackbus}^{min}\\
Q_{G,slackbus}^t &\leq Q_{slackbus}^{max}\\
P_{G,pvbus}^t &= P_{PV,pvbus}^t\\
Q_{G,pvbus}^t &= Q_{PV,pvbus}^t\\
P_{G,notgeneratorandpvbus}^t &= 0\\
Q_{G,notgeneratorandpvbus}^t &= 0\\
P_{PV,pvbus}^t &\geq 0\\
P_{PV,pvbus}^t &\leq P_{PV,pvbus,max}^t\\
Q_{PV,pvbus}^t &\geq -P_{PV,pvbus}^t \times tan(cos^{-1}(PF_{min}))\\
Q_{PV,pvbus}^t &\leq P_{PV,pvbus}^t \times tan(cos^{-1}(PF_{min}))
\end{aligned}$$

5 | Computer implementation

The optimal power flow problem presented in Section 4.6 is solved using The General Algebraic Modeling System (GAMS). The results obtained from running the optimal power flows in GAMS are compared to power flow analysis of the same system performed in MATPOWER. The time resolution of the model is 1 hour for the reason that it was the sampling rate of the smart meters from which the power use data originated.

5.1 Modelling in MATPOWER

MATPOWER is a package of MATLAB M-files for solving steady-state power flow and optimal power flow problems [27]. A power flow is executed in MATPOWER by calling the *runpf* function. The *runpf* function takes in a single MATPOWER case struct (mpc) file as input, containing the necessary information for all nodes in the network for a given point in time, such as bus type and corresponding known information. The voltages and power flows in the network can be calculated by running a load flow solution for every point in the grid with known power consumption values.

In this thesis, MATPOWER is used to perform load flow analysis of the power system to see the effect of different amounts of PV power generation on a system without inverter control. The system without control is referred to as a passive system.

5.2 Modelling in GAMS

General Algebraic Modeling System is a modeling system for mathematical programming and optimization, and the system is specifically designed for modeling linear, nonlinear and mixed integer optimiza-

tion problems. GAMS is found to be an attractive tool because it enables the user to formulate optimization models in a notation similar to their algebraic notation and it has a powerful language, but is yet easy to learn [28]. Some relevant advantages using GAMS are listed below. The list is based on the list of advantages in reference [29].

- The model formulation is independent of the model data. This allows us to run the problem formulation written for the three bus system on the larger system without changing the model formulation.
- The model formulation is independent of the chosen solver. Hence, you can try different solvers without changing the model formulation.
- The output of GAMS is easy to read and use, and can be easily transferred to other programs by GDX (GAMS Data Exchange) files. In this project, large input data is read from and output data is written to Excel.

In this thesis, the optimal power flow presented in Section 4.6 is written and solved using GAMS. Some of the equations in the problem have nonlinear relationships requiring nonlinear programming to solve the optimization problem. The results from the optimization are presented in the form of plots and graphs using Matlab.

6 | Case study description

A distribution power network in Steinkjer, Norway is the basis of this study. The grid and load data have been modified into standard MATPOWER format for conventional load flow analysis in MATPOWER. The modified grid and load data was provided by Lillebø [13]. The solar generation data was simulated using *Renewables.ninja* [30] in my project thesis spring 2018 [14].

6.1 Description of the distribution network

A single line diagram of the distribution power network in Steinkjer can be seen in Figure 6.1. The grid consists of the following main parts:

- 500 kVA distribution transformer.
- 20 distribution feeder lines, A1-M2, branching out from the transformer.
- 54 end-user buses

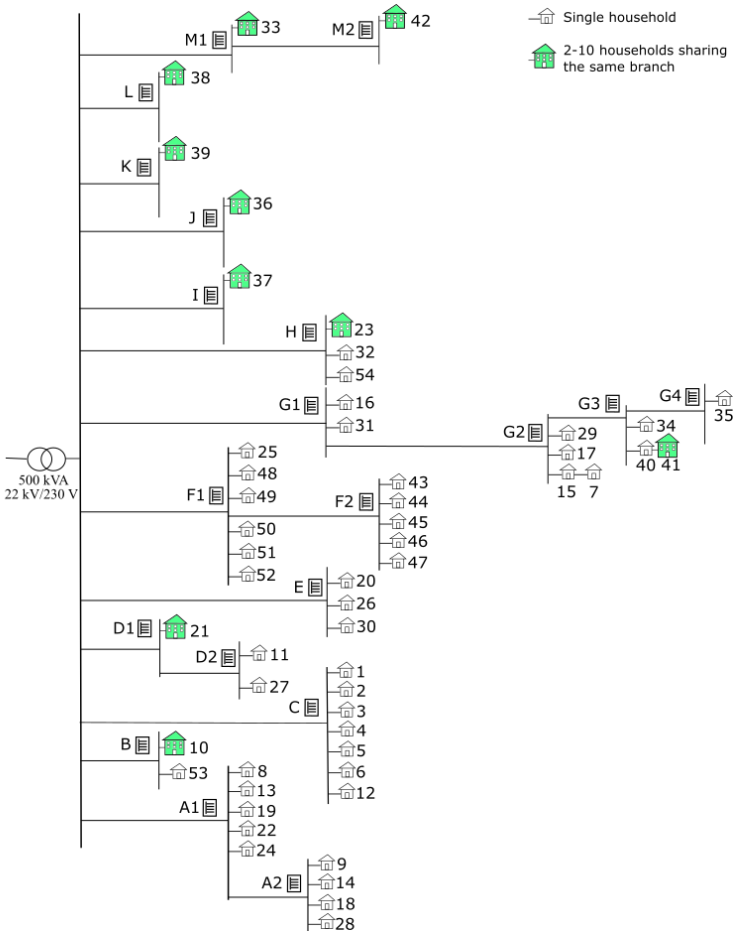

Figure 6.1: The distribution grid in Steinkjer with its 54 consumer nodes. Larger loads sharing the same connection line, such as row houses or apartment blocks, have been aggregated into single loads and are marked with a larger, colorized symbol. Figure from [13].

Larger loads sharing the same connection line, such as row houses or apartment blocks, have been aggregated into single loads. These are referred to as "shared nodes". As a result, the total end-users have been reduced from 95 in the original data set to 54 after the aggregation. In Figure 6.1, the larger nodes are marked with a larger, colorized symbol. As a consequence of the aggregation, the power demands at the aggregated buses are high compared to the rest of the loads. The buses are classified by type of load in Table 6.1.

Table 6.1: Classification of the 54 load buses in the distribution grid.

Type of load	Bus number
Single household	[1-9], [11-20], 22, [24-31], 34, 35, 40, [43-52], 54
Households sharing the same branch	21, 23, 33, [36-39], 41, 42
Eldery care home	10
Grocery store	32
School	53

6.1.1 Load data

Hourly active power measurements for the year 2012 was provided for all end-users in the system by the DSO [13]. The reactive power loads have been calculated based on the DSO´s assumed power factor of 0.98 lagging. Note that 2012 is a leap year, thus the number of hours in the year is 8784 hours.

$$Q_L = P_L \times tan(cos^{-1}(0.98)) \tag{6.1}$$

The load data was converted into per unit values by dividing by the apparent power base, S_{base}, for optimal power flow studies in GAMS. The apparent power base is set to 25 MVA for this case study.

6.1.2 Grid parameters

The line impedances have been converted to per unit values to be able to run the power flow in MATPOWER and in GAMS. The per unit values was calculated with V_{base} equal to 230 V and S_{base} equal to 25 MVA. The line impedance can be converted to per unit values dividing by Z_{base}, given by:

$$Z_{base} = \frac{V_{base}^2}{S_{base}} \tag{6.2}$$

R/X ratio and length of the power lines

The R/X ratio of the power lines impacts the effectiveness of voltage control as explained in Section 2.1.3. Table 6.2 gives the R/X ratio and length of the 20 distribution feeder lines. The lengths and R/X ratios for

the rest of the lines are given in Table 6.3. The R/X ratios of the grid are high and hence the grid is more susceptible to voltage change from active power than reactive power.

Table 6.2: R/X ratio and length for the 20 distribution feeder lines.

	R/X ratio	Length [m]
Average	3.52	79.25
Median	2.86	57.50
Maximum	8.11	249.00
Minimum	1.74	15.00

Table 6.3: R/X ratio and length for the rest of the lines.

	R/X ratio	Length [m]
Average	12.08	22.13
Median	8.11	12.00
Maximum	71.25	98.00
Minimum	2.86	1.00

Nodal admittance matrix

The nodal admittance matrix, Y_{bus}, of the network is an input parameter to the GAMS simulation model. Y_{bus} of the network was calculated using the *makeYbus* function in MATPOWER. The admittance matrix can be divided into Y_m and Y_{ang}, holding the magnitude and phase of each element of Y_{bus}, respectively.

6.1.3 Classification of buses for load flow studies

The upstream power network is modelled as an infinite bus connected to the main feeder. The infinite bus acts like a slack bus, thus balance the active and reactive power in the system while performing power flow studies in GAMS and MATPOWER. The slack bus is modelled with a constant voltage magnitude of 1 pu and voltage angle of 0 radians. The transformer is modelled as a cable based on the transformer impedance and MVA rating, connected in series between the slack bus and the main feeder [13]. The R/X ratio of this line is 0.181. All end-users are modelled as load buses with their respective active and reactive powers. The net load, given by the consumption minus the PV power generation, is assigned to the load

buses for MATPOWER simulations with PV power generation. The bus bars connecting the transformer feeder lines to the end-user branches are modelled as load buses with zero active and reactive loads. In Figure 6.1, these bus bars are denoted with letters A1-M2.

6.2 Solar PV generation data

Hourly PV power generation profiles for each end-user have been generated using simulated PV power generation data simulated using *Renewables.ninja* [14]. The simulated PV power generation data is for a capacity of 1 kWp in Trondheim for the year 2014. The final PV power generation for each end-user with PV is calculated by multiplying the installed capacity of the PV panel for each end-user by the hourly simulated generation for 1 kWp. As the load data provided is for a leap year (2012), an additional day had to be added to the PV generation data. The PV generation at the additional day, 29. February, is chosen to be equal to the PV generation at 28. February.

The PV penetration is assumed to be 100% (all end-users have PV) in this case study and two scenarios for PV installed capacities have been formulated. The PV installed capacity for each end-user is calculated based on its annual consumption. For PV scenario 50%, the PV capacity is found such that the annual PV generation of each end-user is equal to 50% of the annual load for the end-user. The annual PV generation is equal to 100% of the annual load in PV scenario 100%. The PV capacities are rounded down to the nearest whole number for both scenarios. Note that bus 43 have no PV capacity installed due to a low annual consumption of 413.90 kWh/year. The PV installed capacity was rounded down to zero.

6.2.1 Installed solar PV capacities

The median and average installed capacities for the end-users can be seen in Table 6.4. The installed capacities of PV for households in NTEs grid varies from 2.1 kWp to 75 kWp, with an average of 10 kWp [31]. Hence, the calculated capacities are of reasonable magnitude. The average annual load for the 54 consumers is 27 016 kWh/year and the annual total load is 1 459 MWh/year. Thus, the annual PV generation is approximately 50% and 100% of the annual load for the 54 consumers in the two scenarios.

Table 6.4: PV installed capacities and annual PV generation for PV scenarios 50% and 100%.

	PV scenario 50%	PV scenario 100%
Median PV capacity	10 kWp	20 kWp
Average PV capacity	15 kWp	31 kWp
Total installed PV capacity	832 kWp	1688 kWp
Average annual PV active power generation	13 135 kWh	26 648 kWh
Annual total PV active power generation	709 MWh	1 439 MWh

6.3 Time period of analysis

The time period of analysis is chosen to be the day of the year with the highest PV power generation [kWh/day]. The day of highest PV generation is chosen because this day will have most hours with high voltages caused by high amounts of PV generation. This day is found to be 27. of May. The generation and peak power for 1 kWp on 27. May are 6.718 kWh and 0.741 kW, respectively. To avoid confusion it must be noted that 5. of May is the day of the year with highest peak generation. The generation on 5. of May can be seen as the highest peak to the left in Figure 6.2. The generation and peak power for 1 kWp on 5. May are 6.455 kWh and 0.755 kW, respectively. The total PV generation for the two scenarios 50% and 100% as well as the total load in May can be seen in Figure 6.2. The total PV generation and total load on 27. of May is plotted in Figure 6.3. On 27. of May the total load is 2 227 kWh/day, and the generation is 5 589 kWh/day and 11 340 kWh/day for PV scenarios 50% and 100%, respectively. Thus, the PV power generation is approximately 2.5 and 5 times the total load in the PV scenarios.

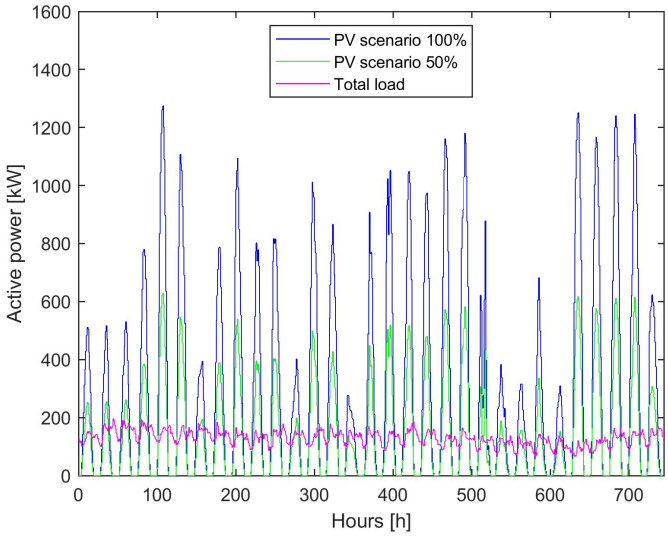

Figure 6.2: Total PV active power generation and load in May. The maximum peak occur on 5. May (highest peak to the left in the figure) and the maximum PV generation occur on 27. May.

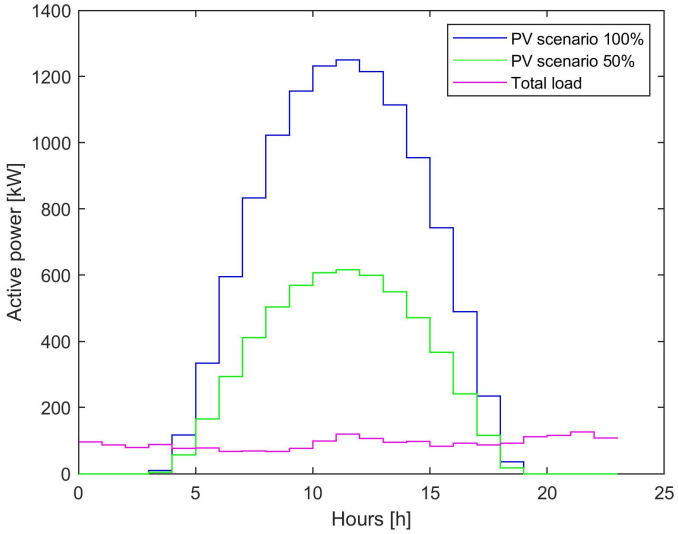

Figure 6.3: Total PV active power generation and load on 27. May, the day of maximum PV active power generation.

7 | Results

In this chapter results from power flow studies and optimal power studies of the distribution network are presented. The power flow studies are preformed in MATPOWER, while the optimal power flow studies are preformed in GAMS. The simulations are carried out on the distribution network presented in Section 6.1 with respective grid and load data, and PV generation data presented in Section 6.2. The equations and constraints are as described in Chapter 4. Table 7.1a presents the parameter values relevant for the system and simulation model.

Table 7.1: Parameter values used for the simulations in GAMS. (a) Input data. (b) Lower and upper limits.

(a)

Parameter	Value
$\|Y_{ij}\|$	Input data
θ_{ij}	Input data
P^t_{Li}	Input data
Q^t_{Li}	Input data
$P^t_{PVi,max}$	Input data

(b)

Parameter	Value
V^{min}	0.95 pu
V^{max}	1.05 pu
δ^{min}	-3.14 rad
δ^{max}	3.14 rad
PF_{min}	0.8
$P^{min}_{slackbus}$	Not binding
$P^{max}_{slackbus}$	Not binding
$Q^{min}_{slackbus}$	Not binding
$Q^{max}_{slackbus}$	Not binding

Section 7.1, *Passive system*, presents results from power flow simulations without solar PV generation and for PV scenarios 50% and 100%. All presented results are for 27. of May, the day of maximum solar PV generation.

In Section 7.2, *Single objective optimization*, results from optimal power flow studies of the distribution network with different objectives are presented. The objectives in Section 4.3 are optimized one by one. First, results for each objective are presented. Second, results from simulations for only active power curtailment and for both reactive power control and active power curtailment are presented and compared. The results are presented for 27. of May in Section 7.2.5 and for a year in Section 7.2.6.

In Section 7.3, *Comparison of the single-objective optimizations*, the main findings from the single-objective optimization results are gathered and compared. This includes results for maximum voltage magnitudes, network active power losses and PV active power curtailment. The operating power factor for the PV inverter at the most critical node is presented for the different objectives in Section 7.3.2. The locations for PV inverter control are identified in Section 7.3.3 and the load ratios for the distribution network cables are presented in Section 7.3.4.

In Section 7.4, *Sensitivity*, results for dual value calculations for the restriction on maximum voltage magnitude at the most critical node are presented for objective 4 and PV scenario 100%. In this case, the dual value represent the change in the objective function if the upper voltage bound is increased by one percentage point, i.e. from 1.05 to 1.06 pu. The results are presented for 27. of May and for a year with only active power curtailment and for both reactive power control and curtailment.

Finally, in Section 7.5, *Multi-objective optimization*, results from multi-objective simulations of objectives 2 and 4 are presented for 27. of May and PV scenario 100%. The PV inverter control strategy includes both reactive power control and active power curtailment.

For each simulation, the network active power losses, maximum voltage magnitude, curtailed PV power generation and total active power losses (network active power losses + curtailed PV power generation) are presented in tables. These values are relevant for evaluation of the distribution network performance. In addition, they represent each of the four objectives to be minimized: (i) network active power losses, (ii) voltage deviations, (iii) PV active power curtailment, and (iv) overall active power losses (network + curtailment). "Total PV generation/ Total active load" denotes the fraction between total PV power generation and total active load in the time period analyzed. If this fraction is more than 100%, excess energy is exported to the upstream network. "Total PV generation/ Total maximum PV generation" denotes the fraction between PV power generation in the distribution network and the maximum available PV power generation in the time period analyzed. This fraction is less than 100% when PV power generation is curtailed.

7.1 Passive system

Power flow studies were preformed for the distribution network in MATPOWER in order to see the present status of the power network and to see the potential impacts from high amounts of solar PV power generation. Results for no PV and PV scenarios 50% and 100% are obtained for 27. of May. The power factor of the PV inverters are set to unity, i.e. PF=1.

Figures 7.1a and 7.1b show the network power losses and the power import at the slack bus without PV on 27. of May. Similar results for PV scenarios 50% and 100% are presented in Figures 7.2 and 7.3, respectively. The network power loss and power export increase as the PV power generation increase.

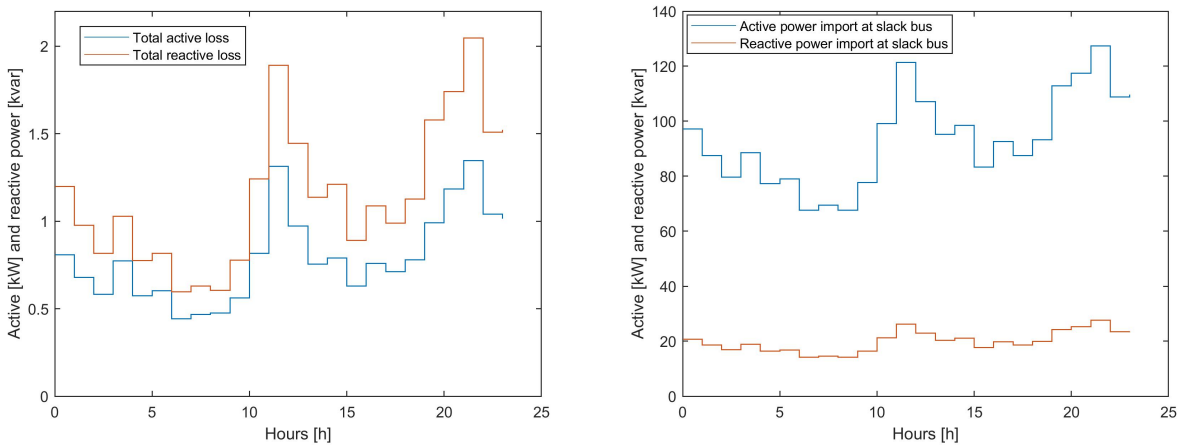

(a) **(b)**

Figure 7.1: Passive system without PV generation on 27. of May. (a) Total network active and reactive power losses. (b) Power import at the slack bus.

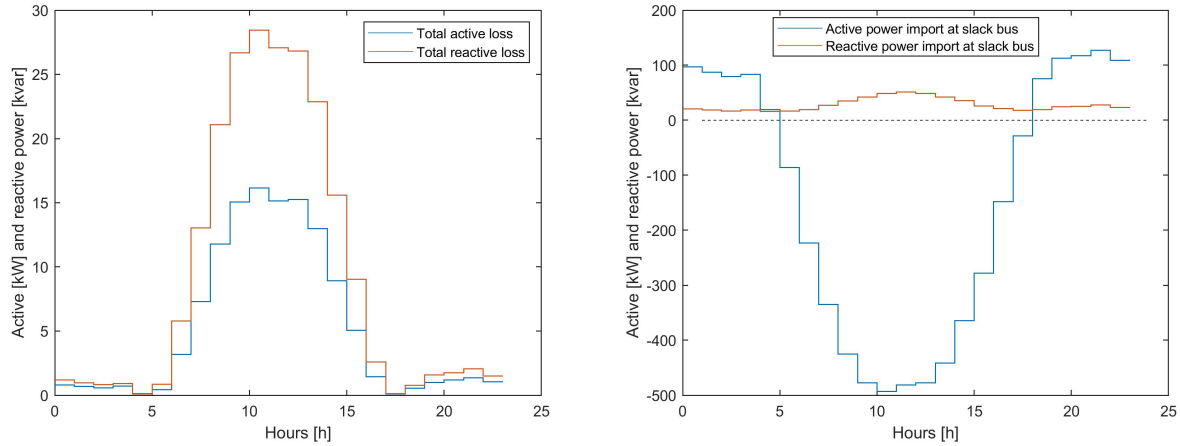

(a) **(b)**

Figure 7.2: Passive system with PV scenario 50% on 27. of May. (a) Total network active and reactive power losses. (b) Power import at the slack bus.

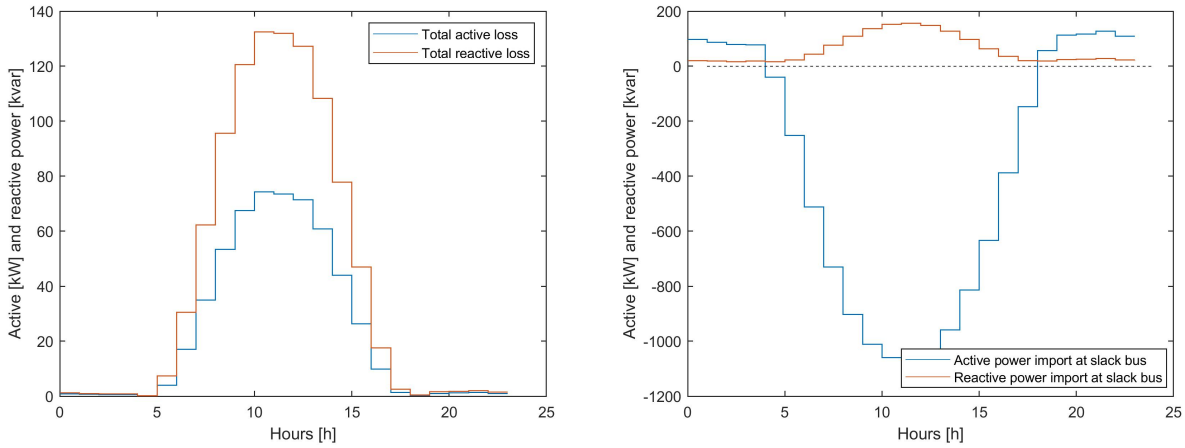

(a) **(b)**

Figure 7.3: Passive system with PV scenario 100% on 27. of May. (a) Total network active and reactive power losses. (b) Power import at the slack bus.

Table 7.2 presents the total PV generation relative to the total active power load, the maximum voltage magnitude and the total network active power loss on 27. of May for each PV scenario. The PV generation is 2.5 and 5 times the load for PV scenario 50% and 100%, respectively. Hence, the distribution network will have high reverse power flows and high export of power to the upstream network. Another consequence is increased voltage magnitudes. The maximum voltage bound of 1.05 pu is exceeded for both PV scenarios 50% and 100%. Bus 32 has the highest voltage magnitude in the system with a voltage magnitude of 1.0541 pu in PV scenario 50% and 1.1138 pu in PV scenario 100%. Note that bus 32 is a

grocery store with a high consumption and consequently high solar PV generation. The relative increase in network active power losses is 538% compared to the case without PV generation for PV scenario 50%. For PV scenario 100%, the relative increase in network power loss is 2 768%. Thus, the high amounts of PV generation increase the network active power loss significantly due to increased line power flows.

Table 7.2: Results for the passive system, i.e. the system without PV inverter control, on 27. of May.

	Without PV	PV scenario 50%	PV scenario 100%
Total PV generation/ Total active load	0%	251%	509%
Maximum voltage magnitude	1.0000 pu	1.0541 pu	1.1138 pu
Network active power loss	19.08 kWh	121.80 kWh	547.24 kWh

The maximum voltage bound of 1.05 is exceeded at 6 buses (bus 23, 32, 40, 41, 54 and 68) on 27. of May for PV scenario 50%. In PV scenario 100%, the voltage magnitudes exceed 1.05 pu at 30 buses and 1.10 pu at 6 buses. This can be seen in Figure 7.4 where the voltage magnitudes at all 76 buses are presented at 11:00, the time of maximum voltage, on 27. of May for all PV scenarios.

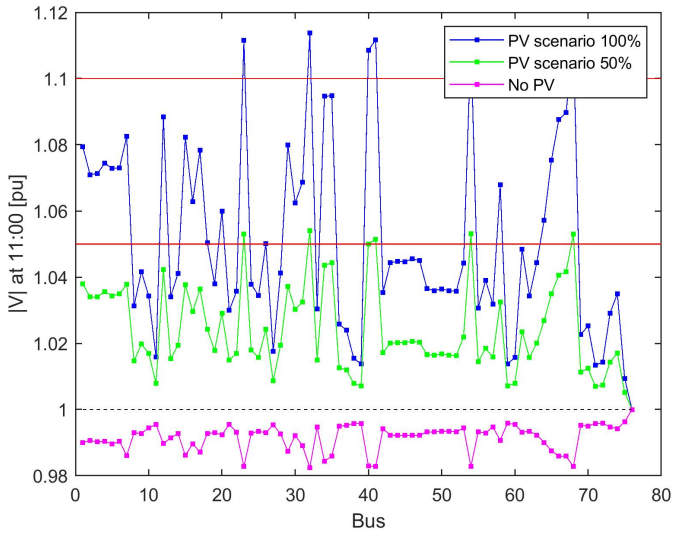

Figure 7.4: Voltage magnitude at all buses for no PV, PV scenario 50% and 100% at 11:00 on 27. of May.

Figure 7.5 shows how the voltage magnitude changes along the lines from bus 76 (slack bus) to bus 35 at 11:00 on 27. of May. The line connecting buses 76 and 75 is "the transformer line", the lines from bus 75 to bus 67 are distribution feeder lines, and the final line connects bus 67 to consumer node 35. The lines connecting bus 75 to bus 35 together comprise 373 m, which is the longest line in the distribution

network. For no PV, the voltage decreases as one move away from the slack bus. For PV scenarios 50% and 100%, the voltage increases towards the end bus (consumer node 35) as a results of reverse power flows.

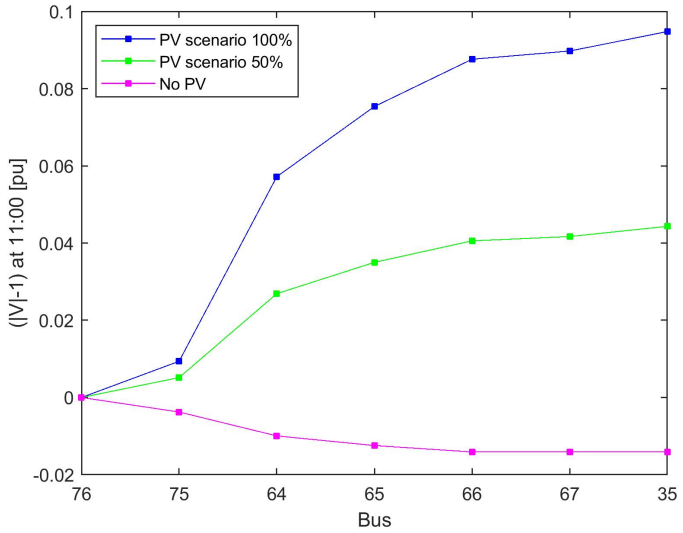

Figure 7.5: Voltage change on lines from bus 76 (slack bus) to bus 35 at 11.00 on 27. of May. Note that the line between buses 76 and 75 is the "transformer line" and buses 64-67 are named G1-G4 in Figure 6.1.

The simulations are preformed with the assumption that the slack bus is considered as the reference for voltage magnitude. Tap-changing transformers in the distribution grid can be utilized to regulate the output voltage such that the bus voltage is larger than 1.00 pu [32]. In a load based distribution network it is beneficial to have a higher voltage than 1.00 pu, for example 1.02 pu, to avoid undervoltage situations. Higher voltage magnitudes are also favorable because the power losses are lower compared to for lower voltage magnitudes (Section 2.2.2). If the voltage at the reference bus in the simulations was set to 1.02 pu, overvoltages would occur for smaller amounts of PV power generation.

The highest voltage magnitude occurs at bus 32, the grocery store. The hourly voltage profiles at bus 32 for no PV, PV scenario 50% and 100% are given in Figure 7.6 for 27. of May. The voltage magnitude increases in the same pattern as the PV generation increases. The figure shows that the upper voltage limit of 1.05 pu is exceeded for a significant number of hours in PV scenario 100%.

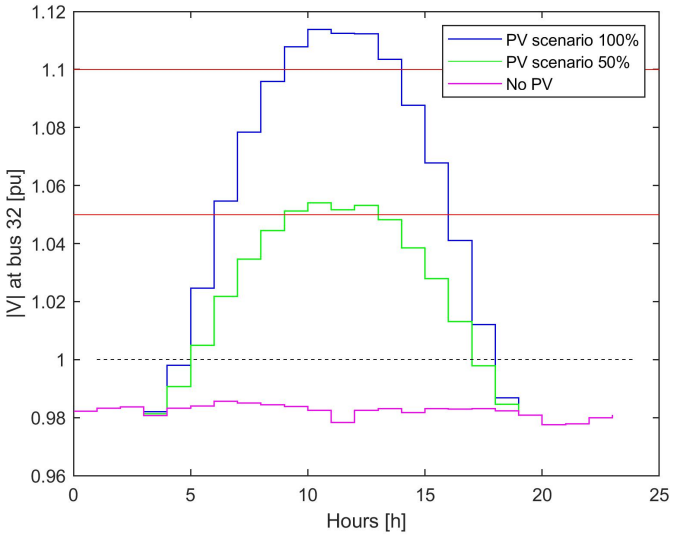

Figure 7.6: Voltage magnitude at bus 32 for no PV, PV scenario 50% and PV scenario 100% on 27. of May.

7.1.1 Effect of constant PV inverter power factor

Table 7.3 and Table 7.4 present the total network active power loss and maximum voltage magnitude for different constant leading power factors (absorbing reactive power) on 27. of May for PV scenarios 50% and 100%, respectively. The results show that lowering the power factor results in increased network active power losses and a lower value for the maximum voltage magnitude. For PV scenario 100%, a power factor of 0.9 is required not to exceed the upper voltage bound of 1.05 pu. A power factor of 0.95 is sufficient for PV scenario 50%.

Table 7.3: Total network active power losses and maximum voltage magnitude for different PV inverter power factors for PV scenario 50% on 27. of May.

PF	Network active active loss	$\|V\|_{max}$
0.90	179.55 kWh	1.0150 pu
0.95	150.93 kWh	1.0276 pu
1.00	121.80 kWh	1.0541 pu

Table 7.4: Total network active power losses and maximum voltage magnitude for different PV inverter power factors for PV scenario 100% on 27. of May.

PF	Network active power loss	$\|V\|_{max}$
0.90	810.39 kWh	1.0328 pu
0.95	680.64 kWh	1.0605 pu
1.00	547.24 kWh	1.1138 pu

7.2 Single objective optimization

Optimal power flow studies were preformed for the distribution grid in GAMS optimizing each objective in Section 4.3 one by one. Numerical results are presented for PV scenario 50% and 100%, while graphs are only presented for PV scenario 50% in this section. The results for PV scenario 100% are similar to the results for PV scenario 50% and can be found in Appendix A. These results are presented for 27. of May. Simulations for only active power curtailment and for both reactive control and active power curtailment are presented and compared for PV scenario 100% for 27. of May and for a year.

7.2.1 Objective 1: Minimization of network active power losses

Objective 1 is to minimize the network active power losses. The network active power losses can be reduced by reducing the line power flows (Equation 2.7). Thus, minimization of objective 1 results in high curtailment of PV power generation in order to reduce the reverse power flows. PV power generation is curtailed and the inverter power factors are adjusted such that net generation minus load equals to zero at each bus in hours of significant PV power generation. Results from minimization of objective 1 are presented in Table 7.5. Note that the network active power losses are lowered by approximately 10 kWh for both PV scenarios compared to the results for no PV on 27. of May.

Table 7.5: Results from minimization of objective 1 on 27. of May.

	PV scenario 50%	PV scenario 100%
Network active power loss	8.99 kWh	8.61 kWh
Total active power loss (network and curtailment)	4 382.63 kWh	10 089.59 kWh
Maximum voltage magnitude	1.00 pu	1.00 pu
Total PV generation/ Total active load	55%	57%
Total PV generation/ Total maximum PV generation	22%	11%

Figures 7.7a and 7.7b show the network active power loss and the power import at the slack bus. The network active power loss and power import at the slack bus are close to zero in hours of PV power generation. This is because the PV inverters adjust the active and reactive power outputs such that the net load at each bus is close to zero.

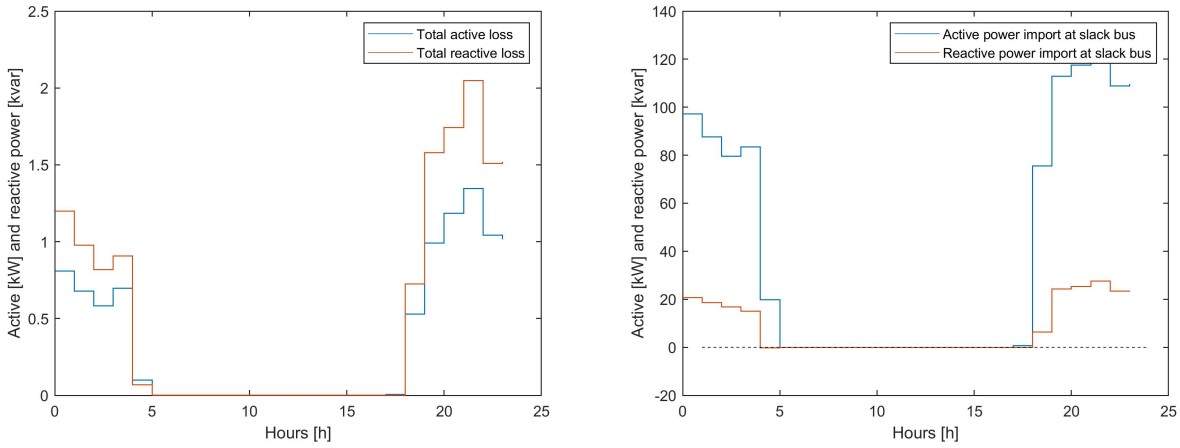

(a) **(b)**

Figure 7.7: Objective 1, PV scenario 50% on 27. of May. (a) Total network active and reactive power losses. (b) Power import at the slack bus.

The total active power load and total PV active power generation are presented in Figure 7.8a. The total active power generation is equal to the total active load in the system in the hours of PV generation. Figure 7.8b shows the PV active power in the system (red area) and curtailed PV active power (blue area). In PV scenario 50%, 78% is the potential PV power generation is lost as a result of PV active power curtailment.

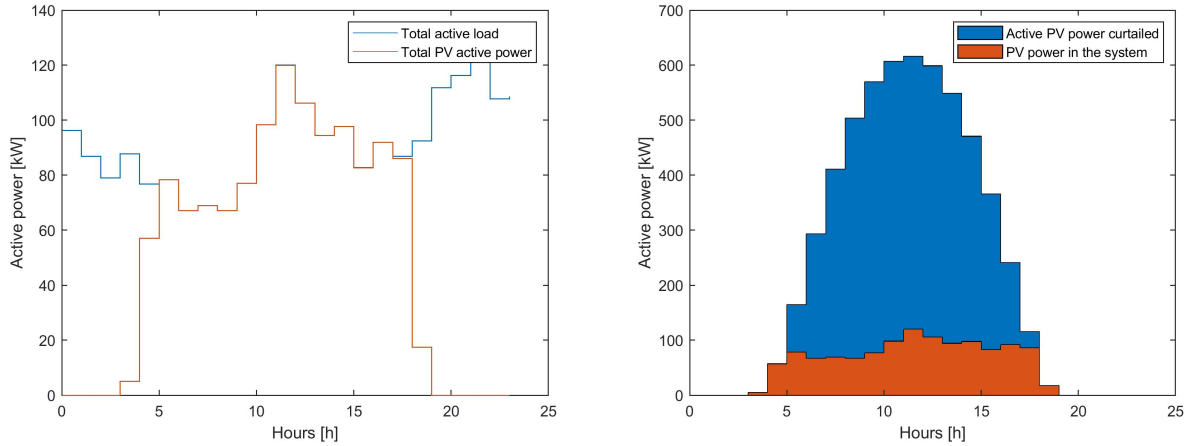

(a) **(b)**

Figure 7.8: Objective 1, PV scenario 50% on 27. of May. (a) Total active power load and total PV generation. (b) Curtailed PV active power and PV active power in the system. The blue area represents the lost energy due to curtailment.

In Figure 7.9, the values of objectives 1, 2, 3 and 4 are plotted when objective 1 is minimized. The absolute values of objectives 1 and 2 are low compared to the values of objectives 3 and 4. The value of objectives 1 and 2 are close to zero in hours of PV generation when the net load at buses with PV generation are zero. The values of objectives 3 and 4 are about the same because the active power losses are very low.

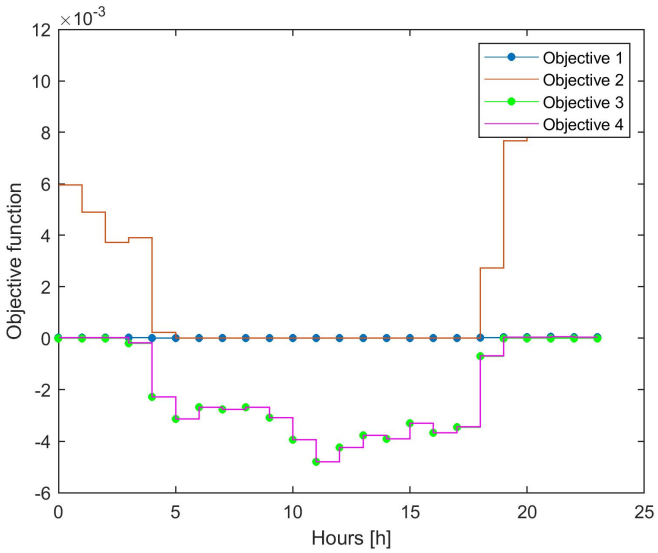

Figure 7.9: Value of objectives 1, 2, 3 and 4 on 27. of May for PV scenario 50%. The plotted values of the objectives are calculated based on per unit values of voltages and powers. Objective 1 is minimized.

7.2.2 Objective 2: Minimization of voltage deviations

Objective 2 is to minimize the voltage deviation from 1 pu at all buses in the system. The voltage magnitude increases when the generation at a bus exceeds the load. As for objective 1, PV active power is curtailed and the PV inverter power factors are adjusted such that the net active and reactive load at each bus reaches zero in hours of PV generation. Results from minimization of objective 2 are given in Table 7.6. The network active power losses are lowered by approximately 10 kWh for both PV scenarios compared to results for no PV.

Table 7.6: Results from minimization of objective 2 on 27. of May.

	PV scenario 50%	PV scenario 100%
Network active power loss	9.19 kWh	8.74 kWh
Total active power loss (network and curtailment)	4 406.39 kWh	10 089.69 kWh
Maximum voltage magnitude	1.001 pu	1.000 pu
Total PV generation/ Total active load	54%	57%
Total PV generation/ Total maximum PV generation	21%	11%

Figure 7.10a and 7.10b show the network power losses and the power import at the slack bus, respectively. The figures show similar results as for objective 1. Voltage deviations from 1 pu are minimized by adjusting the PV inverter active and reactive power outputs such that the net load at each bus is zero. Hence, the power losses and import at the slack bus are close to zero in the hours of PV power generation and the total active load is equal to the total PV power generation.

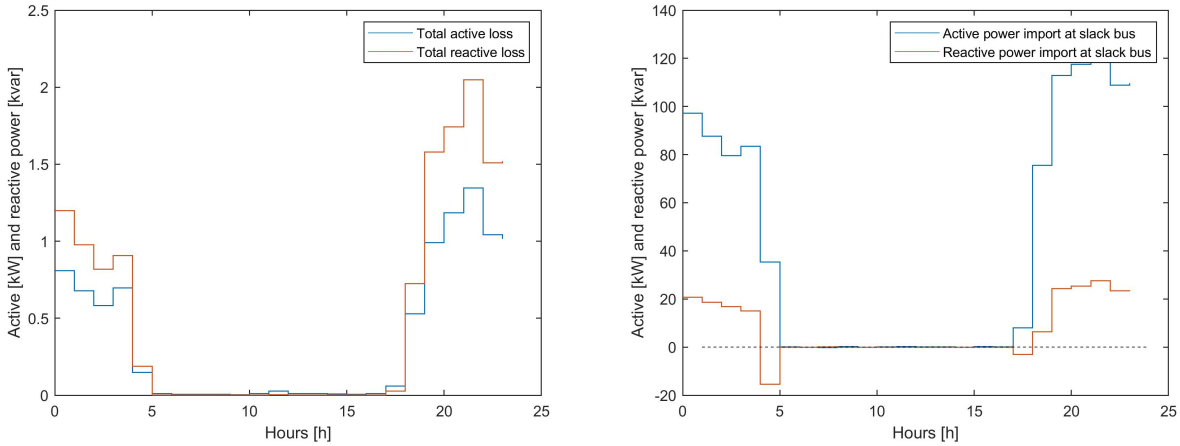

(a) **(b)**

Figure 7.10: Objective 2, PV scenario 50% on 27. of May. (a) Total network active and reactive power losses. (b) Power import at the slack bus.

Figure 7.11a shows the total active power load and total PV active power generation on 27. of May. Figure 7.11b gives the PV active power in the system (red area) and curtailed PV active power (blue area). 79% of the PV active power is lost when objective 2 is minimized.

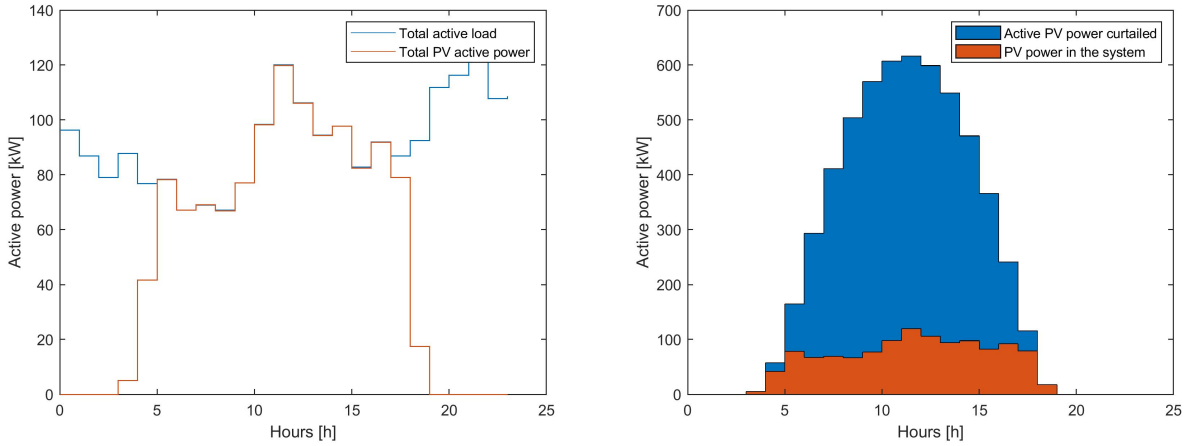

(a) **(b)**

Figure 7.11: Objective 2, PV scenario 50% on 27. of May. (a) Total active power load and total PV generation. (b) Curtailed PV active power and PV active power in the system. The blue area represents the lost energy due to curtailment.

In Figure 7.12, the values of objectives 1, 2, 3 and 4 are plotted when objective 2 is minimized. From the figure it can be seen that the absolute values of objectives 1 and 2 are low compared to objectives 3 and 4. The value of objectives 1 and 2 are close to zero at in hours of PV generation when the net load at buses

with PV generation is zero. Objective 2 is of about the same magnitude as in Figure 7.9 when objective 1 is minimized, and objective 1 is slightly higher. As in the results for objective 1, the values of objectives 3 and 4 are about the same because the active power losses are so low.

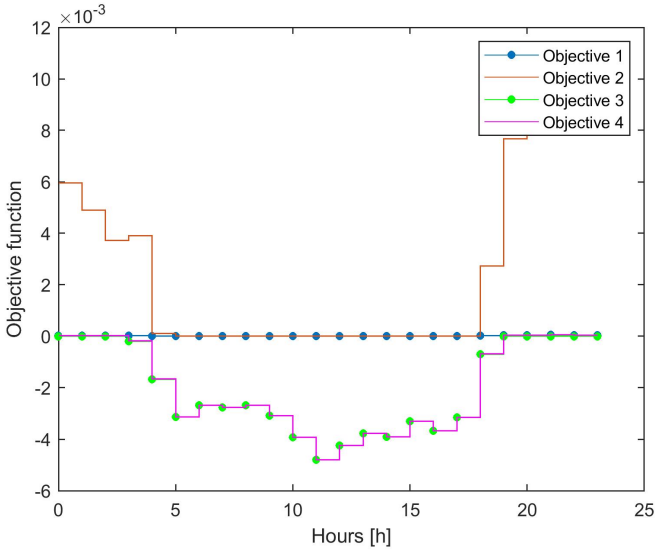

Figure 7.12: Value of objectives 1, 2, 3 and 4 on 27. of May for PV scenario 50%. The plotted values of the objectives are calculated based on per unit values of voltages and powers. Objective 2 is minimized.

7.2.3 Objective 3: Minimization of PV active power curtailment

Objective 3 is to minimize the curtailment of PV active power generation. Table 7.7 presents the main results from minimization of objective 3. The results show that the system is able to host all the PV power generation while ensuring that the voltage magnitudes do not exceed the upper limit of 1.05 pu, by adding reactive power control to the inverters. This holds for both PV scenarios. The PV inverters operate at a leading power factor (absorbing reactive power) to keep the voltages below the upper limit. Hence, the reactive power line flows increase. As a result of increased active and reactive power line flows, the network active power loss is high compared to the results for objective 1 and objective 2.

Table 7.7: Results from minimization of objective 3 on 27. of May.

	PV scenario 50%	PV scenario 100%
Network active power loss	199.41 kWh	870.55 kWh
Total active power loss (network and curtailment)	199.41 kWh	870.55 kWh
Maximum voltage magnitude	1.041 pu	1.050 pu
Total PV generation/ Total active load	251%	509%
Total PV generation/ Total maximum PV generation	100%	100%

The network power losses are presented in Figure 7.13a and the active power export and reactive power import are presented in Figure 7.13b. The active and reactive power losses increase in the same pattern as the PV power generation. The PV power generation exceeds the active power load, and thus active power is exported to the upstream network. Due to reactive power absorption in the inverters, reactive power is imported from the upstream network.

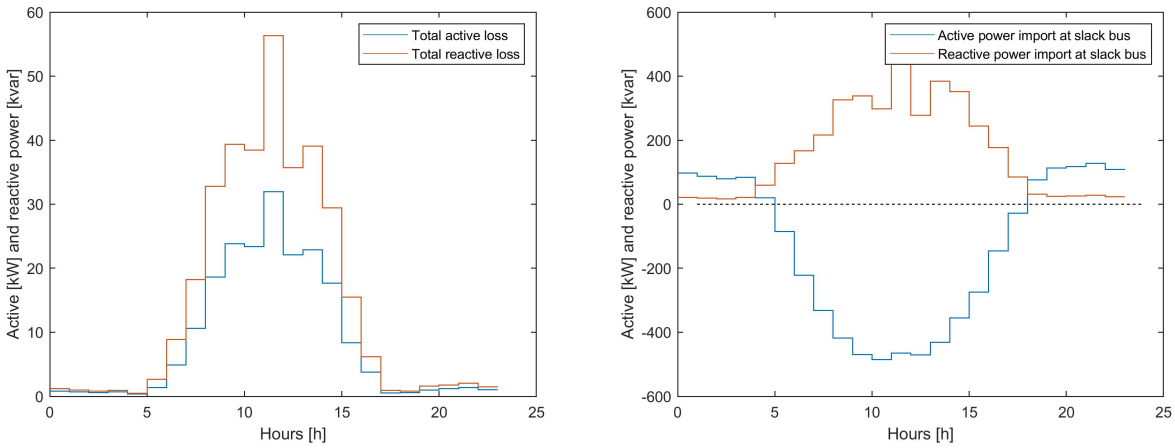

(a) **(b)**

Figure 7.13: Objective 3, PV scenario 50% on 27. of May. (a) Total network active and reactive power losses. (b) Power import at the slack bus.

The total active power load and total PV power generation are presented in Figure 7.14a. Figure 7.14b shows the PV active power in the system (red area). No PV generation is curtailed when objective 3 is minimized.

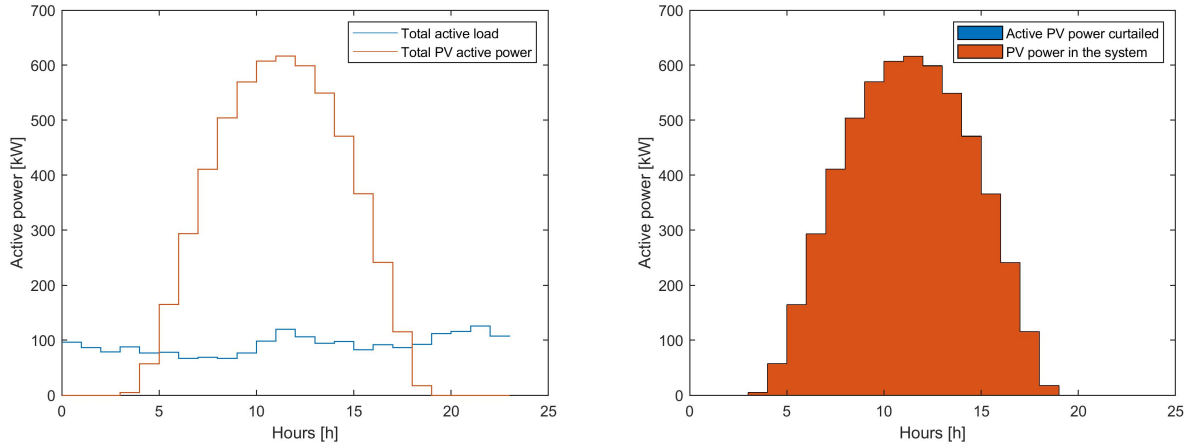

(a) **(b)**

Figure 7.14: Objective 3, PV scenario 50% on 27. of May. (a) Total active power load and total PV generation. (b) Curtailed PV active power and PV active power in the system. No PV active power is curtailed in this case.

Figure 7.15a presents the voltage change on the lines from the slack bus to consumer node 35 at 11:00 on 27. of May. It can be seen that the voltage magnitude drops on the "transformer line" between buses 76 and 75 and increases on the rest of the lines. The voltage drop on the transformer line is due to reactive power import at the slack bus. The resistance and the R/X ratio of the transformer line are low, and hence the line is more sensitive to voltage change from reactive power compared to the other lines in the system. The observed voltage drop on the "transformer line" can be approximated using Equation 2.3. The active power export is 485.60 kW (0.0194 pu) and the reactive power import at the slack bus is 298.13 kvar (0.0119 pu) at 11:00, and the transformer line is given by $R = 0.440$ pu and $X = 2.425$ pu.

$$\begin{aligned} \Delta V &\approx \frac{R \times P_{slackbus} + X \times Q_{slackbus}}{V_N} \\ &\approx \frac{0.440[pu] \times 0.0194[pu] + 2.425[pu] \times (-0.0119)[pu]}{1[pu]} \\ &\approx -0.02[pu] \end{aligned} \tag{7.1}$$

Figure 7.15b shows that there are small variations in voltage magnitude around 1 pu at the buses in the system at 11:00.

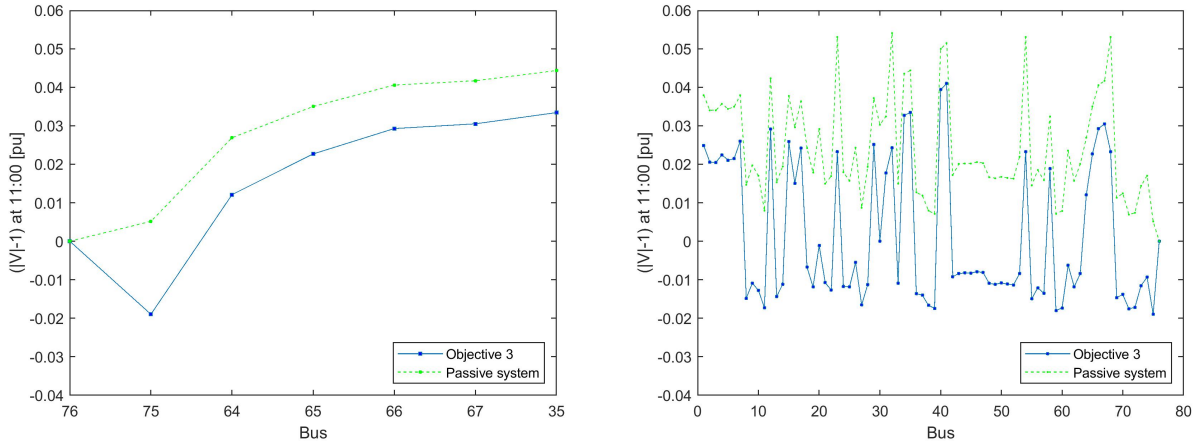

(a) **(b)**

Figure 7.15: Voltage magnitudes at 11:00 on 27. of May for PV scenario 50% for objective 3 (blue) and for the passive without PV inverter control (green). (a) Voltage change on lines from bus 76 (slack bus) to bus 35 (end-user). (b) Voltage magnitude at all buses.

Figure 7.16 shows the values of the objectives 1-4 when objective 3 is minimized. Note that objective 3 is to maximize the PV active power in the system. A more negative value of objective 3 means more PV generation in the system. Objective 3 is more negative in Figure 7.16 compared to objective 3 in Figures 7.9 and 7.12, as desired. The absolute values of objective 1, which represents the active power losses, are low compared to the values of the other objectives, but takes higher values than when objective 1 and 2 are optimized. The voltage magnitudes are higher than 1 pu in the hours of PV generation, and hence objective 2 takes higher values than when objective 1 and 2 are optimized. Objective 4 takes less negative values compared to objective 3. This is because the active power loss takes positive values, hence making the values of objective 4 less negative.

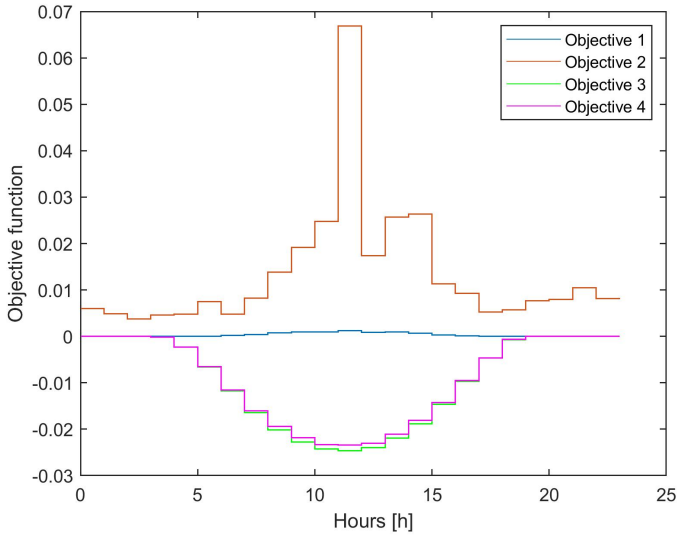

Figure 7.16: Value of objectives 1, 2, 3 and 4 on 27. of May for PV scenario 50%. The plotted values of the objectives are calculated based on per unit values of voltages and powers. Objective 3 is minimized.

7.2.4 Objective 4: Minimization of overall active power losses

Objective 4 is to minimize the total active power loss, denoted as the sum of network active power losses and PV active power curtailment. As for objective 3, no PV active power is curtailed. The PV inverters operate at a leading power factor to ensure voltages below the upper limit. Results from minimization of objective 4 are presented in Table 7.8. The network active power losses are lower for objective 4 compared to for objective 3 as a result of reduced reactive power line flows in the system.

Table 7.8: Results from minimization of objective 4 on 27. of May.

	PV scenario 50%	PV scenario 100%
Network active power loss	121.83 kWh	678.31 kWh
Total active power loss (network and curtailment)	121.83 kWh	678.31 kWh
Maximum voltage magnitude	1.05 pu	1.05 pu
Total PV generation/ Total active load	251%	509%
Total PV generation/ Total maximum PV generation	100%	100%

Figure 7.17a shows the network power losses when objective 4 is minimized. The active and reactive power losses are lower compared to when objective 3 is minimized in Figure 7.13a. The power import

at the slack bus is presented in Figure 7.17b. The reactive power import at the slack bus is significantly reduced for objective 4 due to reduced reactive power absorption in the PV inverters. For the same reason, the power losses are reduced compared to for objective 3. Due to reduced active power losses, more active power is exported to the upstream network compared to the results for objective 3.

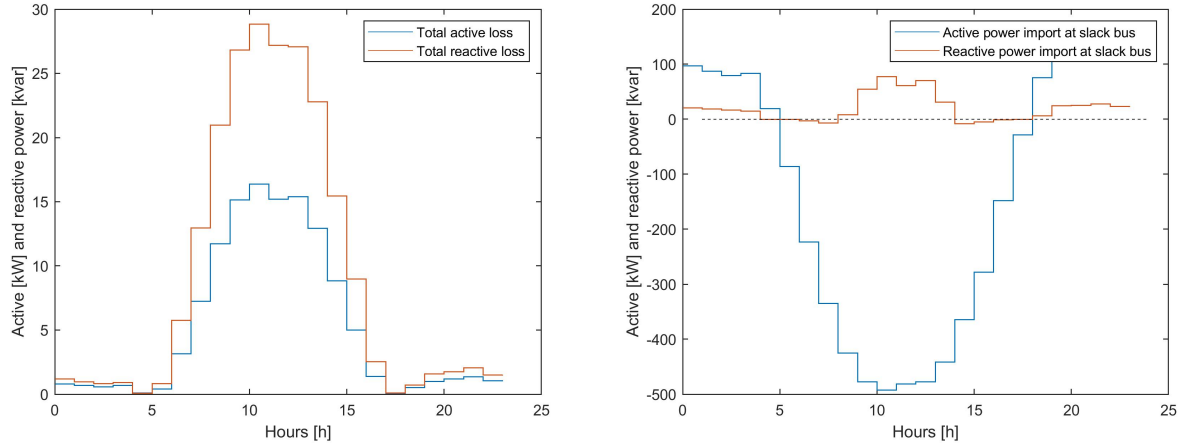

(a) **(b)**

Figure 7.17: Objective 4, PV scenario 50% on 27. of May. (a) Total network active and reactive power losses. (b) Power import at the slack bus.

Figure 7.18a shows the total active power load and total PV active power generation. The PV power generation is much higher than the load in the hours of generation. Figure 7.18b shows the total solar PV power generation in the system (red area). No PV power generation is curtailed.

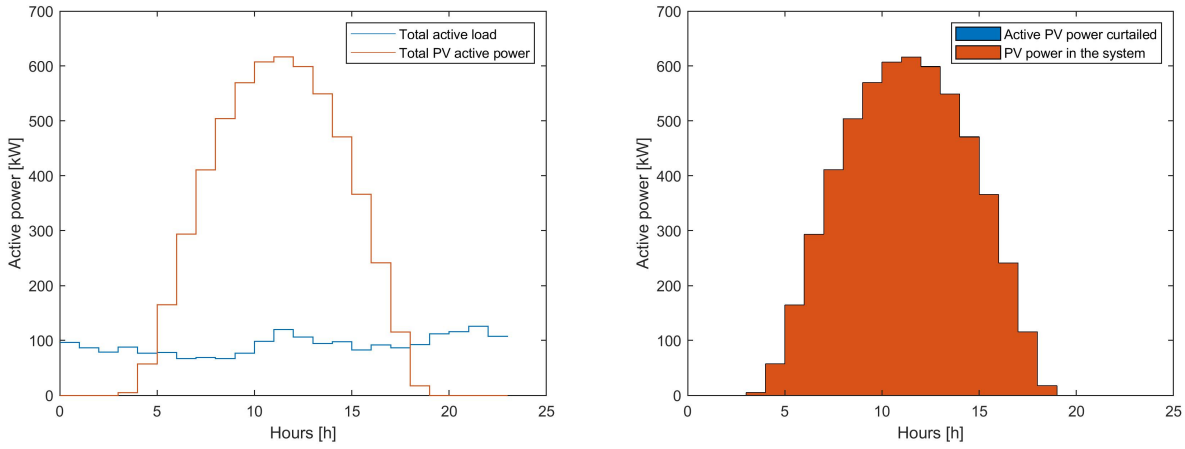

(a) **(b)**

Figure 7.18: Objective 4, PV scenario 50% on 27. of May. (a) Total active power load and total PV generation. (b) Curtailed PV active power and PV active power in the system. No PV active power is curtailed in this case.

Figure 7.19a presents the voltage increase on the lines from the slack bus to consumer node 35 at 11:00 on 27. of May. Unlike for objective 3, there is a voltage increase on the "transformer line" when objective 4 is minimized. This is because the reactive power import at the slack bus is lower for objective 4. The reactive power import at 11:00 is 77.56 kvar for objective 4 compared to 298.13 kvar for objective 3. In Figure 7.19b it can be seen that there are small variations in voltage magnitude around 1 pu at the buses in the system at 11:00. The voltages are somewhat higher compared to for objective 3 in Figure 7.15b because of lower reactive power absorption.

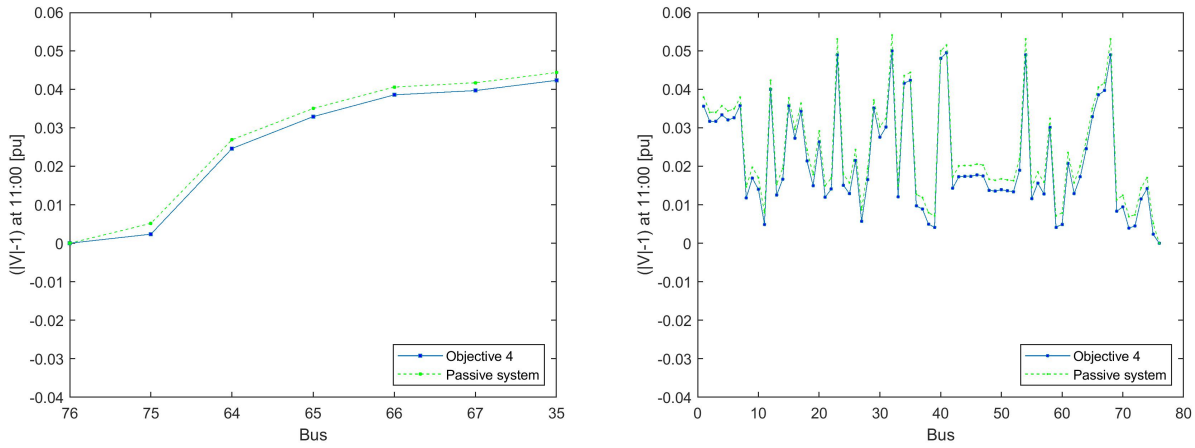

(a) **(b)**

Figure 7.19: Voltage magnitudes at 11:00 on 27. of May for PV scenario 50% for objective 4 (blue) and for the passive without PV inverter control (green). (a) Voltage change on lines from bus 76 (slack bus) to bus 35. (b) Voltage magnitude at all buses.

Figure 7.20 shows the values of the objectives 1-4 when objective 4 is minimized. The value of objectives 1, 3 and 4 are very similar to the values obtained from optimizing objective 3. The losses are reduced when objective 4 is optimized, and hence the absolute value of objective 1 is slightly lower than for minimization of objective 3. The absolute value of objective 2 is higher when objective 4 is optimized for most hours, due to less reactive power compensation and higher voltage magnitudes. As a result of lower power losses, the value of objectives 3 and 4 are more alike compared to the results for objective 3.

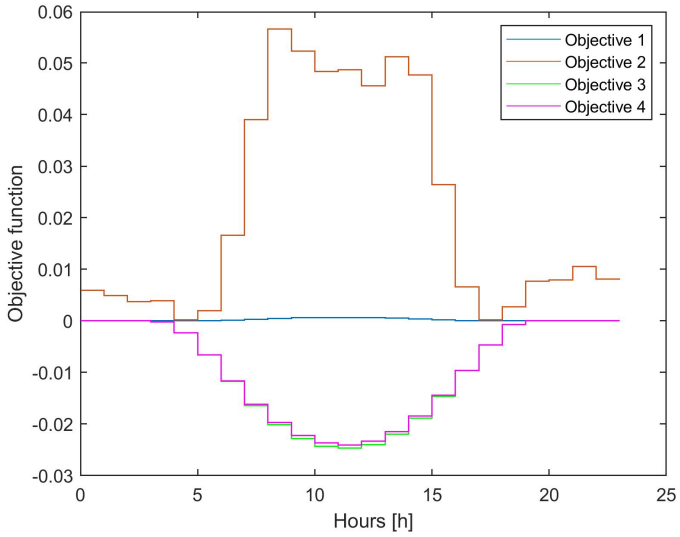

Figure 7.20: Value of objectives 1, 2, 3 and 4 on 27. of May for PV scenario 50%. The plotted values of the objectives are calculated based on per unit values of voltages and powers. Objective 4 is minimized.

7.2.5 Objective 4: APC vs. APC & RPC

The results from the single-objective optimizations show that objective 4 gives best results in terms of lowest network active power losses and no curtailment of PV active power generation. The results show that reactive power control can mitigate overvoltage problems caused by high amounts of PV power generation. However, increased reactive power line flows results in increased loading of the power lines and increased network active power losses. An alternative to reactive power control is only active power curtailment to mitigate overvoltage problems. This technique results in reduced network power losses, but the PV owners will suffer from lost revenue due to lost PV power generation.

In Section 7.1, where the system with PV power generation was analyzed without inverter control, it was found that the voltage magnitudes barely exceed 1.05 pu in PV scenario 50%. Hence, the need for active power curtailment or reactive power absorption to mitigate overvoltage problems is limited. Therefore, PV scenario 100% will be studied when APC and RPC control are compared. Note that active power curtailment is available but not active in the RPC control option. This can be observed because no PV power generation is curtailed.

Table 7.9 presents results for PV scenario 100% on 27. of May for objective 4 for inverter controls only active power curtailment (APC), and for active power curtailment and reactive power control (APC &

RPC). The results show that 1.6 MWh PV power generation is lost for only APC on 27. of May. The network active power losses are lower for APC compared to APC & RPC due to increase in the active and reactive power flows in the latter control option.

Table 7.9: Results from minimization of objective 4 with control options APC and APC & RPC for PV scenario 100% on 27. of May.

	APC	APC & RPC
Network active power loss	323.52 kWh	678.31 kWh
PV active power curtailment	1 575.94 kWh	0 kWh
Total active power loss (network and curtailment)	1 899.47 kWh	678.31 kWh
Maximum voltage magnitude	1.05 pu	1.05 pu
Total PV generation/ Total active load	438%	509%
Total PV generation/ Maximum PV generation	86%	100%

The total network power losses and power import at the slack bus are presented for PV scenario 100% with the two control options in Figures 7.21 and 7.22, respectively. Increased active and reactive power flows for APC & RPC results in increased power losses and increased active power export and reactive power import at the slack bus compared to APC.

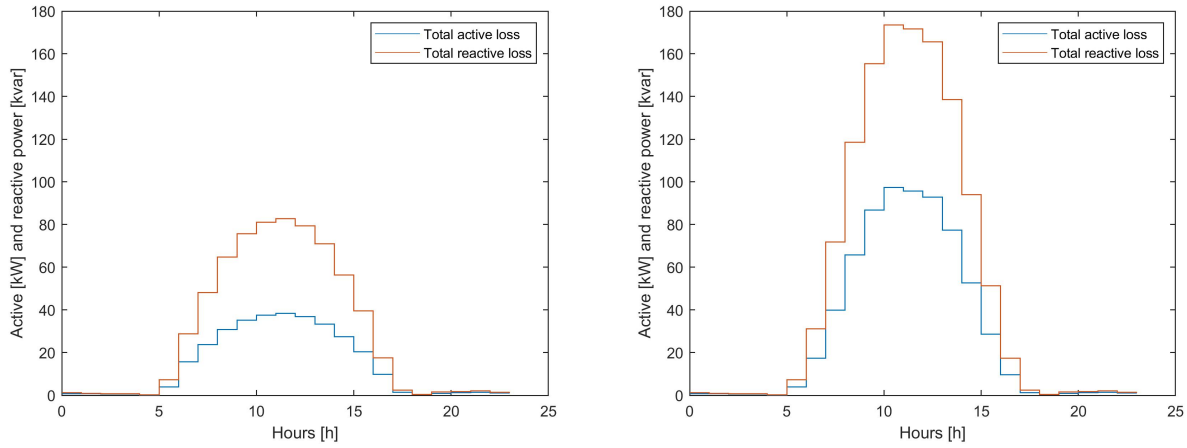

Figure 7.21: Total active and reactive power losses on 27. of May for: (a) APC. (b) APC & RPC.

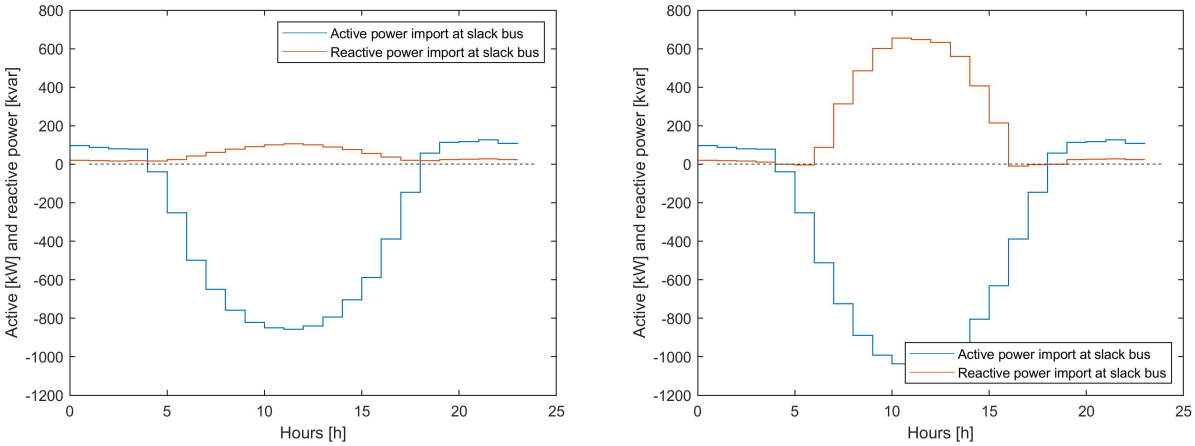

Figure 7.22: Power import at the slack bus on 27. of May for: (a) APC. (b) APC & RPC.

Figure 7.23 shows the total active power load and total active power generation for the two PV inverter controls. In Figure 7.24, the total PV active power in the system (red area) and the total curtailed PV active power generation (blue area) are presented. No PV generation power is curtailed for APC & RPC, while 14% of the generation is lost for APC.

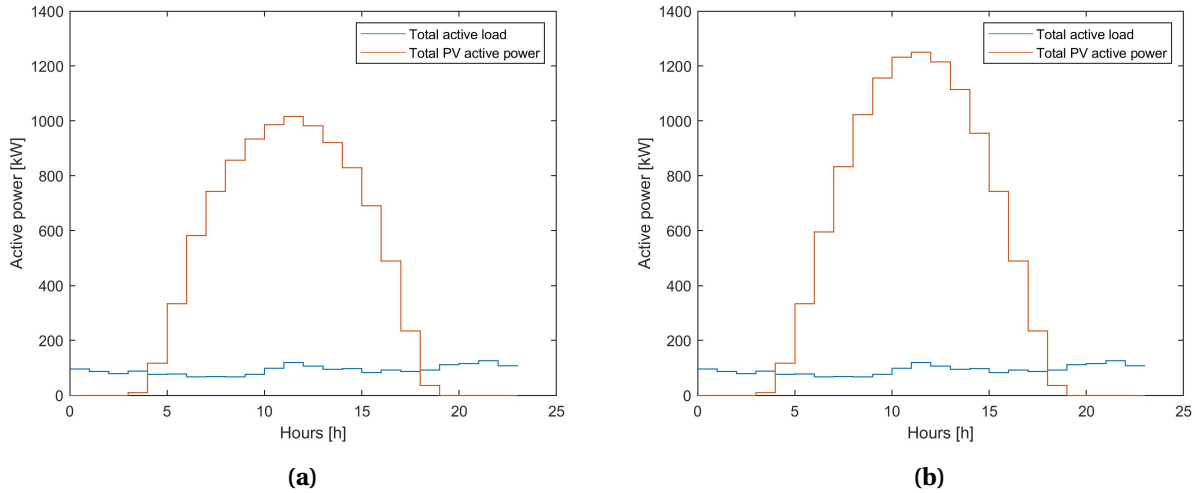

Figure 7.23: Total active power load and total PV generation on 27. of May for: (a) APC. (b) APC & RPC.

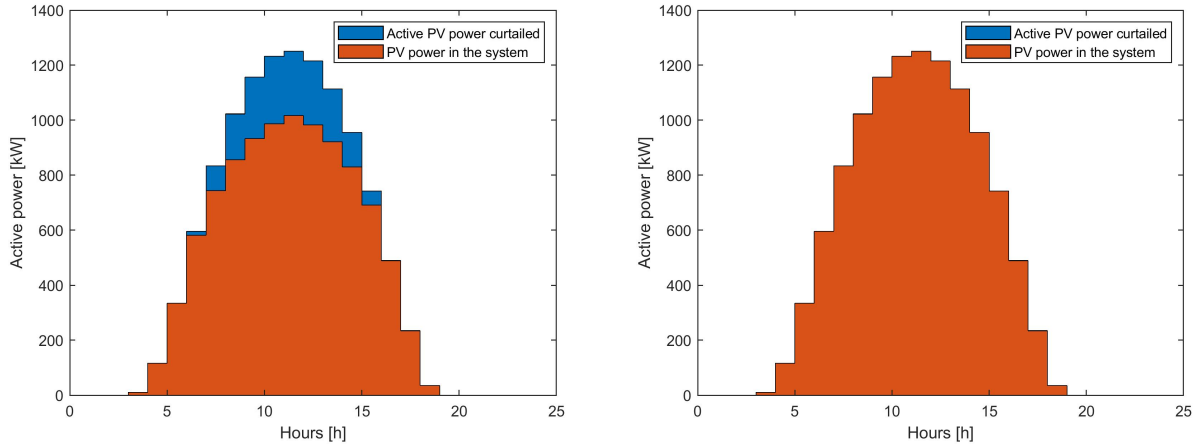

(a) **(b)**

Figure 7.24: PV active power in the system and curtailed PV active power on 27. of May. The blue area represents the lost energy. (a) APC. (b) APC & RPC.

In Figure 7.25, the voltage change on the lines from bus 76 to bus 35 are presented for the two control options. The reactive power absorption in the APC & RPC control results in lower voltage magnitudes compared to only APC.

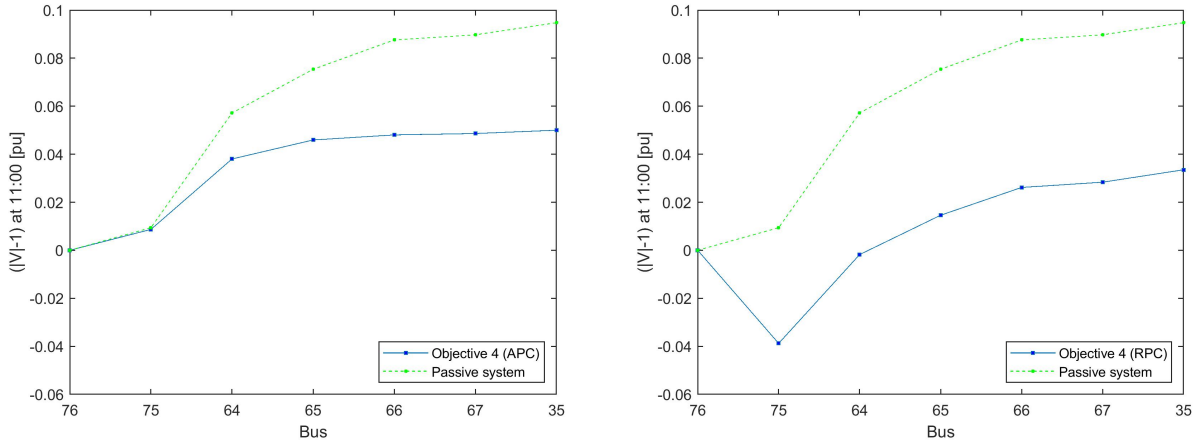

(a) **(b)**

Figure 7.25: Voltage drop on lines from bus 76 (slackbus) to bus 35 at 11:00 on 27. of May for objective 4 (blue) and for the passive without PV inverter control (green). (a) APC. (b) APC & RPC.

7.2.6 Objective 4: APC vs. APC & RPC - Annual analysis

In this section results for an annual analysis of the control options APC and APC & RPC for PV scenario 100% are presented. As in the analysis for 27. of May, no PV active power is curtailed for the APC & RPC control option. An annual analysis is performed to see what impact high amounts of PV power generation and different inverter controls have on the annual total active power losses and on the voltage profile.

Table 7.10 presents some numerical results from annual simulations for the inverter controls and for the system without inverter control and PV scenario 100%. The results for only active power curtailment show that the hosting capacity of PV generation is 1 365.40 MWh/year without exceeding the upper voltage limit of 1.05 pu. The hosting capacity can be increased to 1 439.01 MWh/year by adding reactive power control to the PV inverters. This constitutes a relative increase in annual hosting capacity of 5%.

The network power loss is increased by 15 MWh/year (37%) for APC & RPC compared to only APC, as a result of increased active and reactive power line flows. The annual network active power losses are 5 MWh/year higher for APC & RPC control compared to the results without control due to increased flow of reactive power. Note that no inverter control results in overvoltages. The total active power losses (network power losses and curtailment) are about halved for APC & RPC compared to only APC.

Table 7.10: Results from minimization of objective 4 with control options APC and APC & RPC and for a passive system for PV scenario 100%. The results are presented for a year.

	APC	APC & RPC	Passive system
Annual network active power loss	41.85 MWh	56.41 MWh	51.55 MWh
Annual curtailed PV active power	73.66 MWh	0 MWh	0 MWh
Annual total active power loss	115.51 MWh	56.41 MWh	51.55 MWh
Annual PV active power generation	1 365.40 MWh	1 439.01 MWh	1 439.01 MWh
Maximum voltage magnitude	1.05 pu	1.05 pu	1.12 pu
PV generation/ Maximum PV generation	95%	100%	100%
PV generation/ Active load	94%	99%	99%

Figure 7.26 shows the network power losses for the two PV inverter controls. The network active and reactive power losses are higher for APC & RPC compared to only APC in parts of the year with significant amounts of PV power generation.

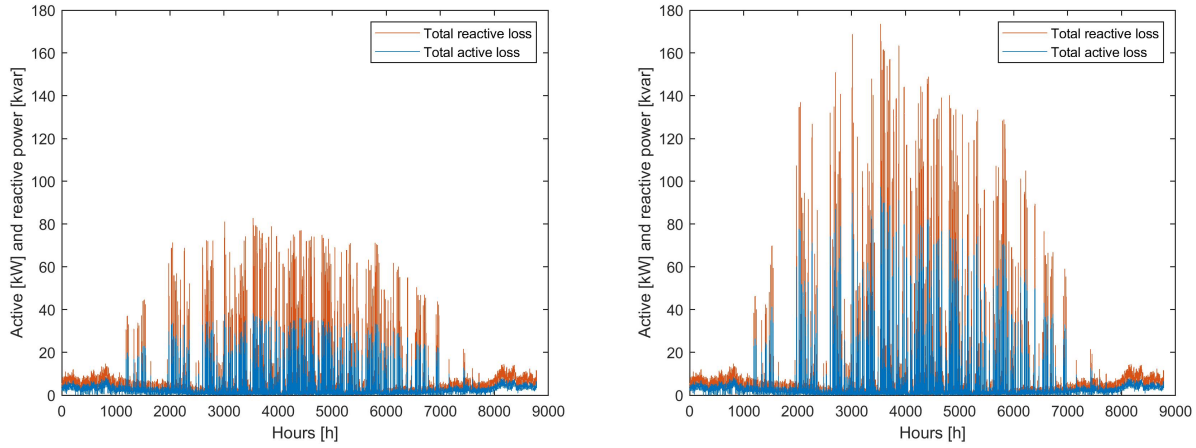

Figure 7.26: Total active and reactive power losses for: (a) APC. (b) APC & RPC.

The power import at the slack bus is presented in Figure 7.27. The most visible difference in the two sub-figures 7.27a and 7.27b is the reactive power import. It can be seen that the reactive power import is high for APC & RPC most of the year. The reactive power import follows the pattern of the active power generation and is highest in the periods of the year with highest PV power generation.

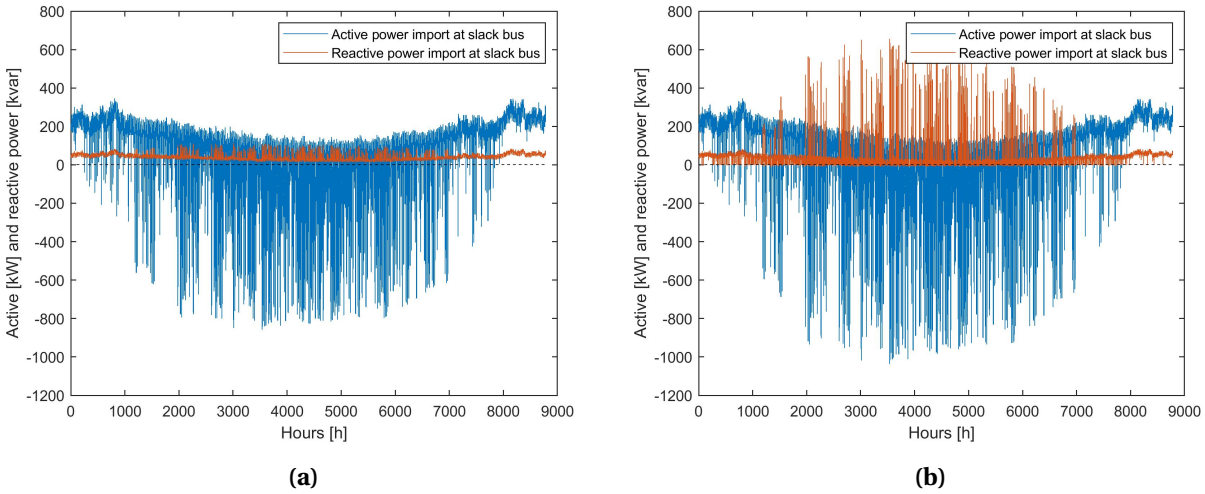

Figure 7.27: Power import at the slack bus for: (a) APC. (b) APC & RPC.

The total active power load and total PV power generation are presented in Figure 7.28. The PV power generation is higher than the load almost all year around for both control options. Figure 7.29 shows the total PV power generation in the system and the curtailed PV power generation. Curtailment is present for the APC option in the summer months and no PV power generation is curtailed in the APC & RPC

option.

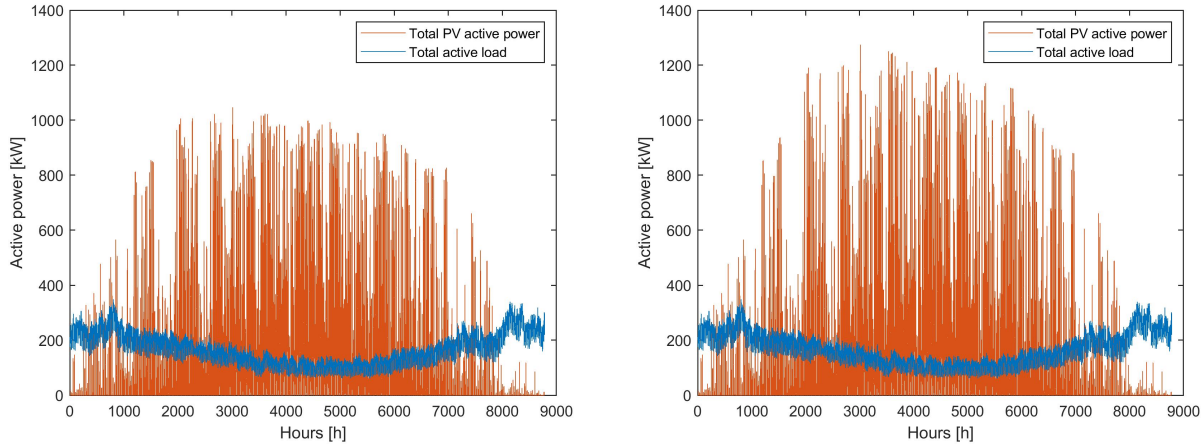

Figure 7.28: Total active power load and total PV generation for: (a) APC. (b) APC & RPC.

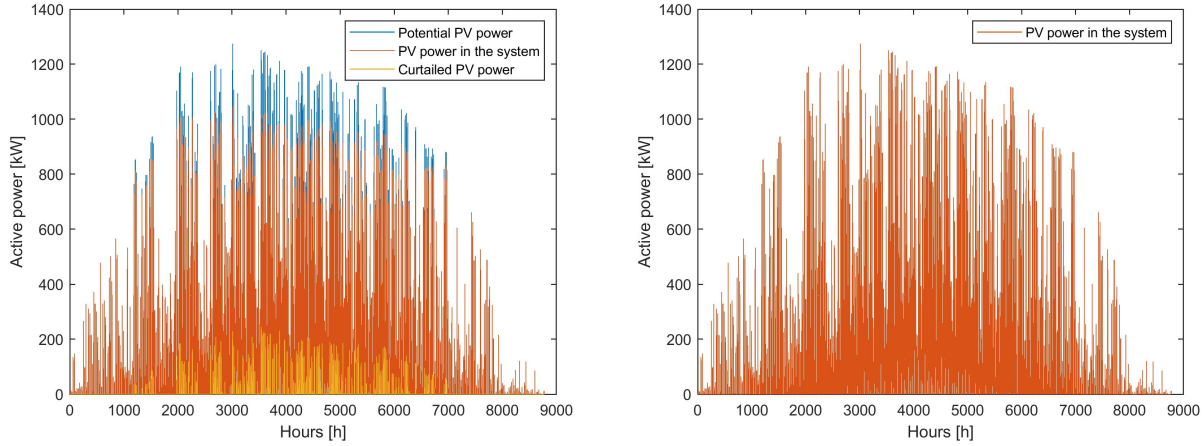

Figure 7.29: PV active power in the system and curtailed PV active power for: (a) APC. (b) APC & RPC.

Active power curtailment and reactive power control ensure that the maximum voltage bound of 1.05 pu is not exceeded. Figure 7.30 shows the annual voltage profile at bus 32 (most critical node) for a passive system without inverter control and for APC & RPC control. Only APC control gives approximately the same voltage profile as APC & RPC control. The figure shows that inverter control is required to regulate the voltage for a great part of the year for the chosen PV capacities in PV scenario 100%.

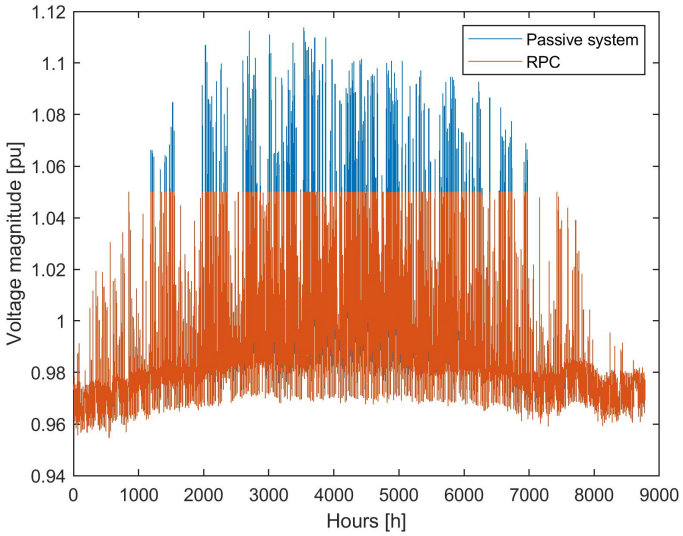

Figure 7.30: Voltage magnitude at bus 32 for a passive system and for APC & RPC control.

7.3 Comparison of the single-objective optimizations

The purpose of this thesis it to investigate how controllable PV inverters can mitigate to solve overvoltage problems caused by high amounts of solar PV power generation, while limiting the overall active power losses. In this section main findings from the single-objective optimizations are summarized and compared considering the purpose of the study.

7.3.1 Comparison of the objectives

The distribution network can take high amounts of PV power generation before overvoltage problems occur. The maximum voltage for PV scenario 50% without inverter control barely exceeds the limit of 1.05 pu, and thus inverter control is not needed for overvoltage mitigation. In Table 7.11, the relative changes in maximum voltage magnitudes, network active power losses and total active power losses from a passive system without inverter control are presented for PV scenario 50%. Values for voltage magnitude, network power losses and total power losses can be found in Table B.1 in Appendix B. It can be observed that the values for objective 4 are about the same as for the passive system because of the limited need for inverter control.

Table 7.11: Relative change from the results for the passive system without inverter controls for PV scenario 50% on 27. of May.

	$\|V\|_{max}$	Network active power loss	Total active power loss
Passive system	1.05 pu	121.80 kWh	121.80 kWh
Objective 1	-4.76%	-92.62%	+3 498.20%
Objective 2	-4.76%	-92.45%	+3 517.70%
Objective 3	-0.95%	+63.72%	+63.72%
Objective 4	0.00%	+0.02%	+0.07%

Table 7.12 presents the same results for PV scenario 100%. Values for voltage magnitudes, network power losses and total power losses can be found in Table B.2 in Appendix B. Note that the results are presented relative to PV scenario 100% without inverter control where the maximum voltage limit is exceeded. For reactive power control, objective 4 give the best results due to lowest network active power losses and no curtailment of PV active power generation. In addition, optimal power flow simulations for objective 4

result in lower network active power losses compared to constant leading power factors of 0.9. Optimal power flow simulations of objective 4 for only APC and for APC & RPC, show that there is a trade-off between lowering the network active power losses or reducing the curtailment of PV power generation. This will be discussed further in the discussion in Chapter 8.

Table 7.12: Relative change from the results for the passive system without inverter controls for PV scenario 100% on 27. of May. Note that the results for the passive system gives overvoltages in PV scenario 100%.

	$\|V\|_{max}$	Network active power loss	Total active power loss
Passive system	1.11 pu	547.24 kWh	547.24 kWh
Constant PF=0.9 (leading)	-7.21%	+48.09%	+48.09%
Objective 1	-9.90%	-98.43%	+1 743.70%
Objective 2	-9.90%	-98.40%	+1 743.70%
Objective 3	-5.41%	+59.08%	+59.08%
Objective 4 (APC & RPC)	-5.41%	+23.95%	+23.95%
Objective 4 (APC)	-5.41%	-40.88%	+247.10%

The network active power loss and the total active power loss (network loss and curtailment) are presented in Figure 7.31 for all objectives. For the purpose of minimizing total active power losses, objective 4 gives the best results.

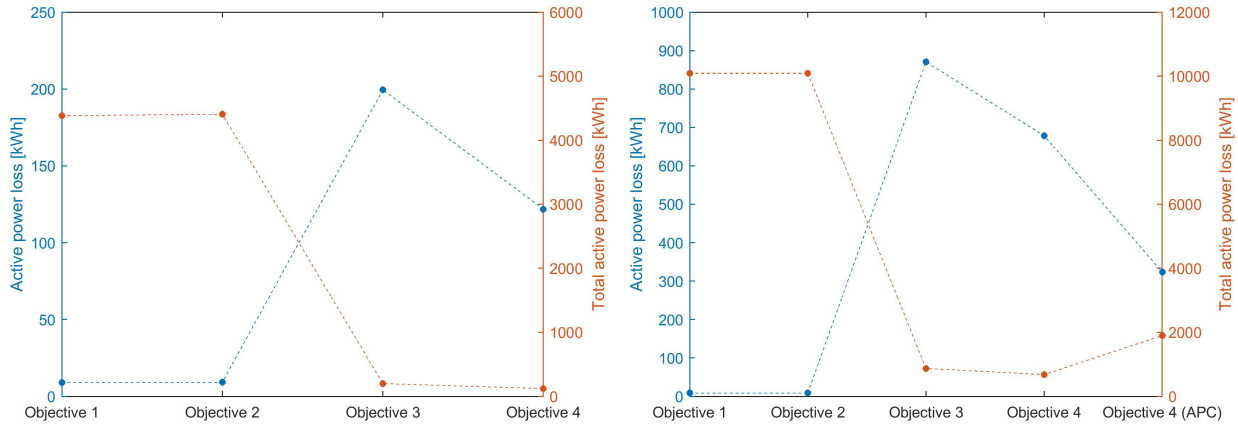

(a) **(b)**

Figure 7.31: Network active power loss and total active power loss (network losses and curtailment) for all objectives on 27. of May. (a) PV scenario 50%. (b) PV scenario 100%.

7.3.2 Inverter power factor at the most critical bus for PV scenario 100%.

In this section, the operating PV inverter power factor is analyzed for bus 32, the most critical bus, on 27. of May for PV scenario 100%. Plots for PV scenario 50% can be found in Appendix C. Figure 7.32a presents the power factor and net load at bus 32 for objective 1, minimization of network active power losses. Figure 7.32b presents the results for objective 2, minimization of voltage deviations. Figure 7.32a shows that the power factor of the PV inverter is equal to the power factor of the load of 0.98 in hours of significant PV active power generation. This is to make sure that both the net active and reactive loads are zero in these hours. As a results, the power flows will be minimized and hence the active power losses. The PV inverter power factor is zero in the hours without PV power generation. The voltage deviation is minimized if the net active and reactive loads are zero. Consequently, the power factor varies around the power factor of the load of 0.98 in Figure 7.32b. The voltage magnitudes are heavily influenced by the active and reactive power flows and hence also by the inverter power factor. This is most likely the reason for more variations in Figure 7.32b compared to in Figure 7.32a.

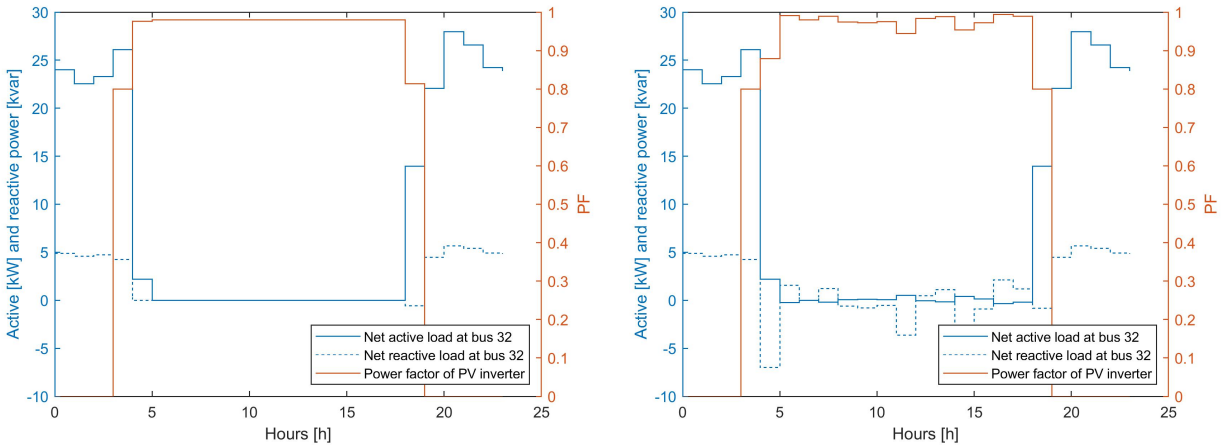

Figure 7.32: Net active and reactive load and power factor of PV inverter at bus 32 (the most critical bus) for PV scenario 100% on 27. of May. (a) Objective 1. (b) Objective 2.

Figure 7.33a shows the power factor and net load at bus 32 for objective 3, minimization of PV active power curtailment. It can be seen that the inverter operates at the minimum power factor of 0.8 for some hours. Remember that more reactive power is absorbed at a lower power factor. Figure 7.33b presents similar results for objective 4, minimization of overall active power losses. Comparing Figures 7.33a and 7.33b it can be seen that the power factor is higher for objective 4. The inverter operates at a higher power

factor and adsorbs less reactive power to lower the network active power losses.

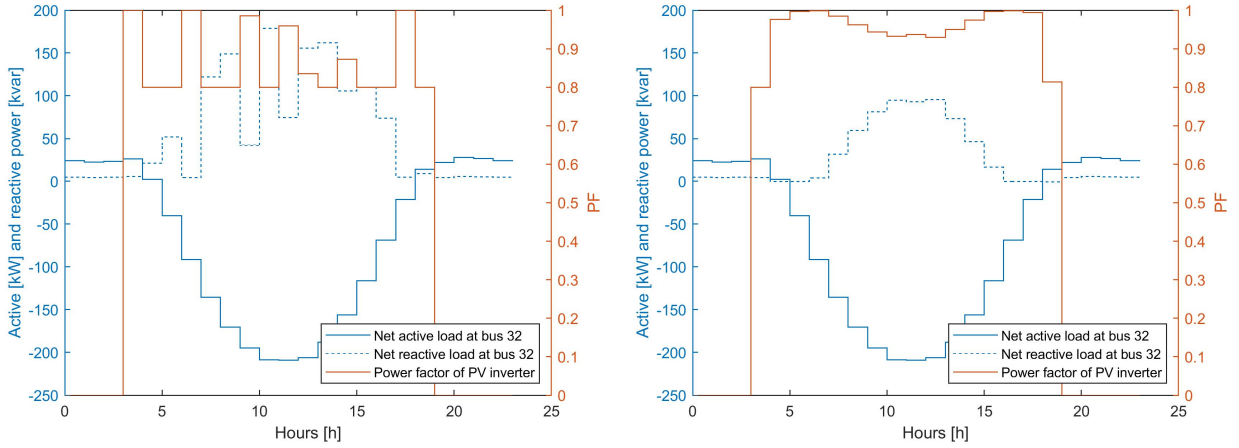

Figure 7.33: Net active and reactive load and power factor of PV inverter at bus 32 (the most critical bus) for PV scenario 100% on 27. of May. (a) Objective 3. (b) Objective 4.

7.3.3 Location for active power curtailment and reactive power control

In Figure 7.34a, the PV active power curtailment and inverter operating power factor for each bus are plotted sorted according to which feeder the buses are connected. The plotted PV active power curtailments are for only APC control, and the power factors are for APC & RPC control. Figure 7.34b shows the PV inverter active and reactive power outputs. In this figure RPC represent the APC & RPC control. High amounts of PV power generation is curtailed at bus 32, the grocery store, connected to feeder H for only APC control. The highest reactive power absorption also takes place at this bus, but the inverter power factor is higher than the minimum value of 0.8. Figure 7.35 shows the voltage magnitudes at all buses sorted according to which feeder they are connected. Comparing Figure 7.34a and 7.35, it can be observed that PV power generation is curtailed at buses with overvoltages. The voltage increases along the distribution feeder lines G1-G4. Therefore, the inverters connected toward the end of the feeder bear the highest share of curtailment. Interestingly, no PV power generation is curtailed at the "shared nodes" connected to buses I-M2 for only APC control, but the inverters contribute with reactive power absorption for APC & RPC control. Reactive power is absorbed although the voltages at these buses are acceptable before inverter control. This also holds for other buses, and hence the number of inverters with reactive power absorption for APC & RPC control is higher than the number of inverters with curtailment for only APC control.

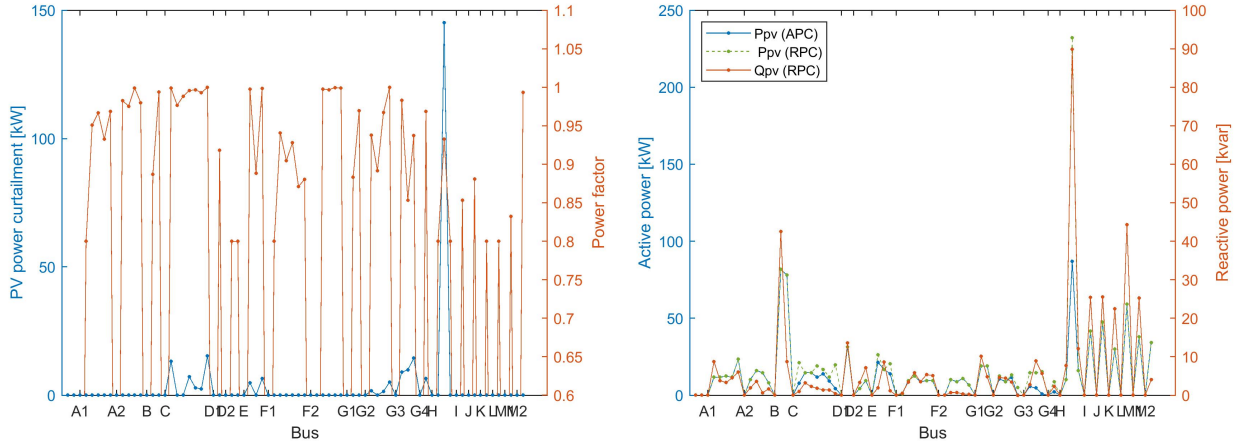

(a) **(b)**

Figure 7.34: Objective 4, PV scenario 100% at 11.00 on 27. of May. (a) PV active power curtailment for APC control and inverter power factors for APC & RPC control. (b) Active power generation and reactive power absorption for only APC control and APC & RPC control (RPC in the figure).

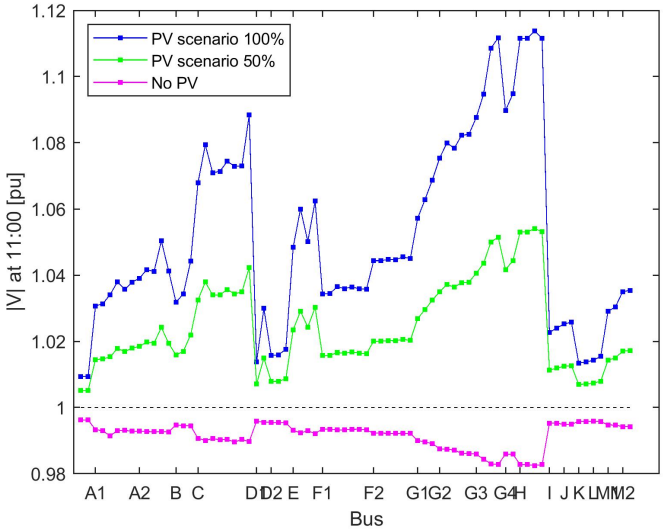

Figure 7.35: Voltage magnitudes at 11:00 on 27. of May for all buses. The buses are sorted according to which feeder the buses are connected.

7.3.4 Load ratio of the power lines

Power cables in a distribution network have a certain current-carrying capability depending on its isolation type, cross-section area and conductor material. The MVA rating of a cable can be calculated from its current-carrying capability. The fraction between the grid power flows and the respective cables rated

power can be defined as the load ratio of the cable. In Figure 7.36, the annual maximum load ratio of each power cable are presented for the distribution network without PV, PV scenario 100% without inverter control, and for PV scenario 100% for control options only APC and APC & RPC. In the figure, the power cables are sorted according to which distribution feeder they are connected. By running an annual analysis of the distribution network with its respective loads and no PV power generation it was found that the cable connecting consumer node 32 to distribution feeder H is overloaded. The remaining lines are loaded below their MVA rating. For PV scenario 100% without inverter control and for control options only APC and APC & RPC, 10, 9 and 16 cables are overloaded, in that order. The lines that are most overloaded are the line connecting consumer node 32 to feeder H, the line from the main feeder to feeder H and the line connecting consumer node 38 to feeder L. Remember that consumer node 32 is a grocery store with a high load (271.63 MWh/year) and consequently high installed PV capacity (318 kWp) compared to the other consumers. Consumer node 38 is a household with a relatively high consumption (69.88 MWh/year).

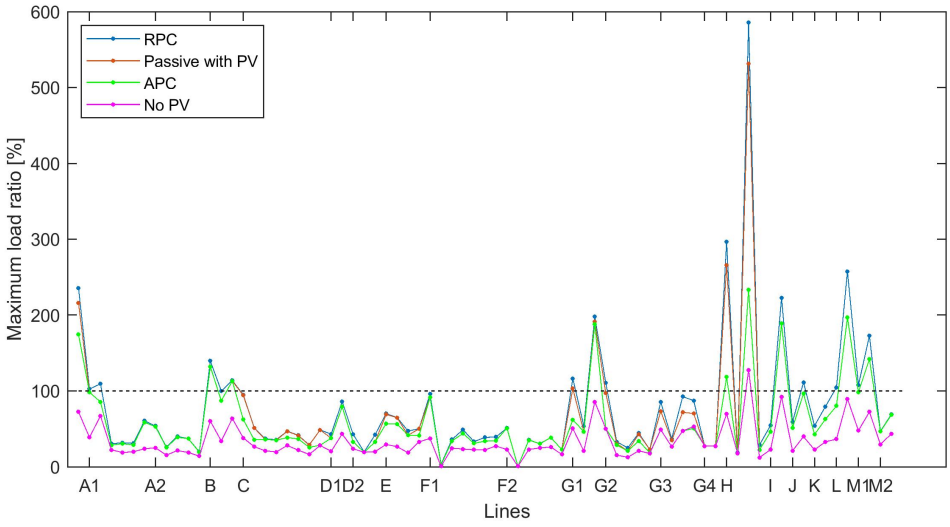

Figure 7.36: Maximum load ratios of the power lines during a year. The load ratio is given by the ratio between the grid power flow and the respective cables rated power threshold. The results are presented for the system without PV (No PV), PV scenario 100% without any control (Passive with PV), and for the controls only APC and APC & RPC (RPC). The lines are sorted according to which feeder they are connected.

7.4 Sensitivity

7.4.1 Dual value for the restriction on maximum voltage magnitude

The upper and lower limits for voltage magnitudes are not absolute and they may vary for different power system operators (Section 2.1.1). The network active power loss depends on the current flowing, and increases when the flow of active- and reactive power increase. As the need of reactive power compensation is reduced if the upper voltage limit is increased, the flow of reactive power is also reduced. Hence, the network active power losses will be reduced by increasing the voltage limit. In addition, less PV active power needs to be curtailed which results in lower overall active power losses.

What impact an increase in the voltage upper bound has on the total active power loss (network and curtailment) can be investigated by determining the dual value (also referred to as shadow price) for the restriction on maximum voltage in the GAMS model. For a specific hour, the dual value gives the change in the value of the objective function if the upper bound is increased by 1 percentage point, i.e. from 1.05 pu to 1.06 pu. The dual values are zero in hours where the restriction on maximum voltage magnitude is inactive.

The dual values are calculated for PV scenario 100% and objective 4 is minimized. As the dual values are the change in the value of the objective, a better understanding of what the value of objective 4 means is required. Objective 4 is to minimize the total active losses including network power losses and solar power curtailment.

$$\begin{aligned} \text{Minimize} \quad F &= \sum_{t=1}^{T}\left(\sum_{i=1}^{N} P_{Gi}^{t} - \sum_{i=1}^{N} P_{Li}^{t} + \sum_{i=1}^{N}(-P_{PVi}^{t})\right) \\ &= \sum_{t=1}^{T}\left(P_{slackbus}^{t} + \sum_{i=1}^{N} P_{PVi}^{t} - \sum_{i=1}^{N} P_{Li}^{t} + \sum_{i=1}^{N}(-P_{PVi}^{t})\right) \\ &= \sum_{t=1}^{T}\left(P_{slackbus}^{t} - \sum_{i=1}^{N} P_{Li}^{t}\right) \end{aligned} \tag{7.2}$$

From Equation 7.2 it can be observed that minimizing objective 4 is the same as minimizing the active power import from the upstream network. This is equivalent to maximizing the active power export to the upstream network, which is achieved by minimizing the network power losses while maximizing the

PV active power generation. It can be observed that the value of objective 4 is the power import at the slack bus minus the total load at time t. Thus, a more negative dual value means increased active power export to the upstream network.

Dual values for 27. of May

Table 7.13 shows the dual values for the restriction on maximum voltage magnitude for bus 32 (most critical bus) on 27. of May for PV scenario 100% when objective 4 is minimized. The most critical bus is analyzed because the voltage at this bus is significantly higher compared to the other buses (Figure 7.4). Remember that this bus is a grocery store. What impact a slack in the voltage bounds has on the whole system is analyzed in the results for multi-objective optimization in Section 7.5.

The dual values are different from zero in the time interval 07.00-16.00 on 27. of May. The net load at bus 32 is positive (i.e. there is export of excess power) from 06.00 to 18.00 for both controls only APC and APC & RPC. However, curtailment only takes place for overvoltage mitigation in the interval 07.00-16.00 for only APC control, and reactive power absorption is only present in the interval 08.00-16.00 for APC & RPC control. This is the reason for the reduced time interval for non-zero dual values.

Table 7.13: Dual values for 1 percentage point increase in the upper voltage magnitude limit for bus 32, i.e. from 1.05 to 1.06 pu, for PV scenario 100% on 27. of May. The results are presented for inverter control options APC & RPC and only APC.

Hour	APC & RPC [kW/0.01 pu]	APC [kW/0.01 pu]
7	-0.40	-19.15
8	-1.93	-18.93
9	-3.11	-18.77
10	-4.02	-18.73
11	-4.59	-18.72
12	-4.57	-18.69
13	-4.64	-18.72
14	-3.70	-18.76
15	-2.58	-18.92
16	-1.29	-19.00
Sum	-30.83 kWh/day	-188.40 kWh/day

The results show that increasing the upper voltage limit results in a reduction in total active power losses and thus increased export at the slack bus. For APC & RPC control, the dual values represent the possible reduction in network active power losses as a result of less reactive power line flows. The network active power losses are 678.31 kWh/day on 27. of May for APC & RPC. Thus, increasing the voltage bound at bus 32 by 1 percentage point may reduce the network active power loss by 4.55%.

For only APC control, the dual values represent the reduction in solar power curtailment. The net power export at bus 32 is 593.71 kWh/day on 27. of May for APC. Thus, increasing the voltage bound at bus 32 by 1 percentage point may increase the net power export at bus 32 by approximately 31.73%. Note that the dual values are the change in the objective value which we saw above was the change in export at the slack bus. Due to power losses during power transfer, the increase in net power export at bus 32 is most likely somewhat higher than 188.40 kWh/day.

Annual calculation of dual values

Dual values have been calculated for the restriction on maximum voltage magnitude for bus 32 for the year of analysis for only APC and for APC & RPC control. These are presented in Figure 7.37. For APC & RPC, the annual network power loss is 56.41 MWh/year. Thus, the total annual change in the objective of 1.55 MWh/year for APC & RPC represents a possible reduction in annual network losses of 2.75%. For only APC, the total annual change in objective 4 is 16.31 MWh/year. The annual net load at bus 32 is 48.81 MWh/year (import) and the degree of curtailment is 18%. Increasing the voltage bound, may reduce the net power import at bus 32 by approximately 33.42% for only APC.

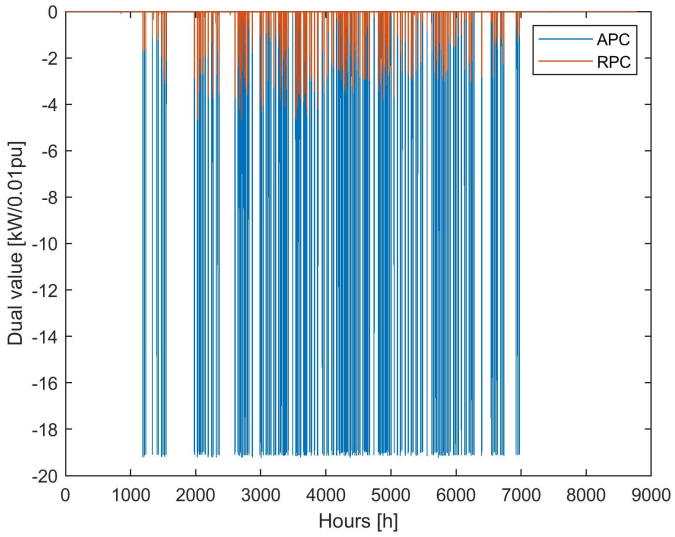

Figure 7.37: Dual values for 1 percentage point increase in the upper voltage magnitude limit for bus 32, i.e. from 1.05 to 1.06 pu, for PV scenario 100%. The results are presented for only APC and APC & RPC (RPC in the figure).

7.5 Multi-objective optimization

The total active power losses in the simulations depend on the maximum limit on voltage magnitude. Section 7.4.1 shows that the total active power losses can be reduced by increasing the upper limit on voltage. The relationship between active power loss and voltage magnitude can also be investigated by multi-objective optimization of objective 2, minimization of voltage deviations, and objective 4, minimization of total active power losses. In a multi-objective optimization of objective 2 and 4, the voltage magnitudes are controlled by including voltage deviation in the objective instead of setting absolute upper and lower bounds by hard constraints. The simulations are done for PV scenario 100% with PV inverter control option APC & RPC on 27. of May.

7.5.1 Determining proper scaling factors

The multi-objective optimization problem is transformed into a single-objective optimization problem using the weighted-sum approach. As stated in Section 3.2.1, the objectives need to be properly scaled to obtain good results from the weighted-sum method for solving a multi-objective optimization problem. For this optimization problem the scaling factors are found in the following way:

- The upper voltage boundary is increased to 2.00 pu, so that objective 2 does the job of voltage regulation.
- The value of the objectives in each hour, t, is observed when each objective is optimized separately.
- The scaling factor for objective 4, s_4, is found as the larges value objective 4 takes when objective 2 is minimized: $s_4 = 0.0048$
- The scaling factor for objective 2, s_2, is found as the larges value objective 2 takes when objective 4 is minimized: $s_2 = 0.4604$

7.5.2 Results for multi-objective optimization of objective 2 and objective 4

The relation between maximum voltage magnitude and total active loss can be found by assigning different weights to the two objectives. Table 7.14 shows the results from single-objective optimization of objective 2 and 4 with an increased upper limit on voltage magnitude, as well as results for a multi-objective optimization when the objectives are equally weighted and scaled as explained above. The results for the latter optimization show that the scaling factors are acceptable because the maximum voltage is reduced compared to the results from single-objective optimization of objective 4 and the power losses are reduced compared to the results for objective 2.

Table 7.14: Results from multi-objective optimization of objectives 2 and 4 for PV scenario 100% on 27. of May.

	Objective 2	Objective 4	Multi-objective
Network active power loss	8.74 kWh	536.90 kWh	646.74 kWh
Curtailed PV active power	10 081.55 kWh	0 kWh	0 kWh
Total active power loss (network and curtailment)	10 090.29 kWh	536.90 kWh	646.74 kWh
Maximum voltage magnitude	1.0001 pu	1.1351 pu	1.0766 pu

The maximum voltage magnitude and total active power loss (network and curtailment) for multi-objective optimization are plotted in Figure 7.38 for different weights of the two objectives. The weight of objective 2, w_2, is varied in the interval [0.9-0], while the weight of objective 4, w_4, is varied in the interval [0.1-1] with a step of 0.1. The weights sums up to 1 for all combinations of weights. The maximum voltage is reduced and the total active power loss is increased when the weight of objective 2 is increased and the weight of objective 4 is reduced. The figure shows that the combination of weights has to be $w_2 = 0.9$

and $w_4 = 0.1$ to obtain a maximum voltage below the bound of 1.05 pu. For this combination of weights the maximum voltage magnitude is 1.044 pu. Results for $w_2 = 1$ and $w_4 = 0$ are not plotted because the total active power loss is very high (10 089 kWh) compared to the total active power losses for the other combinations of weights, due to a much higher PV active power curtailment.

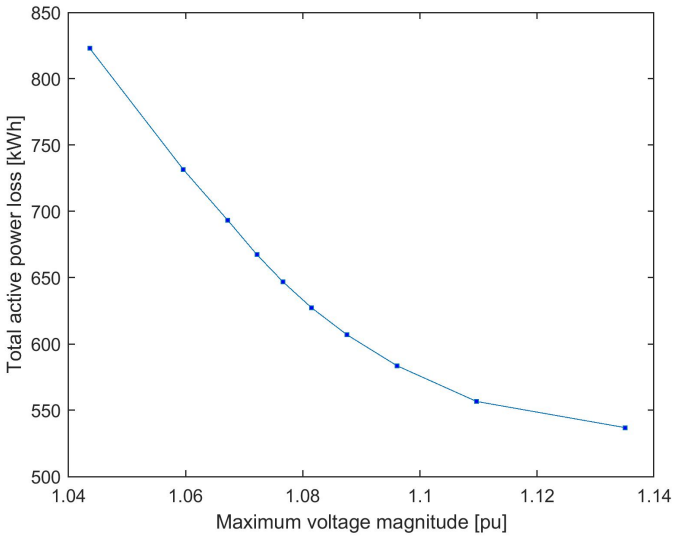

Figure 7.38: Maximum voltage magnitude and total active power losses (network losses and PV curtailment) for different weights for the objectives 2 and 4 on 27. of May. The weights are: $w_2 \in$ [0.9-0] and $w_4 \in$ [0.1-1] with a step of 0.1. Weights [0.9,0.1] corresponds to the dotted point in the upper left of the figure.

8 Discussion

The increasing amount of renewable energy connected to the low voltage grid poses new challenges for the distribution grid operators. Voltage limit violation is one of the important issues that arise. The purpose of this study is to investigate how controllable PV inverters can contribute to overvoltage mitigation, while limiting the network active power losses and curtailment of solar PV active power generation. Active power losses are associated to costs and are therefore minimized. Optimal set-points for the PV inverters have been found by solving single- and multi-objective optimization problems in GAMS. The study is performed for a distribution power network in Steinkjer with simulated PV active power generation data. Two solar PV active power generation scenarios, PV scenario 50% and PV scenario 100%, have been formulated with regards to installed PV capacities. In this chapter, the main findings in Chapter 7 are discussed.

8.1 Impact from high amounts of solar PV

The distribution network is strong and can take high amounts of solar PV power generation before overvoltage problems occur. In PV scenario 50%, the PV penetration is 100% (all consumers have solar PV panels) and the median and average PV installed capacities are 10 kWp and 15 kWp, respectively. The maximum voltage magnitudes barely exceed the upper voltage bound of 1.05 pu when the PV active power generation profiles are added to the load profiles. However, PV scenario 100% results in overvoltages for a significant part of the year. This can be seen in Figure 7.30, where the voltage magnitude at bus 32 (the most critical node) for a passive system is plotted for the year of analysis. The PV capacities of this scenario are high with median and average PV capacities of 20 kWp and 31 kWp, respectively. The highest voltage magnitudes occur at bus 32, the grocery store. A high annual load at this bus results in a high installed PV capacity and hence high reverse power flows.

According to [1], the main issues that arise from high PV penetration in Norwegian distribution grids are assumed to occur at the end of a radial in weak radial distribution networks. The network cables in the distribution grid are relatively short, with a maximum length of 321 m along the distribution feeder lines from the main feeder to distribution feeder G4 (see Figure 6.1). Thus, the network studied has short lines and is not a typical radial weak network, and tolerate integration of solar PV in a better manner. The results implies that the distribution grid is strong. This was confirmed by Lillebø [13] who analyzed the same grid in terms of EV hosting capacity. The EV hosting capacity was found to be good for a majority of the end-users. The distribution grid could tolerate an EV penetration of 50% (50% of the end-users have EV) with regards to a voltage limit for undervoltages of 0.9 pu.

Constant leading power factors can mitigate the overvoltage problems. For PV scenario 100%, constant leading inverter power factors of 0.9 are required to ensure voltages below the upper bound of 1.05 pu. A lower value for the power factor means higher reactive currents, also when the PV active power generation is low and reactive power compensation is not needed. In turn, this leads to increased network active power losses. When all inverters operate at constant leading power factors of 0.9, the network active power loss is increased by 48% (from 547 kWh to 810 kWh), compared to the scenario of unity power factors. Alternatives to adding constant leading power factors are optimal active power curtailment and reactive power control. Optimal set-points for the PV inverter outputs have been found by solving non-linear optimization problems in GAMS with different objectives. The results from optimization with different objectives are discussed in the following sections.

8.2 Single-objective optimization

Optimal set-points for the PV inverters have been found for different objectives. All objectives meets the goal of ensuring that the voltage limits are not violated. Single-objective optimization of objective 1 and 2 (minimization of network active power loss and voltage deviation) give about the same results. To ensure a flat voltage profile in objective 2, the PV inverter active and reactive power outputs at each bus are adjusted such that the net load at the buses are zero in hours of significant PV active power generation. About the same set-points for inverter outputs are obtained from minimization of network active power losses. Net loads of zero means reduced power flows in the lines and hence reduced network active power losses. Optimization of objective 1 and 2 show that solar PV active power generation needs to be included in the objective function in order to maintain high PV active power generation in the network.

No solar PV active power generation needs to be curtailed for single-objective optimization of objectives 3 and 4 (minimize PV active power curtailment and minimize overall active power losses). The PV inverters absorb reactive power to ensure that the voltage limits are not violated. The network active power losses are higher in the simulation results for objective 3 compared to the results for objective 4. For objective 3, the PV inverter reactive absorption is only limited by an upper bound proportional to the active power generation. For objective 4, the reactive power absorption is lower because increased reactive power flows results in increased network active power losses. Moreover, higher reactive power absorption for objective 3 results in a more flat voltage profile compared to in the results for objective 4. With the purpose of minimizing overall active power loss, objective 4 gives the best results as no PV active power generation is curtailed and the network active power losses are minimized for both PV scenarios 50% and 100%.

8.3 Constant PF, APC and RPC for overvoltage mitigation

The overvoltage problems caused by high amounts of PV active power generation in PV scenario 100% can be mitigated by adding constant leading power factors to the PV inverters, curtailment of PV active generation in hours of high generation or by reactive power absorption. In this section the results from these mitigation methods are compared with regards to network active power losses and curtailed PV active power generation. Results for constant leading power factors of 0.9 are compared to simulation results from single-objective optimization of objective 4 with both active- and reactive power control and with only active power curtailment.

Overvoltages considering a limit of 1.05 pu will occur for a significant part of the year for PV scenario 100% without inverter controls, and hence inverter control is necessary for a great part of the year. This can be observed from Figure 7.30, where the voltage magnitude at bus 32 is presented for the year of analysis. The results show that we get the lowest network active power losses if we only use active power control. Compared to results for unity power factors, the network active power losses are reduced by by 41% on 27. of May (the day of maximum PV power generation). This is due to reduced active power line flows from excess PV active power generation. The annual network active power loss is reduced 19% for only active power control. By adding reactive power control (APC & RPC), the network active power loss is increased by 24% on 27. of May compared to unity power factors. The network active power loss is increased by 48% for constant leading power factors of 0.9. The annual network active power loss is increased by 9%

and 43% for APC & RPC and for constant leading power factors of 0.9, respectively. However, APC & RPC and constant leading power factors of 0.9 ensure that no PV active power generation is curtailed. For optimal PV active power curtailment, 14% of the PV active power generation is lost on 27. of May. On an annual basis, 73.66 MWh of the PV active power generation is lost, which represent 5% of the potential annual generation. Hence, adding constant leading power factors of 0.9 results on considerably higher network losses compared to only APC and APC & RPC control on both daily and annual basis. When the possibility of reactive power control is included in the APC & RPC control, the lowest overall losses are obtained (network power loss and curtailment).

Similar observations are found in [4] where optimal set-points for PV inverters in a residential network are found. Compared to the input data in this thesis, the PV capacities are significantly lower, the lines are somewhat shorter and the R/X ratios are of same magnitude. Hence, the voltage change along a line is higher in this thesis, but the effect of reactive power absorption is of the same proportion. Dall'Anese et.al. [4] find that optimal inverter dispatch (APC & RPC) reduce the need for PV power curtailment significantly. Similar to the results from this thesis, the paper states that optimal inverter dispatch gives the lowest overall power losses both on daily and annual basis. However, opposed to the results in this thesis, the paper finds that the network losses are lower for optimal inverter dispatch compared to PV active power curtailment alone. One reason for the difference might be that the amount of reactive power absorption is higher in this case study compared to the reactive power absorption in the paper. Higher PV capacities results in higher reactive power absorption and hence higher network power losses. Similar research in [5] show that activation of RPC compared to APC alone results in reduced power curtailment for overvoltage mitigation. Note that no PV active power is curtailed for the APC & RPC control in the simulations in this thesis. Thus, the inverters do not utilize the entire available operating range given in Figure 2.4c. Indeed, the PV inverters only utilize the operating range in Figure 2.3b.

8.4 Net contribution from extra solar PV active power generation

The simulation results for a passive system with PV scenario 50% show that the voltage magnitudes barely exceed the upper voltage bound of 1.05 pu. This observation shows that the distribution network can host approximately 832 kWp PV capacity, the sum of PV capacities in this scenario, with regards to voltage limitations. When the possibility of reactive power control is included, no PV active power generation is curtailed to mitigate overvoltage problems in PV scenario 100%. By adding reactive power control, the

distribution network can handle an increase in total PV capacity to 1688 kWp, the sum of PV capacities in PV scenario 100%. Hence, the hosting capacity in terms of installed kWp can be increased by at least 103% by adding reactive power control. Note that this only applies if the thermal limitations of the power network are not considered.

Increased PV active power generation results in higher active and reactive power transfer and hence higher network power losses. Thus, the marginal contribution from extra PV active power generation decreases. However, the net energy contribution (power generation minus network power loss) from extra PV generation is high. The increase in net energy contribution on 27. of May (the day of maximum PV power generation) is 95% (increase of 5 194 kWh/day) for APC & RPC and 73% (increase of 3 973 kWh/day) for only APC for PV scenario 100% compared to PV scenario 50% without PV inverter controls. Similar observations are made in [33], where an OPF with the objective of minimizing the expected curtailment from voltage stability considerations in a grid with high wind penetration is done. They find that reactive power generation from the wind farms reduce the need for curtailments, and that the net contribution of extra wind power generation is always positive with regards to increased network power losses.

8.5 Location for APC and RPC in the distribution network

Figure 7.34a shows that active power is curtailed at the buses with the highest voltage magnitudes. The voltage rises along the radial feeder from the distribution transformer to bus 35 along the distribution feeder lines G1-G4. The inverters connected towards the end of the feeder bear the highest share of curtailment. These findings are in agreement with other reports. In [4], the houses located at the end of the feeder curtail more active power and absorb more reactive power than the other houses. Opposed to the results in [4], the inverters at some of the "shared-nodes" in Figure 6.1 operate at a low power factor, but do not have to curtail any PV active power generation. In addition, [4] states that more active power is curtailed at houses with higher PV active power generation. This applies to bus 32, the grocery store, which have the highest PV active power generation and curtailment. Also in [5], it is observed that the power curtailment only takes place at a selection of the buses. Curtailing at a specific bus gives a more favourable distribution of the generated power and acceptable voltages can be maintained. The remaining solar power has a better distribution so that more power can be transferred with lower losses. However, some end-users will suffer a loss in revenue from lost PV active power generation.

8.6 Effectiveness of reactive power control

The effectiveness of reactive power compensation depends on the R/X ratio of the power network. The R/X ratio of the power system studied is high. This means that the voltage is more affected by active power compared to reactive, and a higher amount of reactive power compensation is needed to make up for the voltage change caused by active power. Lillebø [13] added a 22 kVA fast charger in the grid and found that an injection of reactive power corresponding to a power factor of 0.74 leading was required to successfully implement fast chargers in the weakest part of the grid without violating the minimum voltage level of 0.9 pu. Hence, the required power factor was found to be low for successful reactive power compensation in the distribution network. Figure 7.27, which presents the annual active and reactive power import at the slack bus for the control options APC and APC & RPC, shows that a high amount of reactive power import is needed to facilitate a smaller increase in active power generation. In addition, it was found that a constant power factor of 0.9 leading is necessary to get acceptable voltage magnitudes in PV scenario 100%.

Interestingly, in ref. [7] it is found that increasing the PV inverter apparent power rating to enable more reactive power compensation does not improve the network performance much compared to real power curtailment during peak generation. This is because the effect of reactive power control is limited in networks with high R/X ratios. As no PV active power generation is curtailed for optimal reactive control in this thesis, the entire inverter rating is required in hours when the inverters operate at a leading power factor of 0.8. Hence, the inverter overrating of 25% is utilized. An interesting analysis for further work could be to add a restriction for the PV inverter apparent power ratings. Thus, one can investigate if increasing the PV inverter apparent power rating improves the network performance or not.

8.7 Sensitivity analysis on voltage limits

The results in Sections 7.4.1 and 7.5 show that the overall active power losses can be reduced by accepting higher voltage magnitudes. By accepting higher voltage magnitudes less PV active power needs to be curtailed and less reactive power absorption is required to mitigate overvoltage problems. A reduction in active power losses means reduced costs, and hence it is important not to put too strict voltage bounds. Note that reduced curtailment is mainly a benefit for the PV owner, while reduced network power losses

caused by reduced reactive power absorption mainly is a benefit for the distribution grid operator. In the simulations in this thesis the maximum allowable increase and decrease from nominal voltage magnitude was set to 5%. However, the bound on upper and lower voltage magnitudes varies for different power system operators and are not absolute (Section 2.1.1).

In Section 7.4.1 it was proved that the overall active power loss can be reduced by increasing the upper voltage bound at the most critical bus by 1 percentage point, i.e. from 1.05 to 1.06 pu. Also the results for multi-objective optimization of objectives 2 and 4 in Section 7.5 show that reductions in active power losses are obtained by accepting higher voltage variations. The curve in Figure 7.38 flattens around 1.10 pu, meaning that increasing the voltage upper bound above 1.10 pu will not result in that much reduction in total active power losses. Thus, one should carefully consider the consequences when setting absolute voltage boundaries.

In [5] coordinated droop-based APC and RPC control for overvoltage mitigation in a low voltage microgrid was investigated using multi-objective optimal power flow. The objectives were to maintain a flat voltage profile, minimize PV active power curtailment and to maximize the absorbed reactive power at the PV inverters. As in the simulation results in this project, [5] finds that a smaller amount of both curtailed active power and absorbed reactive power can be obtained by decreasing the weight on the objective to minimize voltage deviation. As a result the overall power loss is reduced. Also ref. [6] obtain similar results as this thesis. In the paper, a multi-objective optimization technique that considers all objective simultaneously is investigated. The objectives are to minimize voltage deviation, network power losses and PV power curtailment. The paper states that by being more flexible in voltage deviation, the overall system performance is improved due to reduced import power and reduction in PV active power curtailment.

8.8 Thermal limitations of the distribution network

The PV generation cause high reverse power flows on 27. of May. The maximum active power exchange at the slack bus is increased significantly for both PV scenarios compared to the maximum power import for a passive system without PV power generation. The maximum power import in the passive system is 356.52 kW in the winter. For PV scenario 50% the maximum power export is 492.87 kW. The maximum export is 1059.56 kW in PV scenario 100%. The MVA rating of the transformer is 500 kVA, meaning that the

transformer is loaded close to its limit in PV scenario 50% and is considerably overloaded in PV scenario 100%. In addition, reactive power import at the slack bus due to inverter reactive power control increase the loading of the transformer even more. Hence, in reality the transformer is too small. In this case study it is assumed that the transformer is upgraded such that its capacity is large enough to export all excess energy generation. An alternative to upgrading the transformer could be to install a battery to store the excess energy exceeding the capacity of the transformer.

In [1], overloading of lines is mentioned as one challenge that will arise from increased PV penetration in the Norwegian distribution grid. The maximum load ratio of the network cables was presented in Figure 7.36 without PV and for PV scenario 100% for control options only APC and APC & RPC. It was found that a selection of cables are significantly overloaded for both control options, although the voltages are of acceptable magnitude. Lines connected to end-users with relatively high consumption and generation are most overloaded. These end-users also experience the highest voltage magnitudes. From Figure 7.36 it can be observed that reactive power control increases the loading of the cables. The results show that the power network can tolerate lower amounts of PV generation with regards to maximum loading of the cables, compared to maximum voltage magnitudes. Similar observations were obtained in the analysis of the current network with regards to EV hosting capacity in [13]. It was found that the distribution network could tolerate an EV penetration of 10-20% with regards to the thermal limitation of the cables and 50% with regards to voltage limits.

Thermal limits can be included in the optimization model as hard constraints or in the objective function. Adding thermal limits to the optimization model will probably result in active power curtailment in the APC & RPC control option. The network active power losses will be reduced compared to simulations without thermal limits due to reduction in active and reactive power line flows. As a result APC & RPC control might give lower network power losses compared to APC alone as found in [4].

8.9 Multi-objective optimization and other possible objectives

There are several challenges and many degrees of freedom associated with solving multi-objective optimization problems. Usually, the problem has multiple optimal solutions and a decision process is necessary in order to select a suitable solution. There exist several ways of solving multi-objective problems. The weighted-sum method was used in this thesis to produce a single compromise solution to the multi-

objective problem. To obtain acceptable results from the weighted-sum approach, the objectives were scaled in a way which seemed expedient to get approximately normalized values.

The objectives in this thesis were chosen to be minimization of network active power losses, voltage deviations and PV active power curtailment. As proven by the results, the choice of objective affect the final outcome. An alternative to include thermal limits as hard constraints is to include them in the objective function. Analyzes on thermal limitations require input data with improved time resolution to also include fluctuations within an hour, because high loading of the power lines for short time intervals might be acceptable, while high loading for 10-20 min might not. For that reason an objective including thermal limitations should also include the duration of the loading.

8.10 Local energy generation and energy efficiency

In this case study, the PV capacities in PV scenario 100% were calculated such that the annual PV generation was equal to 100% of the annual load demand for each end-user. As a consequence, high reverse power flows at bus 32, the grocery store, caused overvoltages and overloading of power line connected to it. The definition of zero-energy buildings (ZEB) states that these buildings produce enough renewable energy to compensate for green gas emissions from the entire lifespan of the building. This includes building materials, construction, operation and demolition/recycling [34]. However, these buildings are energy efficient, and thus the required annual generation is lower compared to a less energy efficient building. Thus, for consumers with high load, such as the grocery in this thesis, the potential for reducing the consumption should be investigated when deciding the PV capacity required for 100% annual self-consumption.

8.11 Limitations and assumptions

Several limitations and assumptions have been made for this study, which in turn influence the results. Firstly, the study is performed on one specific grid with specific consumption data and PV active power generation data. Other input data will probably give different results. However, the load profiles and PV active power generation profiles are characteristic and thus the results show characteristic trends. Also, the time resolution of this study is one hour and any peak value happening between two hourly

measurements is not included.

PV active power generation profiles were added to each consumer for different PV capacities. One reference was used for all PV generators in the system, and hence the power generation at all PV units are synchronized. In reality, factors like the tilt and position of the solar panels and shading will results in different PV power generation profiles. In the study it was found that high PV capacities are required to cause overvoltages in the distribution network. Thus, the PV capacities and the costs of the PV panels are high. It might not be realistic for consumers to invest in panels of that size. In addition, a PV penetration of 100% (all consumers have PV panels) is not realistic today.

For solving the load flow problems in MATPOWER and GAMS, it was assumed that both the consumption and PV power generation are equally distributed between the phases. In reality, the loads in the distribution grid will not necessarily be uniformly connected to the phases, and the loads are mostly connected across two phases in an IT-grid. In addition, PV inverers may be connected to one single-phase. As a result unbalance may occur due to excessive loading on one of the phases which in turn worsen the results. However, the PV capacities in this study are large and exceeds the limit for single-phase installations of 3.6 kVA [20].

It is assumed that the PV inverter controls work flawlessly so that the inverters can provide the exact value of the simulated active and reactive power outputs. In addition it is assumed that a centralized controller and a two-way communication infrastructure is available.

9 | Conclusion

In this project optimal control of PV inverters for overvoltage mitigation is analyzed. Optimal PV inverter set-points have been found considering minimization of the different objectives: (i) network active power losses, (ii) voltage deviations, (iii) PV active power curtailment, and (iv) overall active power losses (network and curtailment). The study is performed for a distribution power network in Steinkjer, with simulated PV generation data. Optimal PV inverter control is found to be effective for overvoltage mitigation in the distribution network for high amounts of PV generation.

Two different scenarios for PV generation were constructed; (i) PV scenario 100%, the annual generation is equal to the annual consumption for each end-user, and (ii) PV scenario 50%, the annual generation is equal to half of the annual consumption. The PV penetration is assumed to be 100% (all end-users have solar PV) for both PV scenarios. Considering an upper limit for voltage magnitude of 1.05 pu, PV scenario 50% does not lead to significant overvoltage problems. However, PV scenario 100% causes overvoltages at several of the buses. The PV capacities in this scenaro are very high. Hence, the distribution network is strong and can take high amounts of solar PV generation before overvoltage problems occur.

The single-objective optimization results show that all objectives are effective for overvoltage mitigation. For objectives 1 and 2, PV generation exceeding the load demand is curtailed. No PV generation needs to be curtailed for objectives 3 and 4. It is found that by including the network active power losses in the objective, the reactive currents in the network are reduced. Hence, minimization of objective 4 is most successful for minimization of network power losses and PV power curtailment, while ensuring that the voltages are of acceptable magnitudes.

The results from minimization of overall active power losses (objective 4) show that we get the lowest network active power losses if we only use active power curtailment. When the possibility of reactive power control is included (APC & RPC), the lowest overall active power losses are obtained. Constant

power factors also mitigate overvoltage problems but results in significantly higher network active power losses compared to optimal active power curtailment and reactive power inverter control.

By increasing the PV installed capacities and by adding optimal reactive power control to the inverters, the network active power losses are increased. The increase is caused by increased active and reactive power line flows. However, the net energy contribution (power generation minus network losses) from extra PV generation is high. The increase in net energy contribution from extra PV generation on 27. of May (the day of maximum PV power generation) is 95% (increase of 5 194 kWh/day) for optimal reactive power control and 73% (increase of 3 973 kWh/day) for only optimal active power curtailment for PV scenario 100% compared to PV scenario 50% without PV inverter controls.

More PV power generation is curtailed at end-user nodes with high PV generation and at buses located more far from the main feeder. These buses also have the highest voltage magnitudes. PV power curtailment at a selection of the buses results in a more favourable distribution of the generated power and acceptable voltages. However, some end-users will suffer a loss in revenue from lost generation. Reactive power absorption occurs more randomly and also occur at buses without overvoltages.

The network can take higher amounts of solar PV generation with regards to overvoltage compared to overloading of the cables and exceeding the transformer rating. Due to increased line power flows, optimal reactive power control cause the highest loading of the cables. The concept zero energy buildings require both local energy generation and energy efficiency. Thus, for consumers with high load, such as the grocery in this thesis, the potential for reducing the consumption should be investigated when deciding the PV capacity required for 100% annual self-consumption. Hence, overloading and overvoltages in the distribution network can be limited.

Sensitivity analysis for the restriction on maximum voltage magnitude and the results from multi-objective optimization of objectives 2 and 4 (voltage deviation and overall power loss) show that reductions in overall active power losses (network and curtailment) can be obtained by accepting higher voltage variations. However, increasing the voltage upper bound above 1.10 pu will not result in much reduction in overall active power losses. By allowing higher voltages, the reactive currents and the required amount of curtailed PV power generation can be reduced. Thus, one should carefully consider the consequences when setting absolute voltage boundaries.

10 | Further work

This work has contributed to a better understanding of how utilization of smart photovoltaic inverters can mitigate negative impacts from high amounts of solar photovoltaic active power generation in the distribution networks. Further work is needed to broaden the applicability of the results by studying other distribution network architectures, other load and PV power generation profiles, inverters with local energy storage and expanding the simulation model to also include thermal limitations. In particular, the further works should include:

- Load demand and PV power generation data with improved time resolution can be gathered to see rapid voltage variations and to observe the duration of overloading on the power cables.
- The power network studied has a high R/X ratio and short power transmission lines, and hence the effectiveness of reactive power control is limited. The simulation model can be applied to a power network with a lower R/X ratio and longer lines. In power networks with lower R/X ratios, more of the voltage rise caused by distributed generation can be compensated for by reactive consumption.
- The simulation model can be applied to other PV generation data and different load profiles.
- Investigate other ways to write the restriction for inverter reactive power output, by adding a restriction for the inverter apparent power rating.
- Investigate the benefits of a full-bridge inverter with battery storage, so that the inverters can provide reactive power compensation in undervoltage situations caused by high load demand also when the sun does not shine.
- Investigate the benefits of active and reactive power control in power networks with high amounts of both solar PV and electrical vehicles. Reactive power generation can mitigate undervoltage situ-

ations caused by charging of electrical vehicles.

- Expand the model to also include power and voltage unbalance as excessive loading on one of the phases will worsen the results.
- Investigate the effect of adding thermal limitations of the distribution network (transformer and power cables) as hard constraints or as a part of the objective function.

Bibliography

[1] Multiconsult and Asplan Viak, "Solcellesystemer og sol i systemet," 2018. [Online]. Available: http://solenergiklyngen.no/app/uploads/sites/4/180313-rapport_solkraft-markedsutvikling-2017-endelig.pdf

[2] M. M. Haque and P. Wolfs, "A review of high PV penetrations in LV distribution networks: Present status, impacts and mitigation measures," *Renewable and Sustainable Energy Reviews*, vol. 62, pp. 1195–1208, 2016. [Online]. Available: http://dx.doi.org/10.1016/j.rser.2016.04.025

[3] A. Rodriguez-Calvo, R. Cossent, and P. Frías, "Integration of PV and EVs in unbalanced residential LV networks and implications for the smart grid and advanced metering infrastructure deployment," *International Journal of Electrical Power and Energy Systems*, vol. 91, pp. 121–134, 2017. [Online]. Available: http://dx.doi.org/10.1016/j.ijepes.2017.03.008

[4] E. Dall'Anese, S. V. Dhople, and G. B. Giannakis, "Optimal dispatch of photovoltaic inverters in residential distribution systems," *IEEE Transactions on Sustainable Energy*, vol. 5, no. 2, pp. 487–497, 2014. [Online]. Available: https://ieeexplore.ieee.org/stamp/stamp.jsp?tp=&arnumber=6719562

[5] T. T. Mai, A. N. M. M. Haque, T. Vo, and P. H. Nguyen, "Coordinated active and reactive power control for overvoltage mitigation in physical LV microgrids," 7th International Conference on Renewable Power Generation, Oct 2018 Copenhagen Denmark.

[6] A. Verma, P. P. Verma, A. V. Eluvathiangal, and K. S. Swarup, "An Intelligent Methodology to Improve Distribution System Operational Parameters Utilizing Smart Inverter Functionalities of PV Sources," 7th International Conference on Renewable Power Generation, Oct 2018 Copenhagen Denmark.

[7] X. Su, M. A. Masoum, and P. J. Wolfs, "Optimal PV inverter reactive power control and real power curtailment to improve performance of unbalanced four-wire LV distribution networks,"

IEEE Transactions on Sustainable Energy, vol. 5, no. 3, pp. 967–977, 2014. [Online]. Available: https://ieeexplore.ieee.org/stamp/stamp.jsp?arnumber=6804647

[8] X. Huang, H. Liu, B. Zhang, J. Wang, and X. Xu, "Research on local voltage control strategy based on high-penetration distributed PV systems," 7th International Conference on Renewable Power Generation, Oct 2018 Copenhagen Denmark.

[9] SMA, "PV Grid Integration - Backgrounds, requirements, and SMA solutions," *Technology Compedium 3.4*, 2012. [Online]. Available: http://files.sma.de/dl/10040/PV-Netzint-AEN123016w.pdf

[10] R. K. Varma and E. M. Siavashi, "PV-STATCOM: A New Smart Inverter for Voltage Control in Distribution Systems," *IEEE Transactions on Sustainable Energy*, vol. 9, no. 4, pp. 1681–1691, 2018. [Online]. Available: https://ieeexplore.ieee.org/stamp/stamp.jsp?tp=&arnumber=8299588

[11] P. Brucke, "Reactive Power Control in Utility-Scale PV," *SolarPro Magazine*, no. 7.4, 2014, accessed 2018-11-27. [Online]. Available: https://solarprofessional.com/articles/design-installation/reactive-power-control-in-utility-scale-pv#.XBYsdhNKhTb

[12] K. Turitsyn, P. Šulc, S. Backhaus, and M. Chertkov, "Options for control of reactive power by distributed photovoltaic generators," *Proceedings of the IEEE*, vol. 99, no. 6, pp. 1063–1073, 2011. [Online]. Available: https://ieeexplore.ieee.org/stamp/stamp.jsp?tp=&arnumber=5768094

[13] M. Lillebo, S. Zaferanlouei, A. Zecchino, and H. Farahmand, "Impact of Large-Scale EV Integration and Fast Chargers in a Norwegian LV Grid," *NTNU*, 2018. [Online]. Available: https://brage.bibsys.no/xmlui/bitstream/handle/11250/2497394/18218_FULLTEXT.pdf?sequence=1&isAllowed=y

[14] O. A. Hjelme, "Integration of distributed renewable energy in Trøndelag," *NTNU*, 2018.

[15] S. G. Naik, D. Khatod, and M. Sharma, "Optimal allocation of combined DG and capacitor for real power loss minimization in distribution networks," *International Journal of Electrical Power and Energy Systems*, vol. 53, pp. 967–973, 2013. [Online]. Available: https://ac.els-cdn.com/S0142061513002688/1-s2.0-S0142061513002688-main.pdf?_tid=0eec9392-72da-43dd-83e5-a100ca1b444f&acdnat=1551255066_852e8836eb4293f77ebea118f9d37331

[16] H. Saadat, *Power System Analysis*, 3rd ed. PSA Publishing, 2010.

[17] NVE, "Nett," accessed 2019-01-10. [Online]. Available: https://www.nve.no/energiforsyning-og-konsesjon/nett/

[18] Lovdata, "Forskrift om leveringskvalitet i kraftsystemet - Lovdata," *Lovdata*, p. Kapittel 3. Krav til leveringspålitelighet og spen, 2004, accessed 2019-02-10. [Online]. Available: https://lovdata.no/dokument/SF/forskrift/2004-11-30-1557#KAPITTEL_4

[19] VDE, "German Technical Standard VDE-AR-N 4105 Power generation systems connected to the low-voltage distribution network," 2011.

[20] NTE, "Veileder plusskunder nettanalyse," 2018.

[21] C. Dierckxsens, A. Woyte, B. Bletterie, A. Zegers, W. Deprez, A. Dexters, K. V. Roey, J. Lemmens, J. Lowette, K. Nulens, Y. T. Fawzy, B. Blazic, B. Uljanic, and M. Kolenc, "Cost-effective integration of photovoltaics in existing distribution grids : results and recommendations," Tech. Rep., 2015. [Online]. Available: https://www.ait.ac.at/fileadmin/mc/energy/downloads/MetaPV_Final_Report_Results_and_Recommendations.pdf

[22] G. M. Masters, *Renewable and Efficient Electric Power Systems*, 2nd ed. John Wiley Sons, 2013.

[23] NEK, "Requirements for micro-generating plants to be connected in parallel with public low-voltage distribution networks," 2013.

[24] NVE, "Plusskunder," 2015, accessed 2018-04-26. [Online]. Available: https://www.nve.no/reguleringsmyndigheten-for-energi-rme-marked-og-monopol/nettjenester/nettleie/tariffer-for-produksjon/plusskunder/

[25] K. Deb, *Multi-objective Optimization*. Boston, MA: Springer US, 2014, pp. 403–449, in: Burke E., Kendall G. (eds) Search Methodologies. [Online]. Available: https://doi.org/10.1007/978-1-4614-6940-7_15

[26] C. M. Fonseca and P. J. Fleming, "Multiobjective optimization and multiple constraint handling with evolutionary algorithms - Part I: A Unified Formulation," *IEEE Transactions on Systems, Man, and Cybernetics Part A:Systems and Humans.*, vol. 28, no. 1, pp. 26–37, 1998.

[27] R. D. Zimmerman and C. E. Murillo-Sánchez, "Matpower User´s Manual," vol. 7.0b1, 2018. [Online]. Available: http://www.pserc.cornell.edu/matpower/manual.pdf

[28] GAMS, "An introduction to GAMS," accessed 2018-08-27. [Online]. Available: https://www.gams.com/products/introduction/

[29] "A GAMS Tutorial by Richard E. Rosenthal," accessed 2018-12-09. [Online]. Available: https://www.gams.com/latest/docs/UG_Tutorial.html#UG_Tutorial_Summary

[30] Renewables.ninja, "Renewables.ninja," accessed 2018-06-01. [Online]. Available: https://www.renewables.ninja/

[31] M. Blikø, "Email correspondence with Marianne Blikø, engineer at NTE," 2018.

[32] Circuit Globe, "Tap-changing Transformers," accessed 2019-02-20. [Online]. Available: https://circuitglobe.com/tap-changing-transformers.html

[33] E. Nycander, S. Lennar, R. Eriksson, and C. Hamon, "Minimizing wind power curtailments using OPF considering voltage stability," 2018. [Online]. Available: http://www.diva-portal.org/smash/get/diva2:1264655/FULLTEXT01.pdf

[34] ZEB, "ZEB Definitions," accessed 2019-02-16. [Online]. Available: https://www.zeb.no/index.php/en/about-zeb/zeb-definitions

Appendix A

Results for PV scenario 100%

A.1 Objective 1

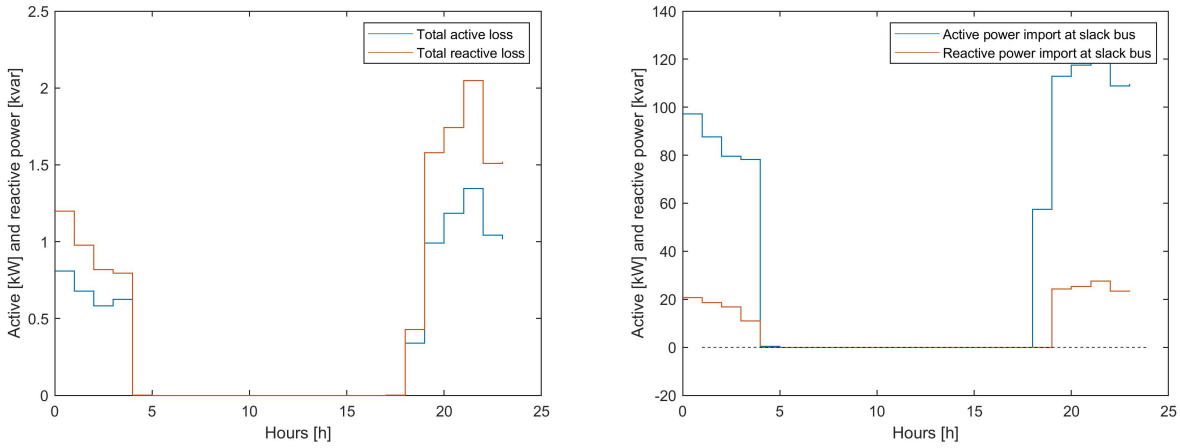

(a) **(b)**

Figure A.1: Objective 1, PV scenario 100% on 27. of May. (a) Total network active and reactive power losses. (b) Power import at the slack bus.

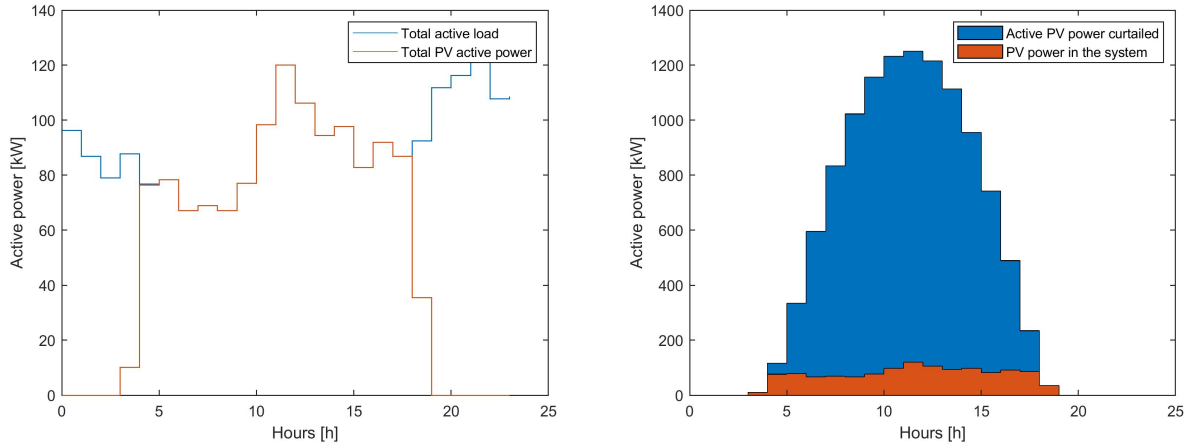

(a) **(b)**

Figure A.2: Objective 1, PV scenario 100% on 27. of May. (a) Total active power load and total PV generation. (b) Curtailed PV active power and PV power in the system. The blue area represents the lost energy due to curtailment.

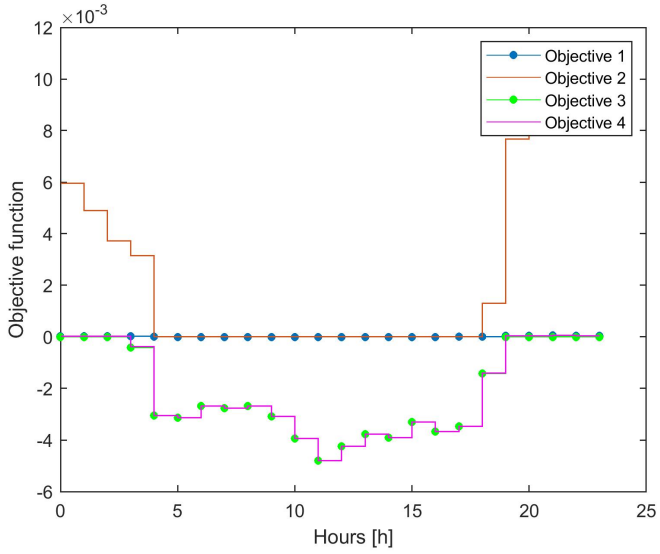

Figure A.3: Value of objectives 1, 2, 3 and 4 on 27. of May for PV scenario 100%. The plotted values of the objectives are calculated based on per unit values of voltages and powers. Objective 1 is minimized.

A.2 Objective 2

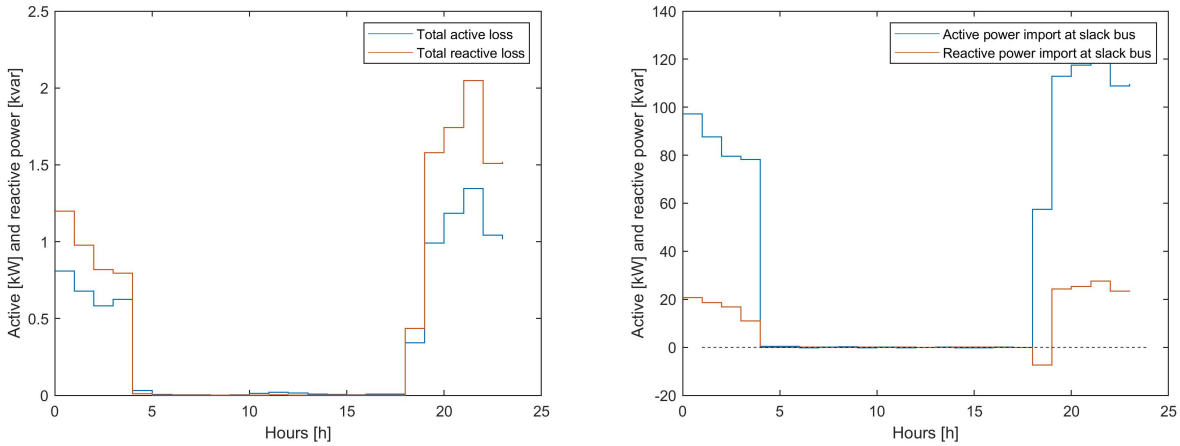

(a) **(b)**

Figure A.4: Objective 2, PV scenario 100% on 27. of May. (a) Total network active and reactive power losses. (b) Power import at the slack bus.

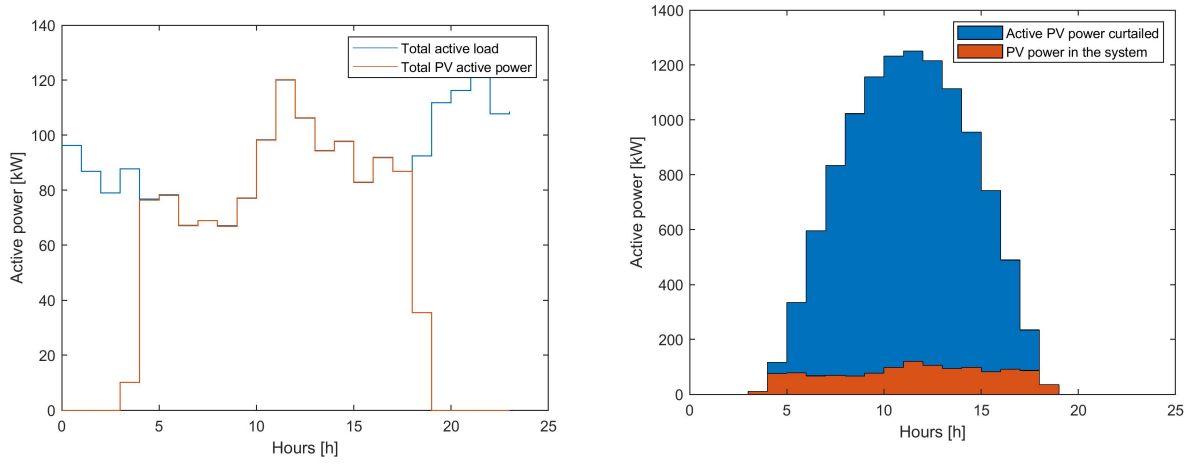

(a) Total active load and PV power.

(b) Active PV power curtailed and active PV power in the system. The blue area represents the lost energy.

Figure A.5: Objective 2, PV scenario 100% on 27. of May. (a) Total active power load and total PV generation. (b) Curtailed PV active power and PV power in the system. The blue area represents the lost energy due to curtailment.

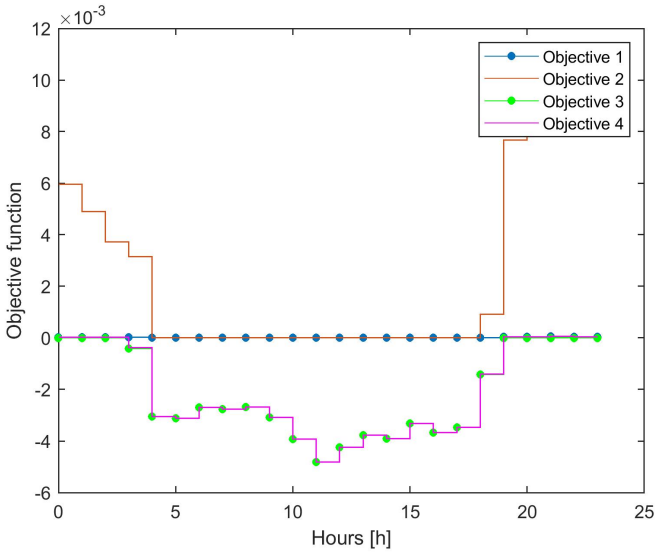

Figure A.6: Value of objectives 1, 2, 3 and 4 on 27. of May for PV scenario 100%. The plotted values of the objectives are calculated based on per unit values of voltages and powers. Objective 2 is minimized.

A.3 Objective 3

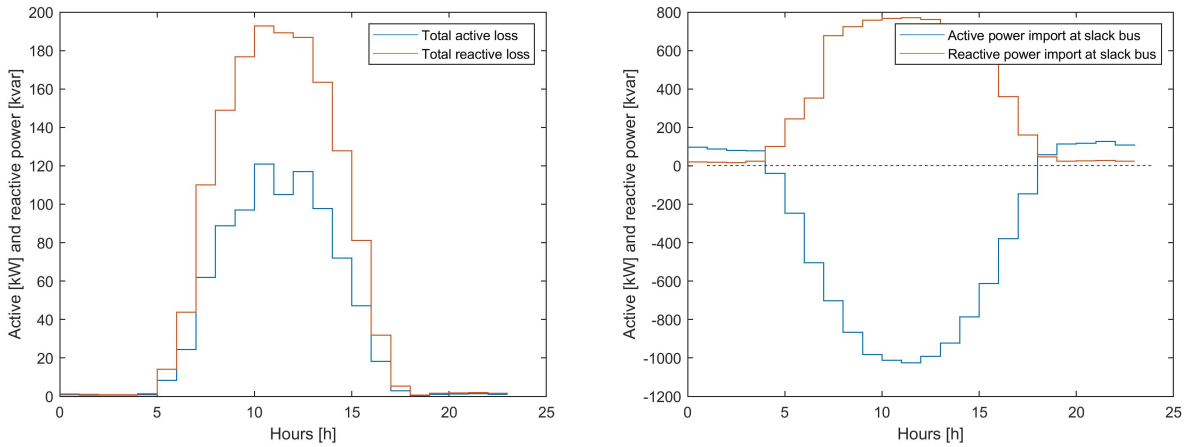

(a) **(b)**

Figure A.7: Objective 3, PV scenario 100% on 27. of May. (a) Total network active and reactive power losses. (b) Power import at the slack bus.

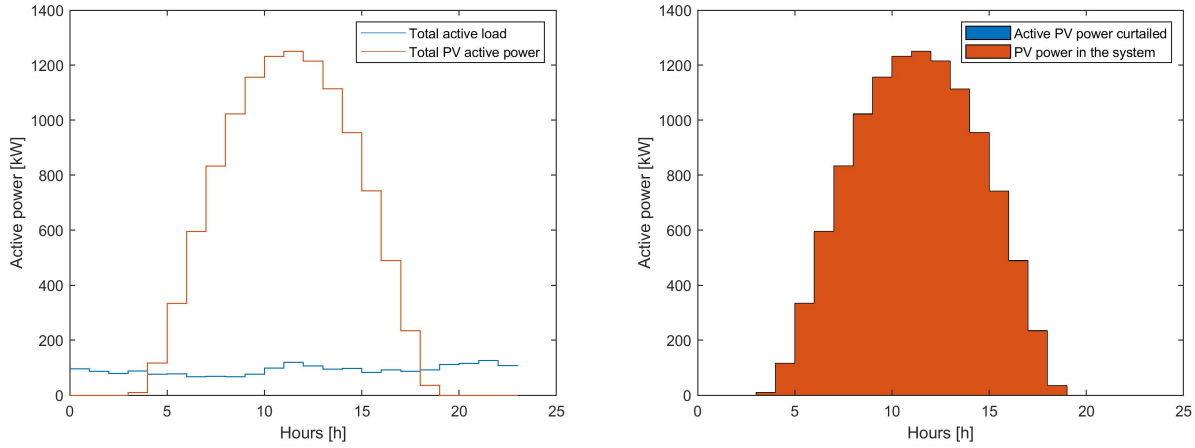

(a) **(b)**

Figure A.8: Objective 3, PV scenario 100% on 27. of May. (a) Total active power load and total PV generation. (b) Curtailed PV active power and PV power in the system. No PV power is curtailed in this case.

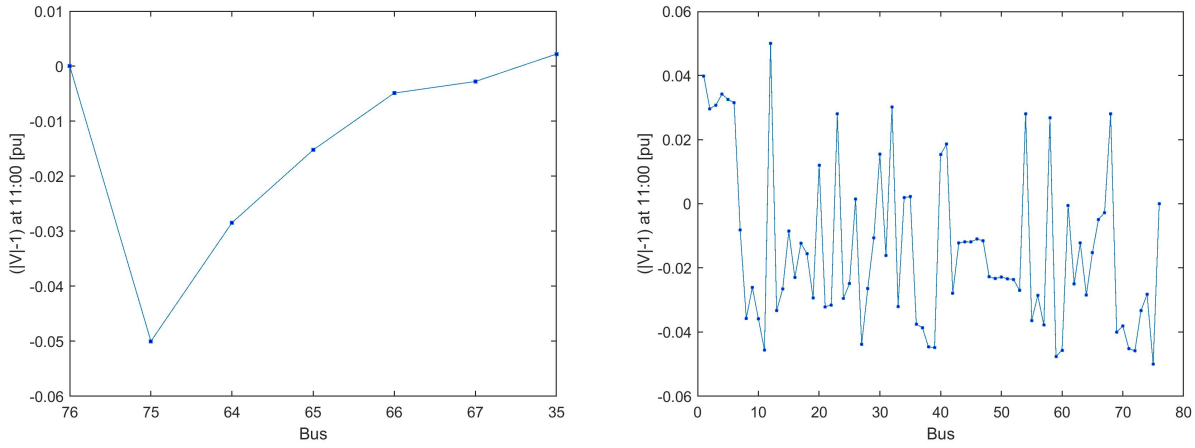

(a) **(b)**

Figure A.9: Voltage magnitudes at 11:00 on 27. of May for objective 3, PV scenario 100%. (a) Voltage change on lines from bus 76 (slack bus) to bus 35. (b) Voltage magnitude at all buses.

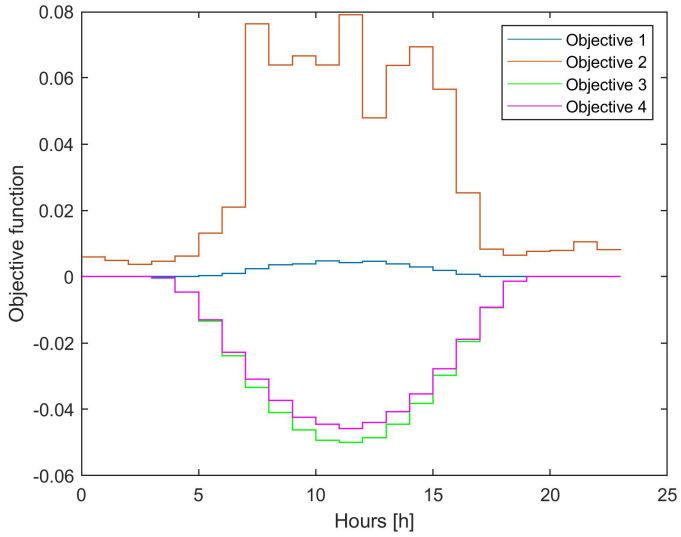

Figure A.10: Value of objectives 1, 2, 3 and 4 on 27. of May for PV scenario 100%. The plotted values of the objectives are calculated based on per unit values of voltages and powers. Objective 3 is minimized.

A.4 Objective 4

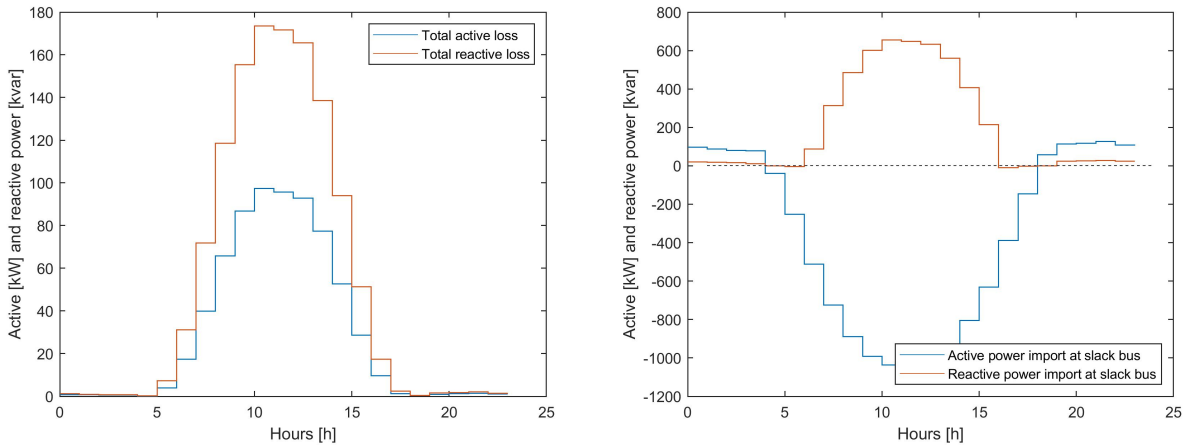

(a) **(b)**

Figure A.11: Objective 4, PV scenario 100% on 27. of May. (a) Total network active and reactive power losses. (b) Power import at the slack bus.

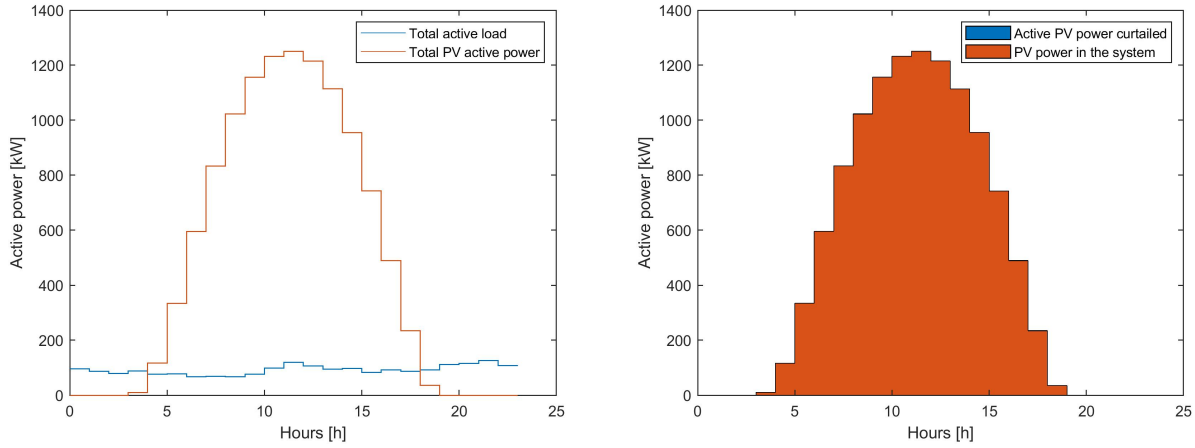

(a) **(b)**

Figure A.12: Objective 4, PV scenario 100% on 27. of May. (a) Total active power load and total PV generation. (b) Curtailed PV active power and PV power in the system. No PV power is curtailed in this case.

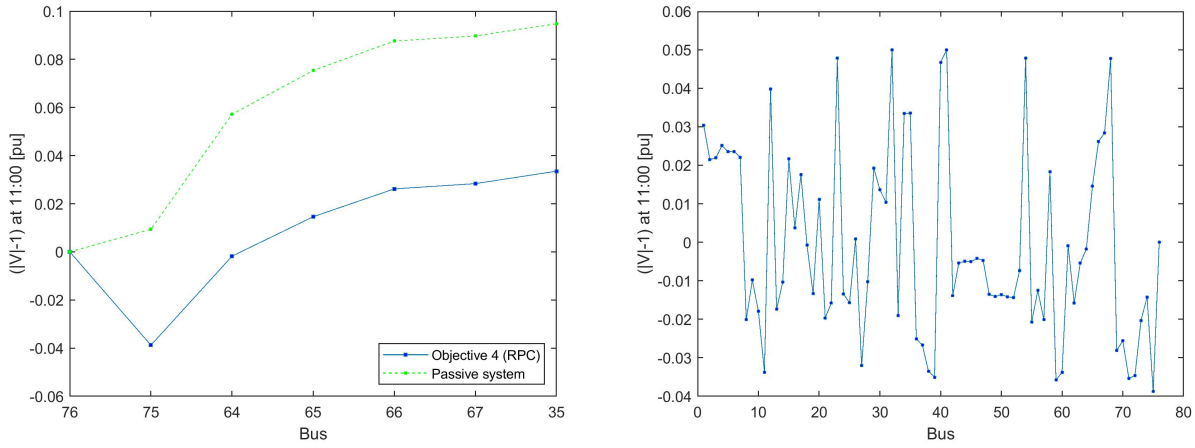

(a) **(b)**

Figure A.13: Voltage magnitudes at 11:00 on 27. of May for objective 4, PV scenario 100%. (a) Voltage change on lines from bus 76 (slack bus) to bus 35. (b) Voltage magnitude at all buses.

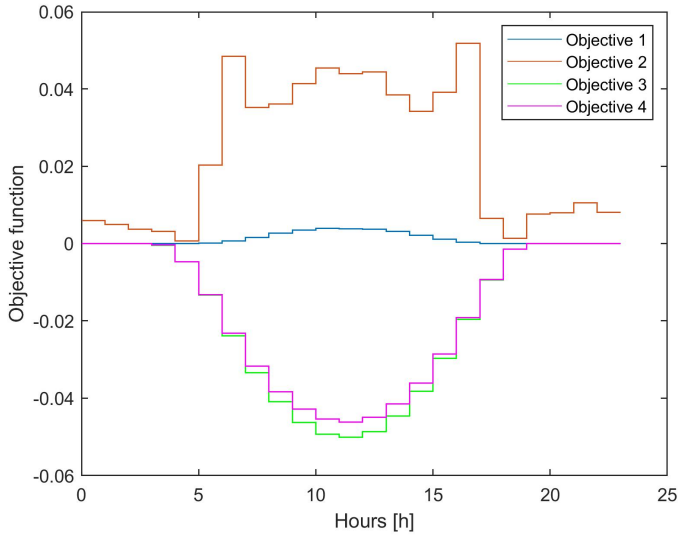

Figure A.14: Value of objectives 1, 2, 3 and 4 on 27. of May for PV scenario 100%. The plotted values of the objectives are calculated based on per unit values of voltages and powers. Objective 4 is minimized.

A.5 Objective 4 (APC only)

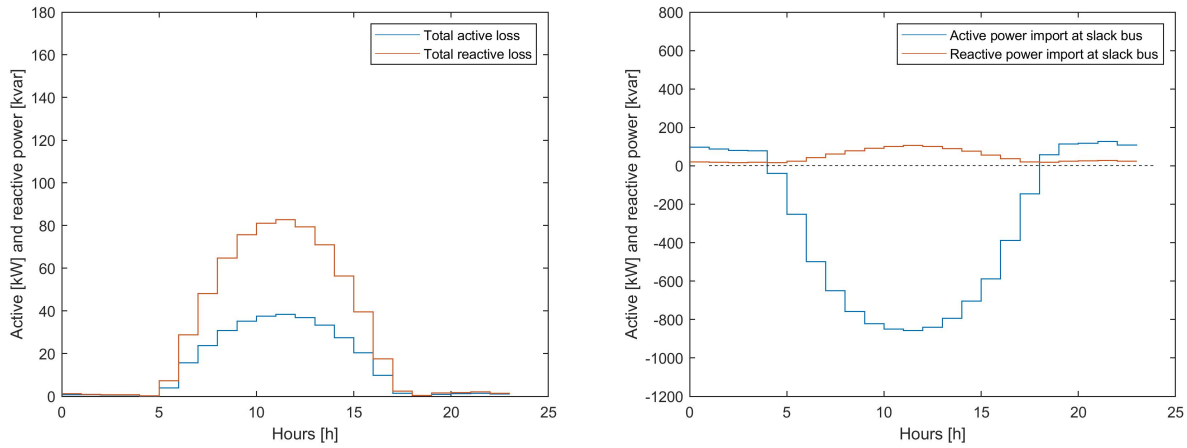

(a) **(b)**

Figure A.15: Objective 4 (only APC), PV scenario 100% on 27. of May. (a) Total network active and reactive power losses. (b) Power import at the slack bus.

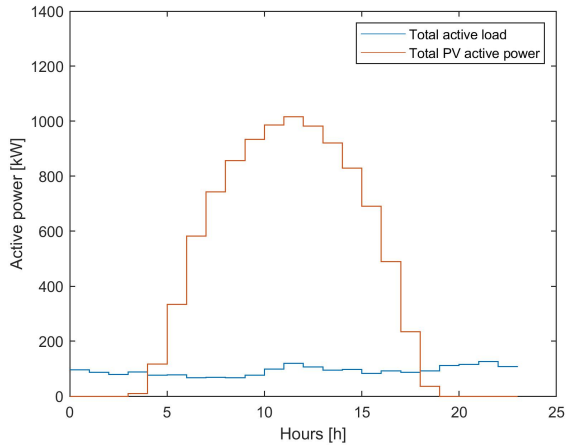

(a) Total active load and PV power.

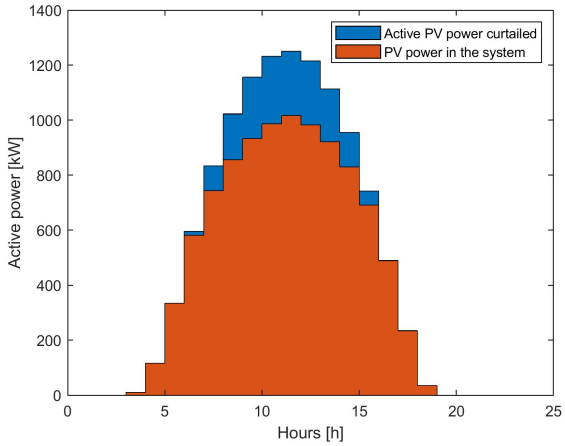

(b) Active PV power curtailed and active PV power in the system. The blue area represents the lost energy.

Figure A.16: Objective 4 (only APC), PV scenario 100% on 27. of May. (a) Total active power load and total PV generation. (b) Curtailed PV active power and PV power in the system. The blue area represents the lost energy due to curtailment.

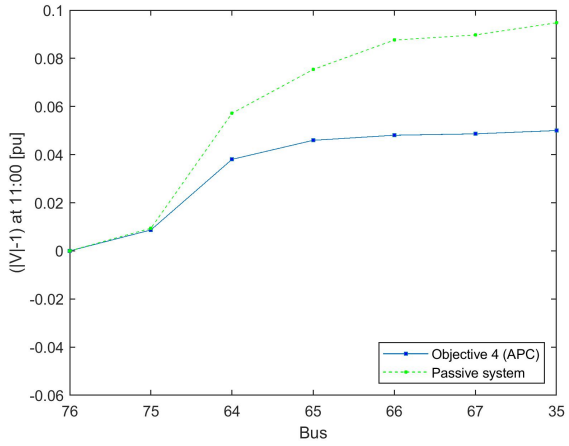

(a)

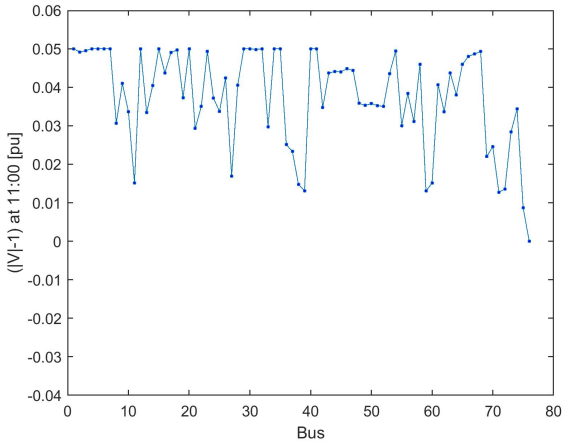

(b)

Figure A.17: Voltage magnitudes at 11:00 on 27. of May for objective 4 (only APC), PV scenario 100%. (a) Voltage change on lines from bus 76 (slack bus) to bus 35. (b) Voltage magnitude at all buses.

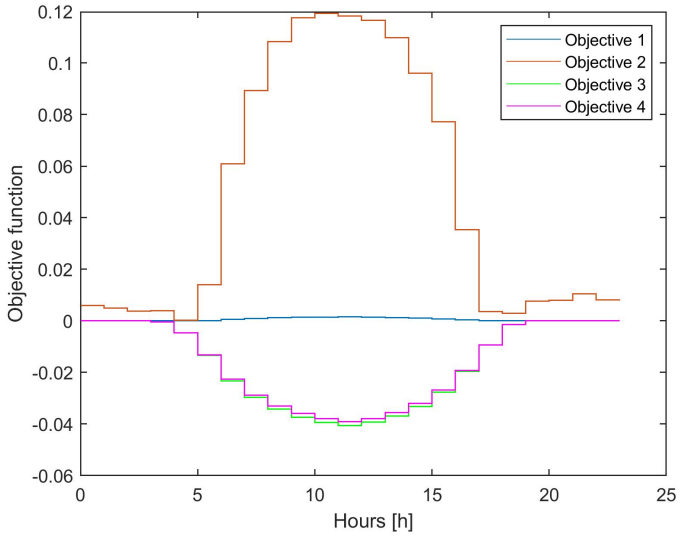

Figure A.18: Value of objectives 1, 2, 3 and 4 on 27. of May for PV scenario 100%. The plotted values of the objectives are calculated based on per unit values of voltages and powers. Objective 4 is minimized.

Appendix B

B.1 Comparison of single-objective optimizations

Table B.1: Results for PV scenario 50% on 27. of May for the passive system and for the single-objective optimizations.

	$\|V\|_{max}$	Network active power loss	Total active power loss
Passive system	1.05 pu	121.80 kWh	121.80 kWh
Objective 1	1.00 pu	8.99 kWh	4 382.63 kWh
Objective 2	1.00 pu	9.19 kWh	4 406.39 kWh
Objective 3	1.04 pu	199.41 kWh	199.41 kWh
Objective 4	1.05 pu	121.83 kWh	121.89 kWh

Table B.2: Results for PV scenario 100% on 27. of May for the passive system and for the single-objective optimizations.

	$\|V\|_{max}$	Network active power loss	Total active power loss
Passive system	1.11 pu	547.24 kWh	547.24 kWh
Constant PF=0.9 (leading)	1.03 pu	810.39 kWh	810.39 kWh
Objective 1	1.00 pu	8.61 kWh	10 089.59 kWh
Objective 2	1.00 pu	8.74 kWh	10 089.69 kWh
Objective 3	1.05 pu	870.55 kWh	870.55 kWh
Objective 4 (APC & RPC)	1.05 pu	678.31 kWh	678.31 kWh
Objective 4 (APC)	1.05 pu	323.52 kWh	1 899.47 kWh

Appendix C

C.1 Inverter power factor at the most critical bus for PV scenario 50%

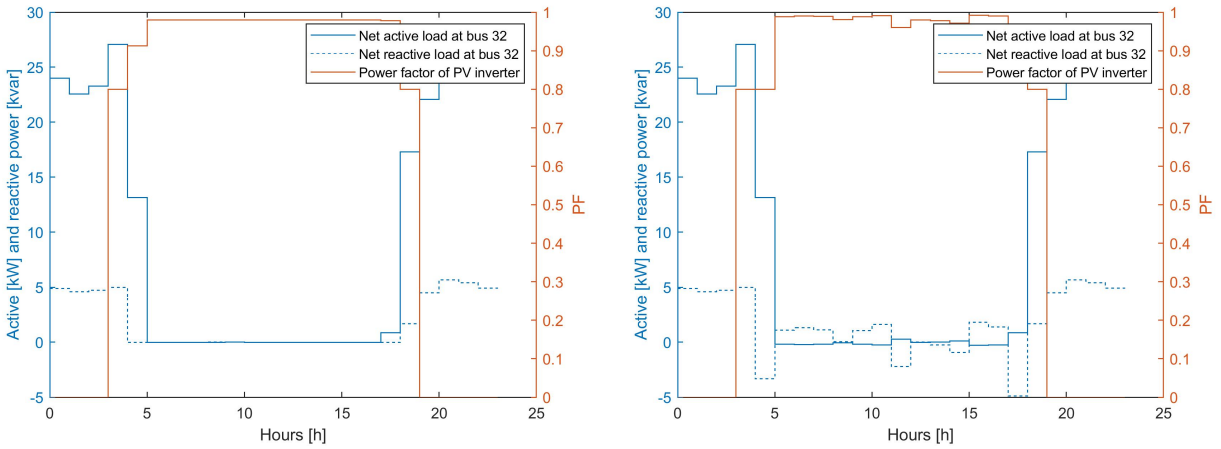

Figure C.1: Net active and reactive load and power factor of PV inverter at bus 32 for PV scenario 50% on 27. of May. (a) Objective 1. (b) Objective 2.

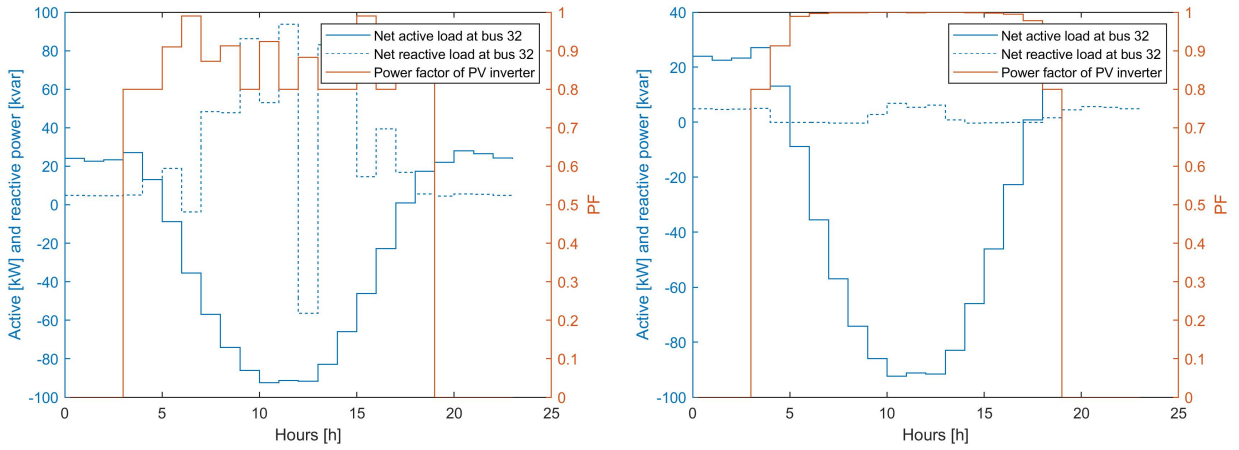

Figure C.2: Net active and reactive load and power factor of PV inverter at bus 32 for PV scenario 50% on 27. of May. (a) Objective 3. (b) Objective 4.

Oda Andrea Hjelme

Optimal PV Inverter Active and Reactive Power Control in Distribution Grids With High Amounts of Solar PV

NTNU
Norwegian University of
Science and Technology